

**THE INFLUENCE OF FOREST MANAGEMENT AND SPATIO-TEMPORAL  
VARIATION ON GREENHOUSE GAS FLUXES FROM RIPARIAN SOILS ALONG  
HEADWATER STREAMS**

by

Teresa K. Silverthorn

B.E.S. (Hon.), University of Waterloo, 2018

A THESIS SUBMITTED IN PARTIAL FULFILLMENT OF  
THE REQUIREMENTS FOR THE DEGREE OF

MASTER OF SCIENCE

in

THE FACULTY OF GRADUATE AND POSTDOCTORAL STUDIES  
(Forestry)

THE UNIVERSITY OF BRITISH COLUMBIA  
(Vancouver)

August 2020

© Teresa K. Silverthorn, 2020

The following individuals certify that they have read, and recommend to the Faculty of Graduate and Postdoctoral Studies for acceptance, a thesis/dissertation entitled:

The influence of forest management and spatio-temporal variation on greenhouse gas fluxes from riparian soils along headwater streams

---

submitted by Teresa K. Silverthorn in partial fulfillment of the requirements for

the degree of Master of Science

---

in Forestry

---

**Examining Committee:**

John Richardson, Forestry

Supervisor

Mary O'Connor, Zoology

Supervisory Committee Member

Sean Smukler, Land and Food Systems

Supervisory Committee Member

Sandra Brown, Land and Food Systems

Additional Examiner

## Abstract

Riparian zones of headwater streams have valuable ecosystem functions, and are particularly vulnerable to forest harvest in coastal British Columbia. Studies of greenhouse gas (GHG; CO<sub>2</sub>, CH<sub>4</sub>, N<sub>2</sub>O) fluxes from these unique ecosystems, with fluctuating water tables, and high soil organic matter, remain limited. My first objective was to quantify the effects of forestry practices on GHG emissions from riparian forest soils, and determine the dominant driver(s) of emissions over the growing season. I compared sites that were clear-cut without a riparian buffer (“no buffer”) or with a buffer (“buffer”) to relatively undisturbed riparian zones (“reference”). I hypothesized that either a rise in the water table, increased soil temperatures, or disturbance of roots and microbes following forest harvest would have the greatest influence on GHG fluxes. My second objective was to examine the effects of temporal and spatial variation on annual GHG fluxes from relatively undisturbed riparian soils. I hypothesized that groundwater discharge (DIS) areas in the riparian zone would have high soil moisture and nutrients, resulting in greater anaerobically produced CH<sub>4</sub> and N<sub>2</sub>O emissions compared to outside of these areas (ND). I further hypothesized that GHG fluxes would peak in the warmest and wettest months. I measured gas fluxes *in situ* alongside headwater streams using static chambers and gas chromatography. I found that N<sub>2</sub>O emissions were 1.71 and 2.12 times lower at buffer and no buffer sites, respectively, than reference sites. Carbon dioxide fluxes were 1.16 and 1.09 times higher at buffer and no buffer sites, respectively, compared to reference sites. Methane fluxes were 1.34 and 2.89 times higher at buffer and no buffer sites, respectively, compared to reference sites. Additionally, CH<sub>4</sub> uptake during the growing season was 2.18 times higher at ND areas than DIS areas. Soil temperature, soil moisture, and depth to the groundwater were significant

predictors of GHG emissions, and emission rates were highest in the spring and summer months. The results of my research provide information on the magnitude and drivers of GHG fluxes in riparian zones to help inform GHG budgets and forest management.

## **Lay Summary**

Riparian zones, or the zones of interaction between terrestrial and aquatic ecosystems, have valuable ecosystem functions, and are particularly vulnerable to forest harvest alongside headwater streams in coastal British Columbia. My objectives were to determine the effects of forest harvest as well as the effects of spatial and temporal variation on greenhouse gas fluxes from riparian soils, in order to inform forest management and improve greenhouse gas budgets for this understudied ecosystem. I found that clear-cutting in the riparian zone without a buffer reduced nitrous oxide fluxes and increased methane fluxes. I also found that methane fluxes were highest in topographic depressions in the riparian zone. Additionally, soil temperature, soil moisture, and depth to the groundwater table were significant predictors of greenhouse gas fluxes. My results further our knowledge of biogeochemical cycling in headwater riparian ecosystems.

## **Preface**

Teresa Silverthorn was the primary author of this work and completed the majority of the field and laboratory work, data analysis, and thesis preparation. Teresa's research project was a part of the Source Stream Protection (SOSTPRO) project led by John Richardson in collaboration with researchers in Sweden (Lenka Kuglerová) and Finland (Timo Muotka). Teresa worked in collaboration with John Richardson, who provided guidance throughout the development of project ideas, experimental design, data analysis, and thesis preparation. Several volunteers and summer assistants (particularly Olivia Hester) provided fieldwork assistance.

Chapters 2 and 3 will be edited for manuscript form to be submitted for publication under co-authorship of Teresa Silverthorn and John Richardson.

# Table of Contents

<b>Abstract .....</b>	<b>iii</b>
<b>Lay Summary .....</b>	<b>v</b>
<b>Preface .....</b>	<b>vi</b>
<b>Table of Contents .....</b>	<b>vii</b>
<b>List of Tables .....</b>	<b>x</b>
<b>List of Figures.....</b>	<b>xii</b>
<b>List of Abbreviations.....</b>	<b>xviii</b>
<b>Acknowledgements.....</b>	<b>xix</b>
<b>Chapter 1: Introduction.....</b>	<b>1</b>
1.1 Greenhouse gases .....	2
1.2 Riparian zones and forestry.....	5
1.3 Review of literature on greenhouse gas fluxes in riparian zones and how they are impacted by forestry.....	7
1.4 Objectives and hypotheses .....	12
<b>Chapter 2: Forest management impacts on greenhouse gas fluxes from riparian soils along headwater streams .....</b>	<b>17</b>
2.1 Introduction .....	17
2.2 Methods.....	21
2.2.1 Site description .....	21
2.2.2 Study design .....	23
2.2.3 Soil sampling .....	24

2.2.4	Greenhouse gas sampling.....	25
2.2.5	Statistical analysis.....	27
2.3	Results.....	34
2.3.1	Environmental variables.....	34
2.3.2	Carbon dioxide .....	35
2.3.3	Methane.....	36
2.3.4	Nitrous oxide .....	37
2.4	Discussion .....	55
2.4.1	Effects of forest harvest .....	56
2.4.2	Effects of local groundwater conditions .....	63
2.4.3	Conclusions .....	64
<b>Chapter 3: Temporal and micro-topographical variations in greenhouse gas fluxes from riparian forest soils along headwater streams .....</b>		<b>66</b>
3.1	Introduction.....	66
3.2	Methods.....	70
3.3	Results.....	71
3.3.1	Environmental variables.....	71
3.3.2	Spatial and temporal variation in greenhouse gas fluxes.....	73
3.4	Discussion .....	86
3.4.1	Spatial variation in greenhouse gas fluxes .....	92
3.4.2	Temporal variation in greenhouse gas fluxes.....	94
3.4.3	Conclusions .....	95
<b>Chapter 4: Conclusions.....</b>		<b>97</b>

4.1	Findings and limitations.....	97
4.2	Implications and future directions .....	99
	<b>References.....</b>	<b>103</b>
	<b>Appendix .....</b>	<b>119</b>

## List of Tables

Table 2.1 Characteristics of riparian study sites alongside headwater streams under differing forestry management conditions in Malcolm Knapp Research Forest, British Columbia.....	33
Table 2.2 Pairwise difference between Treatment levels (reference, R; buffer B; and no buffer NB) using Tukey’s HSD <i>post hoc</i> test for the linear mixed effects models explaining the dynamics of carbon dioxide, methane, and nitrous oxide fluxes, respectively. All models included the autocorrelation term “AR1(Week + 0   Site/Chamber)”. Bolded comparison indicates a significant effect at $p < 0.05$ .....	53
Table 2.3 Summarized output of linear mixed effects models explaining the dynamics of carbon dioxide, methane, and nitrous oxide fluxes, respectively. All models included the autocorrelation term “AR1(Week + 0   Site/Chamber)”. Bolded models indicate a significant effect at $p < 0.05$ . When comparing groundwater discharge (DIS) and non-groundwater discharge (ND) areas, note that ND is the reference level in the DIS_ND term. ....	54
Table 3.1 Summarized output of linear mixed effects model explaining the dynamics of annual carbon dioxide, methane, and nitrous oxide fluxes. All models included the autocorrelation term “AR1(Week + 0   Site/Chamber)”. Bolded models indicate a significant effect at $p < 0.05$ . Note that ND is the reference level in the DIS_ND term. ....	85
Table A.1 Pairwise difference between Treatment levels (reference, R; buffer B; and no buffer NB) for Chapter 2 using Tukey’s HSD <i>post hoc</i> test for the linear mixed effects models explaining the dynamics of carbon dioxide, methane, and nitrous oxide fluxes, respectively. Data includes the influential outliers identified by Cook’s distance. All models included the	

autocorrelation term “AR1(Week + 0 | Site/Chamber)”. Bolded comparison indicates a significant effect at  $p < 0.05$ . ..... 119

Table A.2 Summarized output of linear mixed effects models explaining the effect of groundwater discharge conditions on environmental variables of soil temperature, soil moisture and depth to groundwater table for Chapter 2. All models included an autocorrelation term. Bolded models indicate a significant effect at  $p < 0.05$ . When comparing groundwater discharge (DIS) and non-groundwater discharge (ND) areas, note that ND is the reference level in the DIS\_ND term. .... 120

Table A.3 Pairwise difference between Treatment levels (reference, R; buffer B; and no buffer NB) for soil temperature, soil moisture and depth to the groundwater table using Tukey’s HSD *post hoc* test on the results of linear mixed effects models for Chapter 2. Bolded comparison indicates a significant effect at  $p < 0.05$ . ..... 121

Table A.4 Weekly high and low seven-day maximum and minimum values, respectively, for soil temperature (°C), soil moisture (volumetric water content, %), and depth to the groundwater table (cm) across groundwater discharge (DIS) and non-groundwater discharge (ND) areas in the riparian zone of Mike Ck. and Upper East Ck. in Malcolm Knapp Research Forest for Chapter 3. The date represents the Monday of the week for which the data are averaged. Data are from May 2019 to May 2020, except soil temperature, which only goes to November 2019. .... 123

Table A.5 Summarized output of linear mixed effects model exploring the spatial dynamics of soil temperature, soil moisture, and depth to groundwater for Chapter 3. All models included the autocorrelation term “AR1(Week + 0 | Site/Chamber)”. Note that ND is the reference level in the DIS\_ND term. .... 124

## List of Figures

Figure 1.1 Illustration of study treatments. From left to right: Reference (R), Buffer (B), and No buffer (NB) (n = 3 for each treatment).....	15
Figure 1.2 Conceptual illustration of hypotheses of the effects of forest harvest practices on greenhouse gas emissions from riparian soils. A represents H1: Water table hypothesis, B represents H2: Soil temperature hypothesis, and C represents H3: Disturbance hypothesis. The direction of the arrow indicated an increase (up) or decrease (down) with respect to reference conditions. (Note that predictions are the same for the buffer and no buffer treatments in A, and the buffer treatment is not expected to differ from the reference treatment in B and C).....	16
Figure 2.1 Map of study sites alongside headwater streams at Malcolm Knapp Research Forest, British Columbia.....	29
Figure 2.2 Representative site photos of reference, buffer, and no buffer treatments. Photos taken by Arlo Bryn-Thorn at Upper East, K34B, and E20NB (top to bottom).....	30
Figure 2.3 Conceptual illustration (left) and photo (right) of static chamber used to measure greenhouse gas exchange in riparian soils.....	31
Figure 2.4 Schematic of study design replicated alongside nine headwater streams in Malcolm Knapp Research Forest, British Columbia. Each site had six static chambers to measure greenhouse gas fluxes and six wells to measure the depth to the groundwater table. These experimental units were stratified in groundwater discharge zones (n = 3) and non-groundwater discharge zones (n = 3). The reach length was on average 56 m. ....	32
Figure 2.5 Mean daily air temperature in the riparian zone of headwater streams across reference (R, n = 3), buffer (B, n = 3), and no buffer (NB, n = 3) treatments from June to October 2019. .	38

Figure 2.6 Maximum daily air temperature in the riparian zone of headwater streams across reference (R, n = 3), buffer (B, n = 3), and no buffer (NB, n = 3) treatments from June to October 2019.....39

Figure 2.7 Mean daily soil temperature ~10 cm below the soil surface in the riparian zone of headwater streams in the Pacific coastal rainforest of British Columbia across reference (R, n = 3), buffer (B, n = 3), and no buffer (NB, n = 3) treatments from June to October 2019. ....40

Figure 2.8 Seven-day running maximum soil temperature measured ~ 10 cm below the soil surface in the riparian zone of nine headwater streams in the Pacific coastal rainforest of British Columbia, averaged across three sites per treatment (R, Reference; B, Buffer; NB, No Buffer) from June to October 2019. ....41

Figure 2.9 Mean soil moisture in the riparian zone of headwater streams in the Pacific coastal rainforest of British Columbia across reference (R, n = 3), buffer (B, n = 3), and no buffer (NB, n = 3) treatments as well as in groundwater discharge (DIS) areas and in non-groundwater discharge (ND) areas from June to October 2019. Boxplots display the median, 25<sup>th</sup> and 75<sup>th</sup> percentiles, whiskers (1.5 times the IQR), and individual outliers (dots), for this and all subsequent boxplots. ....42

Figure 2.10 Mean depth to the groundwater table (cm) in the riparian zone of headwater streams in the Pacific coastal rainforest of British Columbia across reference (R, n = 3), buffer (B, n = 3), and no buffer (NB, n = 3) treatments as well as in groundwater discharge areas (DIS) and in non-groundwater discharge areas (ND) from June to October 2019. ....43

Figure 2.11 Riparian forest soil carbon dioxide emission rates from reference (R; n = 3), buffer (B; n = 3), and no buffer (NB; n = 3) treatments, in panel A, and from groundwater discharge

(DIS) and non-groundwater discharge (ND) areas, in panel B, alongside headwater streams in the Pacific coastal temperate rainforest of British Columbia in 2019 (June - October).....44

Figure 2.12 Riparian forest soil carbon dioxide emission rates from reference (R; n = 3), buffer (B; n = 3), and no buffer (NB; n = 3) treatments alongside headwater streams in the Pacific coastal temperate rainforest of British Columbia across five sampling periods from June to October, 2019.....45

Figure 2.13 Relationships between carbon dioxide gas fluxes and the environmental variables of daily mean soil temperature, mean soil moisture, and depth to groundwater table, by treatment. Trend lines are based on LME models accounting for autocorrelation in the relationship between the two variables for reference (R, in green), buffer (B, in blue), and no buffer (NB, in red) treatments. ....46

Figure 2.14 Riparian forest soil methane flux rates from reference (R; n = 3), buffer (B; n = 3), and no buffer (NB; n = 3) treatments, in panel A, and from groundwater discharge (DIS) and non-groundwater discharge (ND) areas, in panel B, alongside headwater streams in the Pacific coastal temperate rainforest of British Columbia in 2019 (June - September). ....47

Figure 2.15 Riparian forest soil methane flux rates from reference (R; n = 3), buffer (B; n = 3), and no buffer (NB; n = 3) treatments alongside headwater streams in the Pacific coastal temperate rainforest of British Columbia across five sampling periods from June to September 2019.....48

Figure 2.16 Relationships between methane gas fluxes and the environmental variables of daily mean soil temperature, mean soil moisture, and depth to groundwater table, by treatment. Trend lines are based on LME models accounting for autocorrelation in the relationship between the two variables for reference (R), buffer (B), and no buffer (NB) treatments. ....49

Figure 2.17 Riparian forest soil nitrous oxide flux rates from reference (R; n = 3), buffer (B; n = 3), and no buffer (NB; n = 3) treatments, in panel A, and from groundwater discharge (DIS) and non-groundwater discharge (ND) areas, in panel B, alongside headwater streams in the Pacific coastal temperate rainforest of British Columbia in 2019 (June - September). .....50

Figure 2.18 Riparian forest soil nitrous oxide flux rates from reference (R; n = 3), buffer (B; n = 3), and no buffer (NB; n = 3) treatments alongside headwater streams in the Pacific coastal temperate rainforest of British Columbia across five sampling periods from June to September 2019.....51

Figure 2.19 Relationships between nitrous oxide gas fluxes and the environmental variables of daily mean soil temperature, mean soil moisture, and depth to groundwater table, by treatment. Trend lines are based on LME models accounting for autocorrelation in the relationship between the two variables for reference (R), buffer (B), and no buffer (NB) treatments. Grey bands represent 95% confidence intervals of the relations. ....52

Figure 3.1 Mean daily soil temperature measured ~10 cm below the soil surface in the riparian zone of two headwater streams in groundwater discharge (DIS, in blue) and non-groundwater discharge (ND, in red) conditions from June 2019 to November 2019. See Figure A.1 in Appendix B for mean soil temperature by site for the entire study period. ....76

Figure 3.2 Mean volumetric soil water content (%) in groundwater discharge (DIS) and non-groundwater discharge (ND) areas of riparian soils alongside along two headwater streams in southwestern British Columbia from May 2019 to May 2020. Lines connecting the points are for visual effect only and are not meant to indicate continuous measurements.....77

Figure 3.3 Mean depth to the groundwater table (cm) in groundwater discharge (DIS) and non-groundwater discharge (ND) areas of riparian soils alongside along two headwater streams in

southwestern British Columbia from May 2019 to May 2020. Lines connecting the points are for visual effect only and are not meant to indicate continuous measurements.....78

Figure 3.4 Riparian forest soil carbon dioxide emission rates ( $\text{mg CO}_2\text{-C m}^{-2} \text{ h}^{-1}$ ) from groundwater discharge (DIS) and non-groundwater discharge (ND) areas of forested riparian areas alongside two headwater streams in the Pacific coastal temperate rainforest of British Columbia from May 2019 to May 2020. Boxplots display the median, 25<sup>th</sup> and 75<sup>th</sup> percentiles, whiskers (1.5 times the IQR), and individual outliers (dots), for this and all subsequent boxplots. ....79

Figure 3.5 Riparian forest soil methane emission rates ( $\mu\text{g CH}_4\text{-C m}^{-2} \text{ h}^{-1}$ ) from groundwater discharge (DIS) and non-groundwater discharge (ND) areas of forested riparian zones alongside two headwater streams in the Pacific coastal temperate rainforest of British Columbia from May 2019 to May 2020. ....80

Figure 3.6 Riparian forest soil nitrous oxide emission rates ( $\mu\text{g N}_2\text{O-N m}^{-2} \text{ h}^{-1}$ ) from groundwater discharge (DIS) and non-groundwater discharge (ND) areas of forested riparian zones alongside two headwater streams in the Pacific coastal temperate rainforest of British Columbia from May 2019 to May 2020. ....81

Figure 3.7 Relationships between carbon dioxide gas fluxes and the environmental variables of daily mean soil temperature, mean soil moisture, and depth to groundwater table, by site. Trend lines are based on LME models accounting for autocorrelation in the relationship between the two variables for Mike Ck. and Upper East Ck.....82

Figure 3.8 Relationships between methane gas fluxes and the environmental variables of daily mean soil temperature, mean soil moisture, and depth to groundwater table, by site. Trend lines

are based on LME models accounting for autocorrelation in the relationship between the two variables for Mike Ck. and Upper East Ck.....83

Figure 3.9 Relationships between nitrous oxide gas fluxes and the environmental variables of daily mean soil temperature, mean soil moisture, and depth to groundwater table, by site. Trend lines are based on LME models accounting for autocorrelation in the relationship between the two variables for Mike Ck. and Upper East Ck.....84

Figure A.1 Mean daily soil temperature measured ~10 cm below the soil surface in the riparian zone of two headwater streams (Mike Ck. and Upper East Ck.) from June 2019 to May 2020. 122

## List of Abbreviations

B: Buffer

BC: British Columbia

CO<sub>2</sub>: Carbon dioxide

CH<sub>4</sub>: Methane

DEM: Digital elevation model

DIS: Groundwater discharge

GHGs: Greenhouse gases

GW: Groundwater

LME: Linear mixed effects

NA: Not applicable

ND: Non-groundwater discharge

NB: No buffer

N<sub>2</sub>: Nitrogen gas

N<sub>2</sub>O: Nitrous oxide

PVC: Polyvinyl chloride

Q-Q: Quantile-quantile

R: Reference

*SD*: Standard deviation

Tukey's HSD: Tukey's honest significant difference

USA: United States of America

## **Acknowledgements**

Firstly, I would like to thank my supervisor, John Richardson, for being a wonderful mentor. I am grateful for his support and guidance throughout my Master's. I would also like to thank my committee members, Mary O'Connor and Sean Smukler, for their insightful and helpful feedback on my thesis.

For field and laboratory assistance, I would like to thank Olivia Hester, as well as the countless others who helped me in the field. Additional thanks to Ionut Aron and the staff at Malcolm Knapp Research Forest for your assistance.

For my funding, I thank my supervisor, the Natural Sciences and Engineering Research Council (NSERC), and the Faculty of Forestry.

Last, but certainly not least, I am ever grateful for the support of my family, my boyfriend, my friends, and my lab mates.

## Chapter 1: Introduction

The cycling of materials is a critical ecosystem process. Human-mediated changes in these biogeochemical cycles can fundamentally alter ecosystem functioning (Chapin, Matson, Vitousek, & Chapin, 2011). Understanding the controls on the rates of these fluxes is important for understanding how they contribute to global change and for predicting how they may be altered by it (Chapin et al., 2011). Greenhouse gases (GHGs; namely carbon dioxide, methane, and nitrous oxide) are critical for life on earth; however, human activities have caused an unprecedented increase of GHG concentrations in the atmosphere, leading to climate change (Serrano-Silva, Sarria-Guzmán, Dendooven, & Luna-Guido, 2014).

Soils play an important role in climate change, as the Earth's soils contain three times more carbon than the atmosphere (Lal, 2004). Depending on the conditions, soils can be a source of GHGs to the atmosphere or they can be a sink of carbon and nutrients (Oertel, Matschullat, Zurba, Zimmermann, & Erasmi, 2016). Therefore, increasing stocks of carbon in the soil and reducing emissions of GHGs to the atmosphere are crucial climate change mitigation strategies (Derrien et al., 2016).

Human-caused disturbance can influence the status of the soil as a source or sink of GHGs. Disturbances are often associated with nutrient losses from an ecosystem (Walley, Van Kessel, & Pennock, 1996). For example, removing vegetation can alter soil ecosystem functions because vegetation plays an important role in regulating biogeochemical cycles (Likens, Bormann, Johnson, Fisher, & Pierce, 1970). Forest harvest can alter biogeochemical processes in soils by

altering plant uptake, soil temperature, water fluxes, and soil microbial activity (Kreutzweiser, Hazlett, & Gunn, 2008). However, biogeochemical responses to logging are highly variable and site specific due to variability in local abiotic and biotic conditions (Kreutzweiser et al., 2008). Therefore, region-specific empirical studies are needed to explain these responses and to advance forest management guidelines for sustaining forest soil productivity, limiting nutrient losses, and mitigating climate change (Kreutzweiser et al., 2008).

### **1.1 Greenhouse gases**

Greenhouse gases can be characterized by their presence in the Earth's atmosphere and their ability to absorb terrestrial infrared radiation, trapping heat in the atmosphere (National Research Council, 2001). Greenhouse gases are critical for life on earth by maintaining liveable temperatures (Solomon, Manning, Marquis, & Qin, 2007). The sun controls the Earth's climate by radiating energy in the form of shortwave radiation (Solomon et al., 2007). Some of that energy is absorbed by the earth's surface and warms it; some of that heat radiates from Earth in the form of longwave radiation and passes back through the atmosphere; and some of that energy is trapped by GHGs in the atmosphere (Solomon et al., 2007). This is the greenhouse effect, which human activities have intensified through the burning of fossil fuels and land-use change, causing increased global temperatures leading to climate change (Serrano-Silva et al., 2014; Solomon et al., 2007). In my research, I focused on three important GHGs that are produced in soils: carbon dioxide (CO<sub>2</sub>), methane (CH<sub>4</sub>), and nitrous oxide (N<sub>2</sub>O). Each gas has its distinct mechanisms of production, primarily produced by living organisms in the soil, which are influenced dissimilarly by various abiotic and biotic factors.

Most natural ecosystems are a net sink of CO<sub>2</sub>, since plants fix carbon during photosynthesis, and this carbon is added to the soil as the plants are consumed and decomposed (Dalal & Allen, 2008). Carbon is lost to the atmosphere in the form of CO<sub>2</sub>, which is produced as a by-product of metabolism that yields energy or carbon intermediates needed for maintenance, growth, or reproduction of organisms (Luo & Zhou, 2006). Soil respiration, or the release of CO<sub>2</sub> from the soil, consists of the combined emissions from root respiration (autotrophic respiration) as well as microbial and faunal breakdown of organic matter in the soil (heterotrophic respiration) (Luo & Zhou, 2006). Soil respiration generally accounts for about 70% of total ecosystem respiration, while aboveground respiration (e.g. from leaves and branches) accounts for the rest (Luo & Zhou, 2006). The processes contributing to soil respiration are mainly affected by soil temperature, soil moisture, and substrate availability (Luo & Zhou, 2006). Typically, soil respiration increases with soil temperature until a maximum, and then declines (Luo & Zhou, 2006). The temperature sensitivity of soil respiration is often expressed as the Q<sub>10</sub> coefficient, or the factor by which the rate of a chemical or biological process increases for every 10°C increase in temperature (Meyer, Welp, & Amelung, 2018). The interactive effect of temperature and soil moisture on soil respiration is quite variable (Meyer et al., 2018). The interactive effects of these and additional environmental factors on soil respiration are complex and poorly understood (Luo & Zhou, 2006).

Methane has a global warming potential about 20 times stronger than that of CO<sub>2</sub> over a 100-year horizon (Conrad, 2007). Global warming potential is the time-integrated radiative forcing of a GHG in the atmosphere, relative to CO<sub>2</sub> (Boucher, Friedlingstein, Collins, & Shine, 2009).

Temperate forest soils are typically well-aerated and act as CH<sub>4</sub> sinks (Frey, Niklaus, Kremer,

Luscher, & Zimmermann, 2011), while wetlands are considered CH<sub>4</sub> sources (Dalal & Allen, 2008). When soil conditions such as waterlogging and compaction restrict soil aeration, the likelihood of CH<sub>4</sub> emission, rather than uptake, increases (Frey et al., 2011). Methane is produced by the breakdown of organic compounds by methanogenic Archaea under anaerobic conditions (Frey et al., 2011; Oertel et al., 2016). Methane is consumed and oxidized by methanotrophic Bacteria under aerobic conditions (Conrad, 2007; Oertel et al., 2016). As such, CH<sub>4</sub> emissions are favoured in oxygen-poor environments where soil moisture content is high (Oertel et al., 2016). Methane oxidation and production is related to the presence, diversity, and abundance of these methanotrophic and methanogenic communities (Christiansen, Levy-Booth, Prescott, & Grayston, 2016). Environmental factors such as soil temperature, soil pH, and substrate availability impact CH<sub>4</sub> emission rates by influencing microbial community abundance and activity (Serrano-Silva et al., 2014). Forest harvest has been shown to reduce CH<sub>4</sub>-oxidation, and even turn soils into a CH<sub>4</sub> source, due to compaction and reduced evapotranspiration, which promote waterlogging and anaerobic conditions (Christiansen, Levy-Booth, Prescott, & Grayston, 2017).

Nitrous oxide is a potent GHG, with a global warming potential 298 times higher than CO<sub>2</sub> over a 100-year horizon (Lavoie, Kellman, & Risk, 2013). Temperate and tropical forest soils are typically sources of N<sub>2</sub>O to the atmosphere (Dalal & Allen, 2008). Nitrogen is often the limiting nutrient in temperate forests (Blevins, Prescott, & Van Nijenhuis, 2006) due to tightly coupled nitrogen-cycling consumptive and productive processes with limited losses (Kreutzweiser et al., 2008; Walley et al., 1996). Forest litter is decomposed to release organic nitrogen, which is subsequently mineralized by microbial activity to inorganic nitrogen (Kreutzweiser et al., 2008).

Inorganic nitrogen can be transformed by microbes into  $N_2O$  and nitrogen gas ( $N_2$ ), and lost to the atmosphere (Kreutzweiser et al., 2008). Nitrous oxide is mainly produced by denitrification under anaerobic conditions, in addition to nitrification under aerobic conditions (Oertel et al., 2016). Nitrogen deposition and fertilization, soil temperature, soil moisture, and soil pH are among the factors that have been shown to influence  $N_2O$  emissions (Dalal & Allen, 2008).

## **1.2 Riparian zones and forestry**

The study system for my research, the riparian zones of headwater streams in southwestern British Columbia, was chosen for its ecological importance, unique conditions, and vulnerability to forest harvest. Riparian zones, that is, the three dimensional zones of direct interaction between terrestrial and aquatic ecosystems (Gregory, Swanson, McKee, & Cummins, 1991), are important for nutrient cycling (Hinshaw & Dahlgren, 2016), biodiversity (Ramey & Richardson, 2017), carbon sequestration (Hazlett, Gordon, Sibley, & Buttle, 2005), and reducing erosion among other benefits (Dosskey et al., 2010). As a result of moist conditions, riparian zones can sequester more carbon than upland forests (Gundersen et al., 2010). On the other hand, due to their shallow water tables and high soil organic matter content, riparian zones have the potential to contribute significant amounts of anaerobically produced  $CH_4$  and  $N_2O$  to the atmosphere (Vidon, Welsh, & Hassanzadeh, 2018).

Headwater streams are ecologically significant tributaries at the most upstream reaches of a stream network. These small streams have an important role in influencing downstream water quality as well as providing refuge for species from larger, impaired water bodies (Biggs, Von Fumetti, & Kelly-Quinn, 2017). The precise definition of a headwater stream is difficult to

determine, with some researchers using catchment size, stream width, mean annual discharge and/or stream order in their definition (Richardson & Danehy, 2007). Headwater streams may constitute up to 80% of stream length in a given drainage network and their riparian zones are particularly vulnerable to forest harvest (Richardson & Danehy, 2007; Richardson, 2019). For example, in British Columbia, fishless streams under 3 m in average channel width are afforded the least amount of protection, with retention of trees long the stream not required, when compared to wider and/or fish-bearing streams (British Columbia Forest Service, 1995).

The Pacific coastal temperate rainforest of British Columbia is one of the most productive terrestrial biomes in the Northern hemisphere (Christiansen et al., 2017). As such, forestry has been, and is still, a dominant industry throughout the biome, with the province of British Columbia producing the largest volume of timber annually in Canada (Basiliko, Khan, Prescott, Roy, & Grayston, 2009; Natural Resources Canada [NRCAN], 2018). The rate of forest harvest in Canada was 766,659 hectares per year in 2016 (NRCAN, 2018). Forest loss negatively influences biodiversity, soil, air and water quality, as well as wildlife habitat (NRCAN, 2018). Under the United Nations Framework Convention on Climate Change, Canada is obligated to annually report on GHG emissions from managed forests (NRCAN, 2018). However, given the lack of knowledge about riparian forest soil GHG emissions, they are not explicitly considered in forestry GHG estimates, despite the unique conditions in riparian zones with high potential for gas emissions after forest harvest. Forest harvest can have dramatic impacts on the biogeochemical processes in soils that control GHG fluxes by changing forest composition, soil temperature and moisture regimes, soil microbial activity, and water fluxes (Kreutzweiser et al., 2008). Therefore, it is important to improve our understanding about how forest harvest influences soil GHG fluxes in riparian soils in southwestern British Columbia.

The most common method of protecting streams and riparian areas from the negative impacts of forest harvest is the use of riparian buffer zones (Richardson & Danehy, 2007). A riparian buffer consists of a strip of trees adjacent to the stream that is either left uncut or has some limited harvesting of trees (Richardson & Danehy, 2007). Studies have shown that riparian buffers are effective in reducing the impacts of forest harvest by intercepting sediments, maintaining bank stability and organic matter inputs, providing shading, and moderating temperature (Richardson, Naiman, & Bisson, 2012). Nevertheless, riparian buffers remain a controversial issue, in headwater systems in particular, due to the large volume of timber that buffers potentially remove from commercial use (Richardson & Danehy, 2007). Additionally, there is no consensus as to the ideal width of a riparian buffer zone, with vastly different rules and regulations across different jurisdictions (Richardson et al., 2012). Moreover, the common practice of using fixed-width buffers is neither economically nor ecologically optimal as it ignores small-scale heterogeneity in the riparian zone (Kuglerová, Ågren, Jansson, & Laudon, 2014). In sum, riparian buffer zones protect some streams and riparian areas from forest harvest, although headwater streams are often unprotected.

### **1.3 Review of literature on greenhouse gas fluxes in riparian zones and how they are impacted by forestry**

No one has yet examined the convergence of how maintaining buffers contrasts with clear-cutting riparian forests around headwater streams to influence rates of GHG fluxes in a forest management context. Several studies have evaluated GHG fluxes from soils of riparian ecosystems (De Carlo, Oelbermann, & Gordon, 2019; Goodrick, Connor, Bird, & Nelson, 2016; Soosaar et al., 2011). However, very few of these studies examine forested riparian zones of

streams (De Carlo et al., 2019); most of the research has been conducted in wetlands (Audet, Elsgaard, Kjaergaard, Larsen, & Hoffmann, 2013; Nag, Liu, & Lal, 2017) or in agricultural contexts (Skinner et al., 2014; Tufekcioglu, Raich, Isenhardt, & Schultz, 2001).

Studies about riparian GHG fluxes have found that soil temperature and soil moisture are two of the most important predictors of flux rates. In particular, the position of the groundwater table is often correlated with flux rates. Carbon dioxide emission rates from tropical riparian rainforest soils were significantly related to soil temperature, soil water content and depth to the water table (Goodrick et al., 2016). Additionally, higher groundwater table levels were found to significantly increase CH<sub>4</sub> emissions, and decreased CO<sub>2</sub> and N<sub>2</sub>O emissions (Soosaar et al., 2011). Riparian forest soil N<sub>2</sub>O emissions alongside a creek in southern Ontario, Canada were influenced by soil characteristics and seasonality, rather than vegetation or spatial position (De Carlo et al., 2019). An experimental manipulation of groundwater table levels in a riparian grey alder stand in Estonia found that flooding significantly increased CH<sub>4</sub> emissions and decreased both CO<sub>2</sub> emissions and N<sub>2</sub>O emissions from the soil (Mander et al., 2015). Not necessarily riparian, but wet forest soils in Denmark doubled the global warming potential from N<sub>2</sub>O and CH<sub>4</sub> emissions when they were accounted for in the catchment (Christiansen, Vesterdal, & Gundersen, 2012). Higher N<sub>2</sub>O emissions were also measured from forested wetland soils than from well-drained forest soils in eastern Canada (Ullah, Frasier, King, Picotte-Anderson, & Moore, 2008).

Landscape features that dictate soil characteristics, such as microtopography and hydrogeomorphic settings, have been found to be important for predicting riparian GHG emissions. Landscape topography can affect the spatial distribution of soil moisture, nutrients,

and organic matter, and consequently the intensity of GHG emissions (Jacinthe & Vidon, 2017). A study comparing greenhouse gas fluxes from two Estonian riparian alder forests found that local microtopographical differences were sometimes greater than those between sites of different ages with varying land-use histories (Soosaar et al., 2011). Hydrogeomorphic setting was important for predicting CH<sub>4</sub> fluxes in a riparian forest in central Indiana, where a topographic depression in a riparian forest accounted for 78% of annual CH<sub>4</sub> emissions, despite only covering <8% of the total land area (Jacinthe, Vidon, Fisher, Liu, & Baker, 2015). Hydrogeomorphic setting was found to be a strong predictor of GHG emissions in riparian zones across the mainstem and tributaries of the White River in Indiana, USA (Jacinthe & Vidon, 2017). They found that the till plain depressions near headwater streams emitted CO<sub>2</sub> at rates 1.6 times higher than other stream sites (incised narrow valleys and broad floodplains), likely due to higher soil carbon quantity, illustrating one of the many possible differences between riparian hydrogeomorphic settings (Jacinthe & Vidon, 2017).

In terms of seasonal trends, riparian GHG fluxes have been found to vary seasonally, with highest fluxes in wetter seasons and/or warmer seasons. The rate of N<sub>2</sub>O flux was higher in the wet season than in the dry season in a tropical riparian ecosystem in northern Thailand (Kachenchart, Jones, Gajasen, Edwards-Jones, & Limsakul, 2012). Variations in N<sub>2</sub>O emission rates were strongly correlated with microbial biomass carbon, denitrification, and water-filled pore space (Kachenchart et al., 2012). Soil respiration rates were significantly different among seasons, and significantly correlated with soil moisture and soil temperature at rehabilitated and undisturbed riparian zones along Washington Creek in southern Ontario, Canada (Oelbermann & Raimbault, 2015). The body of scientific literature on GHG emissions from riparian soils shows

us that soil characteristics, groundwater table levels, landscape setting and seasonality are key controllers of GHG production. Nevertheless, to date, none of these riparian studies have considered the impacts of forest harvest.

There have been several studies evaluating the effects of clear-cutting on GHG fluxes from forest soils (Kähkönen, Wittmann, Ilvesniemi, Westman, & Salkinoja-Salonen, 2002; Lavoie et al., 2013; Ullah, Frasier, Pelletier, & Moore, 2009). Clear-cutting can increase CH<sub>4</sub> efflux due to greater soil moisture and temperature (Wu et al., 2011), increase N<sub>2</sub>O emissions due to increased nitrogen availability (Takakai et al., 2008), and have inconsistent effects on CO<sub>2</sub> emission rates (Striegl & Wickland, 1998; Ullah, Frasier, Pelletier, & Moore, 2009).

Forest harvest may turn soils into a CH<sub>4</sub> source, due to compaction and reduced evapotranspiration, which promote waterlogging and anaerobic conditions (Christiansen et al., 2017). Clear-cutting was found to turn a temperate spruce forest in southern Germany into less of a sink for CH<sub>4</sub>, likely due to increased soil temperature and moisture (Wu et al., 2011). A similar trend was seen in spruce forest soils in Finland, where clear-cutting turned the stand from sink to source of CH<sub>4</sub> through a 40% decrease in CH<sub>4</sub> consumption rates (Kähkönen et al., 2002). Clear-cutting of an alder wetland in Québec, Canada also resulted in creating a strong CH<sub>4</sub> source, with 131 times greater CH<sub>4</sub> emissions than in undisturbed soils (Ullah et al., 2009). This increase in CH<sub>4</sub> production was attributed to higher average summer soil temperatures, volumetric water content, and dissolved organic carbon concentrations in the clear-cut wetland (Ullah et al., 2009). Clear-cutting appears to have inconsistent effects on soil respiration, with some studies reporting a decline (Striegl & Wickland, 1998), an increase (Paul-Limoges, Black, Christen, Nesic, &

Jassal, 2015), or no change (Kähkönen et al., 2002) in emissions following harvest. Soil CO<sub>2</sub> emissions declined following the clear-cutting of a jack pine stand in Saskatchewan (Striegl & Wickland, 1998). This reduction was attributed to the disruption of the soil surface and death of tree roots (Striegl & Wickland, 1998). Soil respiration rates were higher in clear-cut Chinese fir and evergreen broadleaved forest plots than control plots in the first three to four months after treatment in mid-tropical China (Guo et al., 2010). However, for the subsequent two years the soil respiration in the clear-cut plots fell below the control plots (Guo et al., 2010). In contrast, forest harvest changed a former forest carbon sink into a net source due to reduced photosynthetic uptake and increased ecosystem respiration in the first year after harvesting a Douglas-fir stand on Vancouver Island, British Columbia (Paul-Limoges et al., 2015). The authors speculated that the significant reduction in autotrophic respiration due to loss of respiring roots was compensated for by an increase in heterotrophic respiration (Paul-Limoges et al., 2015). Conversely, cumulative annual soil respiration did not change after clear-cutting a mature Norway spruce forest in Finland, despite an increase in soil temperatures (Kähkönen et al., 2002). However, this was attributed to a potential methodological error of not including logging residues in the measurement chambers.

Forest harvest can increase soil moisture and mobilize soil nitrogen, promoting N<sub>2</sub>O losses from logged forest sites (Kreutzweiser et al., 2008). Nitrous oxide emissions were 2.7 times higher in clear-cut than in mature black spruce forest soil in Québec, Canada (Ullah et al., 2009). Slightly higher N<sub>2</sub>O fluxes were also observed following forest harvest in the taiga region of eastern Siberia, Russia (Takakai et al., 2008). This increase was attributed to greater soil moisture following harvest (Takakai et al., 2008). Conversely, no increase in N<sub>2</sub>O emissions was

measured after thinning a boreal forest stand in Germany (Dannenmann, Gasche, & Papen, 2007). A study of subsurface N<sub>2</sub>O concentrations in northeastern Nova Scotia, Canada found that there was greater production of N<sub>2</sub>O following forest harvest (Kellman & Kavanaugh, 2008). However, this did not translate into positive surface fluxes due to consumption of N<sub>2</sub>O during vertical transport through the soil profile (Kellman & Kavanaugh, 2008).

Although some trends in GHG fluxes following clear-cutting are relatively consistent (e.g. increased CH<sub>4</sub> emissions), others are quite variable (e.g. CO<sub>2</sub> emissions). What is more, although a few studies examined GHG responses to forest harvest in moist soils (e.g. alder wetland in Ullah et al., 2009), none of these studies were conducted specifically in a riparian forest context. The unique conditions of riparian ecosystems make them quite distinct from upland forest. Therefore, the results from studies examining the effects of forest harvest on greenhouse gas fluxes on forest soils are not generalizable to riparian forest soils. For instance, riparian zones typically have hydromorphic (wet) soils with high carbon content (Gundersen et al., 2010), shallow and fluctuating water tables (Goodrick et al., 2016), and they can be strongly influenced by groundwater, creating hotspots for plant diversity (Kuglerová, Jansson, Ågren, Laudon, & Malm-Renöfält, 2014). As a result of these and other potential differences, the typical GHG responses to harvest seen in upland forests studies will unlikely be analogous in riparian forests.

#### **1.4 Objectives and hypotheses**

The overarching objective of this study was to evaluate how forestry management practices can alter biogeochemical processes that subsequently affect greenhouse gas fluxes from riparian soils. To address this goal, I had three specific objectives.

My first objective was to quantify the effects of forest harvest practices, specifically contrasting riparian sites that were clear-cut all the way to the stream with or without a riparian buffer zone of trees left standing to relatively undisturbed riparian forests (Figure 1.1), on soil GHG flux rates and to determine the dominant driver(s) of gas fluxes. The competing hypotheses that I tested, illustrated in Figure 1.2, were that: a) forest harvest, regardless of a riparian buffer, reduces transpiration rates, causing an increase in soil moisture due to higher water table levels, creating conditions that will promote greater anaerobically produced CH<sub>4</sub> and N<sub>2</sub>O emissions, and lower aerobically produced CO<sub>2</sub> emissions compared to reference sites (H1: Water table hypothesis); b) forest harvest in the riparian zone without a buffer will reduce shading and increase soil temperatures, stimulating CO<sub>2</sub>, CH<sub>4</sub>, and N<sub>2</sub>O emissions compared to buffer and reference sites (H2: Soil temperature hypothesis); c) forest harvest in the riparian zone without a buffer will disturb soil microbial activity and tree roots, reducing emissions of CO<sub>2</sub>, CH<sub>4</sub>, and N<sub>2</sub>O compared to buffer and reference sites (H3: Disturbance hypothesis). These competing hypotheses were tested by taking measurements of soil gas fluxes and relevant environmental variables from replicate, riparian forest sites that were clear-cut with or without a riparian buffer, or were relatively undisturbed. These environmental variables were chosen as they are consistently identified in the literature as major factors influencing GHG emissions (Dalal & Allen, 2008; Luo & Zhou, 2006; Serrano-Silva et al., 2014). My aim was to determine which, if any, of these factors is the dominant driver influencing any changes in GHG fluxes following forest harvest.

My second objective was to quantify the effects of riparian groundwater conditions on soil GHG rates. I hypothesized that groundwater discharge (DIS) areas, or topographic concavities in the riparian zone, will have higher soil moisture and nutrients from groundwater influence compared to outside of groundwater discharge areas (ND), resulting in greater anaerobically produced CH<sub>4</sub> and N<sub>2</sub>O emissions.

My third objective was to examine the effects of temporal variation on GHG fluxes from riparian soils. I hypothesized that riparian soil GHG fluxes would have significant temporal variation, with peak gas emissions occurring in the warmest and wettest season.

My research will advance our knowledge of spatial and temporal GHG dynamics in riparian soils alongside headwater streams and how they are impacted by forest harvest to inform forestry management practices and more accurate GHG budgets for climate change mitigation.

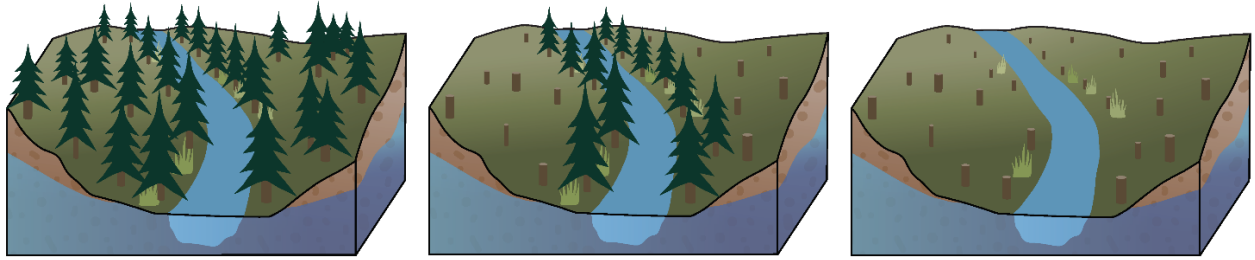


Figure 1.1 Illustration of study treatments. From left to right: Reference (R), Buffer (B), and No buffer (NB) ( $n = 3$  for each treatment).

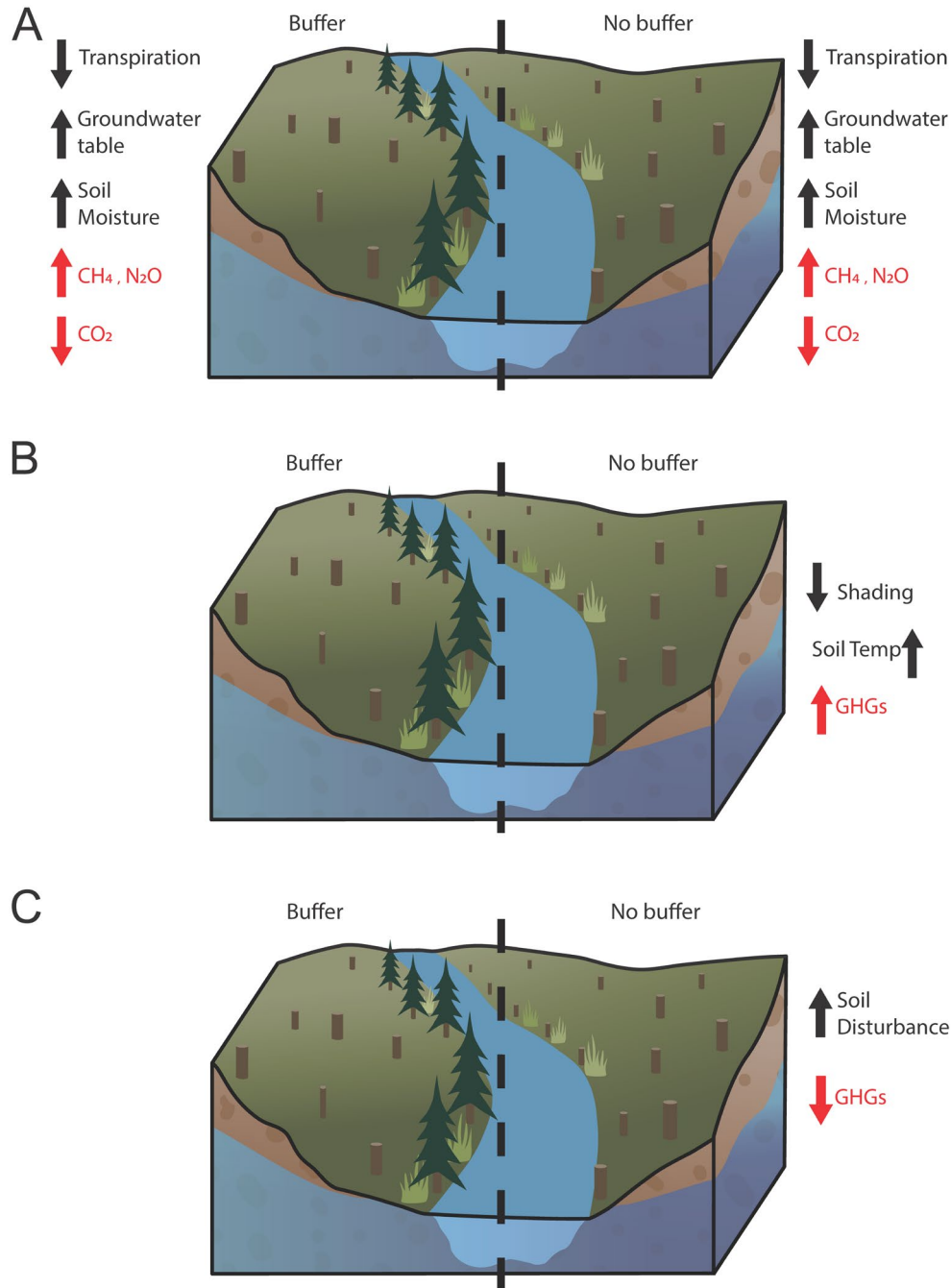


Figure 1.2 Conceptual illustration of hypotheses of the effects of forest harvest practices on greenhouse gas emissions from riparian soils. A represents H1: Water table hypothesis, B represents H2: Soil temperature hypothesis, and C represents H3: Disturbance hypothesis. The direction of the arrow indicated an increase (up) or decrease (down) with respect to reference conditions. (Note that predictions are the same for the buffer and no buffer treatments in A, and the buffer treatment is not expected to differ from the reference treatment in B and C)

## **Chapter 2: Forest management impacts on greenhouse gas fluxes from riparian soils along headwater streams**

### **2.1 Introduction**

Soils play an important role in climate change. Depending on the conditions, soils have the potential to store carbon or to be a source of greenhouse gases (GHGs) to the atmosphere (Oertel et al., 2016). Disturbances, such as forest harvest, can alter biogeochemical processes in soils (Kreutzweiser et al., 2008), subsequently resulting in a change in the GHG emission rates (Lavoie et al., 2013). However, soil ecosystem responses to logging are highly variable and site specific due to micro-site level differences in variables such as soil properties, moisture conditions, and biological interactions (Kreutzweiser et al., 2008). Therefore, the results from the many upland forest studies are likely to differ from other ecosystems, such as riparian zones. Riparian zones are the three dimensional zones of direct interaction between terrestrial and aquatic ecosystems (Gregory et al., 1991). Riparian ecosystem are a priority for management and restoration due to their disproportionately high value and diversity of ecological functions combined with their high level of vulnerability to anthropogenic pressures (Capon & Pettit, 2018). Their unique conditions, including shallow water tables, high soil organic matter content, and high soil nitrogen concentrations, create the potential to contribute significant amounts of anaerobically produced methane and nitrous oxide to the atmosphere (Knoepp & Clinton, 2009; Vidon et al., 2018).

Greenhouse gases are critical for life on earth by maintaining liveable temperatures; however, human activities have intensified the natural greenhouse effect, resulting in climate change (Serrano-Silva et al., 2014; Solomon et al., 2007). This study examines the three important GHGs produced in soils: carbon dioxide (CO<sub>2</sub>), methane (CH<sub>4</sub>), and nitrous oxide (N<sub>2</sub>O). As with many biological processes, soil-atmosphere GHG exchanges are strongly affected by environmental factors.

The production of all three major gases is strongly controlled by soil temperature and soil moisture (Luo & Zhou, 2006). Carbon dioxide emissions consist of the combined emissions from root respiration (autotrophic respiration) and microbial decomposition of organic matter (heterotrophic respiration) (Luo & Zhou, 2006). As such, CO<sub>2</sub> emissions are also affected by substrate availability (Luo & Zhou, 2006). Methane is produced by methanogens in anaerobic conditions, and consumed by methanotrophs in aerobic conditions (Oertel et al., 2016). Besides low-oxygen conditions and soil temperature, the environmental factors of soil pH and substrate availability impact microbial community contributing to CH<sub>4</sub> exchange (Serrano-Silva et al., 2014). Nitrous oxide is mainly produced by denitrification under anaerobic conditions, in addition to nitrification under aerobic conditions (Oertel et al., 2016). Additional important factors influencing these processes are nitrogen deposition and fertilization and soil pH (Dalal & Allen, 2008).

The most common method of protecting streams and riparian areas from the negative impacts of forest harvest is the use of riparian buffer zones, consisting of a strip of trees adjacent to the stream that is either left uncut or has some limited harvesting (Richardson & Danehy, 2007). The

riparian zones of headwater streams are particularly vulnerable to forest harvest. Headwater streams are the ecologically significant, small tributaries at the most upstream ends of a stream network that make up to 80% of stream length in a given drainage network (Richardson, 2019). Although studies have shown that riparian buffers are effective in reducing the impacts of forest harvest by intercepting sediments, maintaining bank stability, and providing shading among other benefits (Richardson et al., 2012); their usage remains contentious in headwater systems, due to the large volume of timber that buffers potentially remove from commercial use (Richardson & Danehy, 2007).

Studies have examined soil-atmosphere exchange of GHGs in riparian ecosystems (De Carlo et al., 2019), and studies have evaluated the effects of clear-cutting on GHG fluxes from forest soils (Kähkönen et al., 2002). Research in riparian zones has found that soil temperature and soil moisture are two of the most important predictors of GHG flux rates. In particular, the position of the groundwater table is often correlated with GHG flux rates. At the same time, clear-cutting has been found to increase soil temperatures (Hashimoto & Suzuki, 2004) and increase the elevation of the groundwater table (Bliss & Comerford, 2002; Hotta et al., 2010). These changes can be attributed to the drastic reduction in leaf area after harvesting, which reduces catchment-wide transpiration rates (Bliss & Comerford, 2002) and allows for an increase in incoming shortwave radiation, warming up the soil (Hashimoto & Suzuki, 2004). Clear-cutting can increase CH<sub>4</sub> emissions due to greater soil moisture and temperature (Wu et al., 2011) and increase N<sub>2</sub>O emissions due to greater soil moisture and increased nitrogen availability as a result of increased rates of nitrogen mineralization and/or reduced competition from roots (Kellman & Kavanaugh, 2008; Takakai et al., 2008). Clear-cutting has inconsistent effects on CO<sub>2</sub> emission

rates, with some studies reporting a decline (Striegl & Wickland, 1998), an increase (Paul-Limoges et al., 2015), or no change (Kähkönen et al., 2002) in emissions following harvest. However, no one has yet examined the convergence of how maintaining buffers contrasts with clear-cutting riparian forests around streams to influence rates of GHG fluxes in a forest management context.

Landscape features that dictate soil characteristics, such as local microtopography, can be important for predicting riparian GHG emissions as they may affect the spatial distribution of soil moisture, nutrients, and organic matter, thus consequently affecting the intensity of GHG emissions (Jacinthe & Vidon, 2017; Soosaar et al., 2011). Local groundwater discharge conditions may create particularly important micro-site variation in the riparian zones of streams. Groundwater discharge (DIS) areas, or discrete riparian inflow points, occur when upland-originating groundwater converges and discharges in a depression in the topography of the riparian zone (Kuglerová et al., 2014b). Soil conditions in DIS areas have been found to have higher base cations, soil moisture, pH levels, and nitrogen concentrations when compared to surrounding soils (Giesler, Högberg, & Högberg, 1998). These conditions can result in hotspots of riparian plant species richness (Kuglerová et al., 2014b). These soil conditions may also influence the processes controlling soil GHG fluxes. For instance, a topographic depression in a riparian forest accounted for 78% of annual CH<sub>4</sub> emissions, despite only covering <8% of the total land area (Jacinthe et al., 2015). Recent evidence suggests that in-stream GHG fluxes peak downstream of DIS areas, likely from lateral gas inputs from riparian soils (Lupon et al., 2019). However, it is also unknown how forest harvest in the riparian zone might influence the conditions in riparian DIS areas, and how GHG fluxes may subsequently be influenced.

In this study, I evaluated how forestry management practices can alter biogeochemical processes that subsequently affect greenhouse gas fluxes from riparian soils. The objectives were: (1) to quantify the effects of forest harvest practices on soil GHG flux rates; (2) to determine which of soil temperature, soil moisture, and/or groundwater level were the dominant driver(s) of gas fluxes; and (3) to determine if local groundwater conditions result in soil conditions that dictate the spatial occurrence of GHG fluxes. I hypothesized that GHG flux rates would be most influenced by soil temperature, soil moisture and/or groundwater level. If my results were in line with H1, the Water Table Hypothesis, I predicted that forest harvest, regardless to what degree, would increase CH<sub>4</sub>, and N<sub>2</sub>O emissions and lower CO<sub>2</sub>, emissions. If my results followed H2, the Soil Temperature Hypothesis, I predicted that GHG emissions would be the greatest at the clear-cut sites compared to the buffer and reference sites. Lastly, if my results were in line with H3, the Disturbance Hypothesis, I predicted that the lowest GHG emissions would be observed at the harvested sites compared to the buffer and reference sites. I further hypothesized that DIS areas will have greater soil moisture and nutrients from groundwater influences, compared to ND areas, resulting in greater anaerobically produced CH<sub>4</sub> and N<sub>2</sub>O emissions.

## **2.2 Methods**

### **2.2.1 Site description**

The study sites for this research were located in the Malcolm Knapp Research Forest (MKRF), at the foothills of the Coast Mountains, about 40 km east of Vancouver, British Columbia (49° 16' N, 122° 34' W) (Figure 2.1). This 5,157 ha forest is managed by the University of British Columbia's Faculty of Forestry as an educational, research, and demonstration facility

(University of British Columbia, 2011). My research sites were located roughly within the southern half of the Forest, below 390 m in elevation (Table 2.1). This portion of the Forest is located in the Coastal Western Hemlock biogeoclimatic zone (Klinka, Chourmouzis, & Varga, 2005). The forest is mostly comprised of approximately 90-year old second growth, naturally regenerated following widespread fire in 1925, and again in 1931 (Klinka et al., 2005). The dominant tree species are Western Hemlock (*Tsuga heterophylla*), Douglas-fir (*Pseudotsuga menziesii*), and Western Red Cedar (*Thuja plicata*) (Klinka et al., 2005).

The climate is maritime, with slight continental influence due to the mountains and inland location (Klinka et al., 2005). The primary climate (Köppen) classification is *Cfb*, temperate oceanic climate (Kottek, Grieser, Beck, Rudolf, & Rubel, 2006). The climate is characterized by mild temperatures, with wet, mild winters, and cool and relatively dry summers (Klinka et al., 2005). Mean annual precipitation and temperature at the Environment Canada climate station located at the Research Forest (Haney UBC RF Admin, station number 1103332) are 2131 mm and 9.7°C, respectively (data for 1962 to 2006).

Glacial till and colluvium are the predominant parent materials in the Forest (Klinka, 1976). In the southern portion of the Forest, surficial deposits include glacio-fluvial and glacio-marine deposits from Pleistocene era glaciation, overlaying compacted till or bedrock (Klinka et al., 2005; Klinka, 1976). The soils formed on these materials are shallow and can be expected to be coarse, acid, and low in basic cations (Klinka et al., 2005). Digging a soil pit at each site revealed that the soils were a Humo-Ferric Podzol at all the sites, except one site (E10B) had soil of the Organic Order (likely a Hydric Mesisol).

### 2.2.2 Study design

This study compared different forest management practices in and near the riparian zone of headwater streams. A total of nine ( $n = 9$ ) headwater streams were chosen as field sites; three sites were not recently logged ( $\sim 90$  year-old stands), representing relatively undisturbed reference conditions (“R”); three sites had a riparian buffer (reserve) zone of trees left standing alongside the stream (“B”); and three sites were clear-cut all the way to the stream without a riparian buffer zone (“NB”) (Figure 2.2). The harvesting system used at the sites was clear-cutting with reserves, and a machine-free zone was maintained around all streams. Furthermore, a ground-based harvest method was used (except at E10 where hoe-forwarding was used), with hand or mechanical felling (I. Aron, personal communication, July 30, 2020).

Field site selection criteria were chosen *a priori* to identify comparable streams and riparian zones (Table 2.1). Using geographic information system (GIS) data provided by MKRF, I identified clear-cut cut-blocks that were harvested no more than five years earlier, in Arcmap 10.6.1 (ESRI, Redlands, CA, USA). The final sites were logged on average  $3.7 \pm 0.82$  (mean  $\pm$  *SD*) years earlier. Ideally the logged sites would have been studied fewer years post-harvest, but there were not enough suitable sites that fit this criteria. The study sites can be defined as headwater systems as all of the streams met Richardson and Danehy’s (2007) criteria for a headwater stream of a mean width  $<3$  m and catchment area  $<100$  ha (much smaller). When possible, the study reaches were not located downstream of any weir or road to reduce confounding effects by these disturbances. The streams all had a slope gradient below  $15^\circ$ , with an overall average stream slope of  $7.6^\circ \pm 4.0$ . The riparian zones at the study reaches had a

gentle slope gradient below 30°, with an average bank slope of  $13.2^\circ \pm 8.4$ . This ensured comparability of groundwater table dynamics between sites, since stream water levels have more control on riparian water table levels when the stream bank slope has a lower gradient (Burt et al., 2002).

### **2.2.3 Soil sampling**

On each gas sampling date, volumetric soil moisture was recorded at each chamber using a ProCheck portable probe (Decagon Devices, Inc., Washington, USA) by using the mean of three readings, each no more than 0.5 m from each chamber. The depth to the water table was also measured on each sampling date by blowing into a thin tube attached to a meter stick lowered into a perforated PVC pipe wrapped in landscape fabric installed at least 40 cm deep into the soil. Over the entire sampling period, continuous soil temperature readings were taken at 1 hr intervals using iButton® dataloggers (DS1992L- Thermochron and DS1923- Hygrochron, Maxim Integrated Products, USA) buried about 10 cm below the soil surface. At each site, two iButtons were buried in a DIS and ND area respectively, and two iButtons were buried 0.5 m and 1.5 m from stream bank-full width, respectively. Air temperature and relative humidity was measured at each site using two HOBO U23 Pro v2 data loggers (Onset Computer Corporation, MA, USA) located 0.5 m and 1.5 m from the stream bank-full width at each study reach. I dug a soil pit at a representative location at each site, within 2 m of the stream bank-full width in a topographic middle-ground (neither on a hummock nor in a hollow). I designated the soil horizons and classified soil colour (Munsell Color, 2010), percentage of coarse fragments, soil texture, root characteristics (Watson, 2009), humus forms (Klinka, Green, Trowbridge, & Lowe, 1981), and the soil type (Canadian Agricultural Services Coordinating Committee, 1998).

#### **2.2.4 Greenhouse gas sampling**

The net terrestrial biosphere-atmospheric exchange of CO<sub>2</sub>, CH<sub>4</sub>, and N<sub>2</sub>O was measured using closed, static chambers (Figure 2.3). Gas samples were collected on approximately a monthly basis from May to September, 2019. At each site, six chambers were placed, on level ground, about 1 to 2 m from the stream bank-full width, in order to capture an area within the zone of influence of the stream (Gregory et al., 1991). Chambers (diameter of 30.5 cm, height of 23 cm) made of grey PVC pipe were permanently inserted about 10 cm below the soil surface at least 10 days (on average 23 days) prior to the first gas sampling to reduce the effects of soil and root disturbances. To facilitate ease of sampling, the length of each stream reach under study (i.e. the distance from the first to the last chamber) was no more than 100 m, and on average  $55.6 \pm 23.2$  m.

At each site, the chambers were stratified according to local groundwater discharge conditions, in groundwater discharge (DIS) and non-groundwater discharge (ND) microsites (Figure 2.4), in order to account for some of the high spatial variability associated with GHG fluxes from soils (Vidon, Marchese, Welsh, & McMillan, 2015). These DIS areas, or discrete riparian inflow points, occur when upland-originating groundwater converges and discharges in a depression in the topography of the riparian zone (Kuglerová et al., 2014b). The DIS areas were identified in Arcmap 10.6.1 using a 1 m digital elevation model (DEM) (MKRF, 2016) and flow accumulation modelling using a channelization threshold of 1 ha. This modelling process assumes that topography and gravity control water movement, and that the groundwater flow path follows the ground surface (Kuglerová et al., 2014b). The DIS areas were then confirmed

with field observations of topography, wetness, and hydrophilic vegetation. Based on the groundwater table level data from the wells installed at each chamber, eight DIS areas were re-classified after the fact in cases where the well was dry for at least 80% of the sampling occasions.

During gas sampling, a PVC lid was placed on top of the chamber and headspace air samples were taken at 0, 15, 30, and 45 minutes after closure. The chamber lids were spray-painted white to prevent heat build-up during measurement. The lids had two rubber septa, one for sampling and one for a thermometer to measure headspace air temperature. Headspace air samples of 20 mL were taken from a rubber septa sampling port in the middle of the lid using a 23 gauge needle and a 50 mL syringe after pumping 20 mL of the headspace gas twice to facilitate mixing. The gas sample was then injected into a pre-evacuated 12 mL exetainer (LabCo Ltd., Lampeter, Wales) until over-pressurized. After gas sampling, air temperature of the headspace was recorded and two ambient air samples were taken for reference.

Sampling was performed between 9:15 and 16:30 h to capture peak fluxes and reduce the effects of diurnal variation (Parkin & Venterea, 2010). Given the difficulty of sampling 54 chambers in one day, three sites were sampled per day over three days, in randomized order within treatment, each month. Gas samples were analysed on a 7890A gas chromatograph (Agilent Technologies Inc., CA, USA) equipped with a flame ionization detector and an electron capture detector, using a PAL auto-sampler (Agilent Technologies Inc., CA, USA). Gas flux rates were calculated by linear regression of gas concentrations over time. This method was chosen because it has been found to be the least sensitive to analytical precision and chamber deployment time, and it tends

to provide high accuracy in statistical comparisons among treatments (Kravchenko & Robertson, 2015; Parkin, Venterea, & Hargreaves, 2012). Each time series was evaluated for goodness of fit by visual inspection (Collier, Ruark, Oates, Jokela, & Dell, 2014). Additional quality control measures included visual inspection for abnormally high and low values outside the range of reported riparian emissions, as well as Cook's Distance statistical test to identify influential outliers (Zuur, Ieno, & Smith, 2007). In sum, these quality control measures resulted in the removal of 11% of flux rate data points for CO<sub>2</sub>, 26% for CH<sub>4</sub>, and 34% for N<sub>2</sub>O. Linear mixed effects models of treatment effect on GHG fluxes were performed on the data with the influential outliers identified by Cook's distance and the abnormal values outside the range of reported riparian emissions included, without a substantial change in the model outcomes, when model convergence was achieved (Table A.1). Using the ideal gas law, the flux rate was converted to μmol, and then the molecular mass was used to translate this value into μg or mg. These equations are described by Collier et al. (2014).

### **2.2.5 Statistical analysis**

For statistical analysis, I used the software *R* 3.6.1 (R Core Team, 2020). I used linear mixed effects (LME) models to evaluate the forest management effects on GHG fluxes using the “glmmTMB” package (Brooks et al., 2017). The models included the autoregressive covariance structure AR(1) to account for temporal autocorrelation and repeated measures (Kravchenko & Robertson, 2015). The model residuals were tested for normality and homogeneity of variance using normal probability (Q-Q) and Residuals vs Fitted diagnostic plots, respectively. When the model residuals violated the assumption of normality, they were transformed and tested again. In the case of models with N<sub>2</sub>O flux rate as the response variable, the flux data was log-

transformed. I used a *post hoc* Tukey's HSD test to compare pairwise differences in treatment levels. For all statistical analyses, significance was accepted at  $p < 0.05$ .

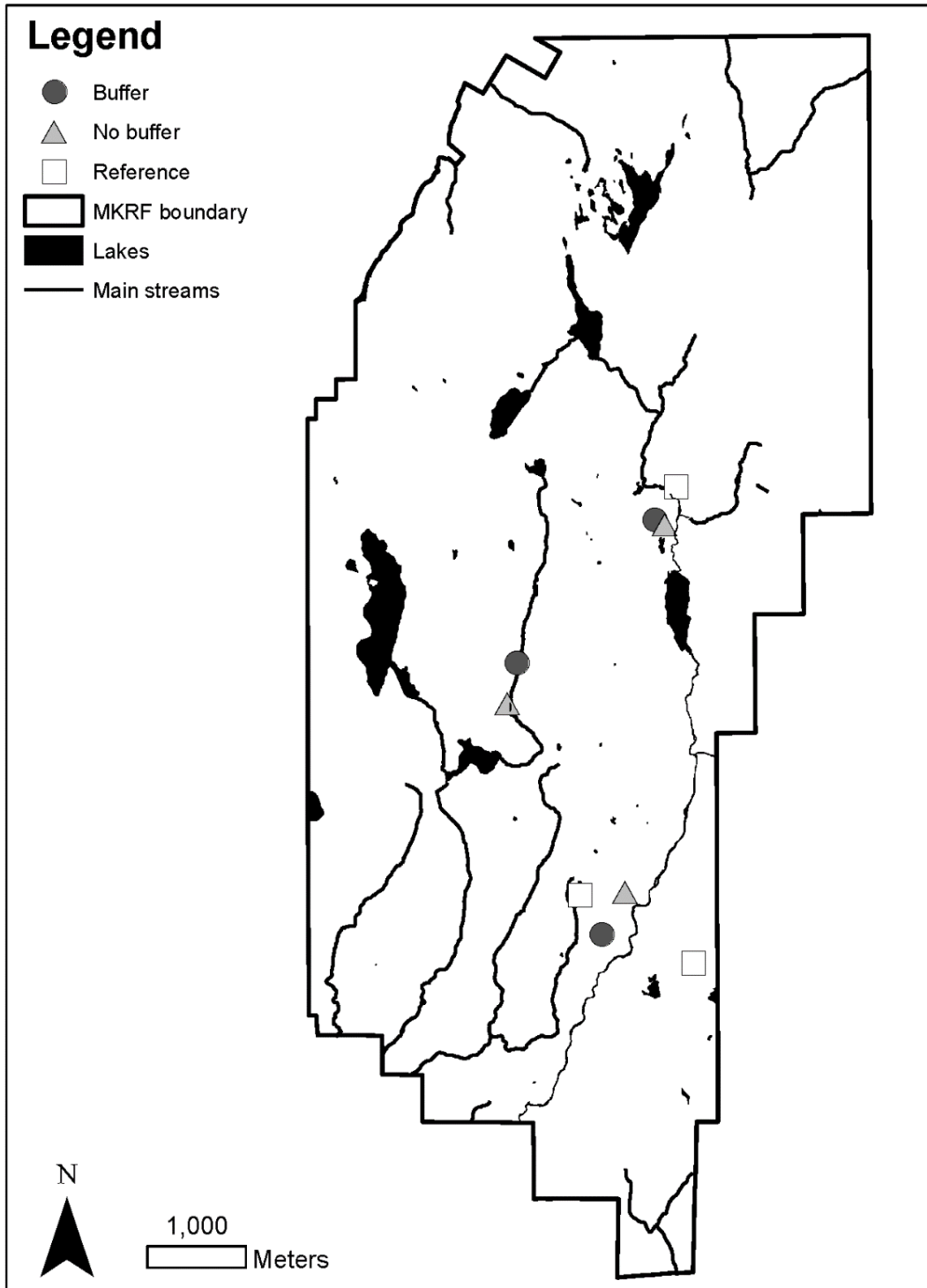


Figure 2.1 Map of study sites alongside headwater streams at Malcolm Knapp Research Forest, British Columbia.



Figure 2.2 Representative site photos of reference, buffer, and no buffer treatments. Photos taken by Arlo Bryn-Thorn at Upper East, K34B, and E20NB (top to bottom).

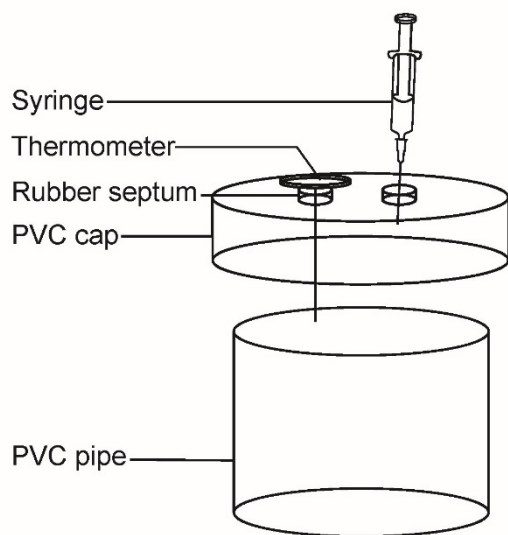


Figure 2.3 Conceptual illustration (left) and photo (right) of static chamber used to measure greenhouse gas exchange in riparian soils.

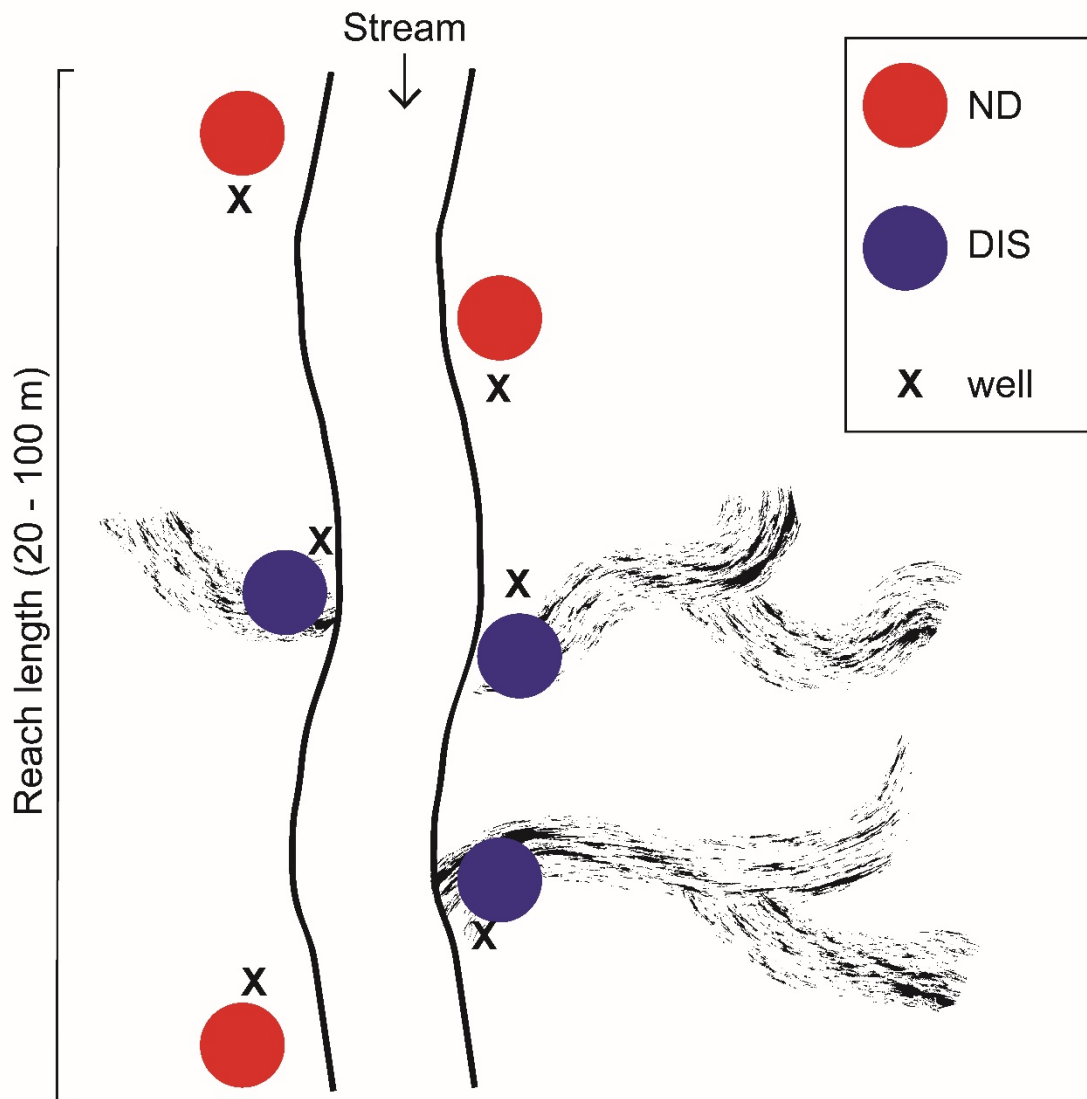


Figure 2.4 Schematic of study design replicated alongside nine headwater streams in Malcolm Knapp Research Forest, British Columbia. Each site had six static chambers to measure greenhouse gas fluxes and six wells to measure the depth to the groundwater table. These experimental units were stratified in groundwater discharge zones ( $n = 3$ ) and non-groundwater discharge zones ( $n = 3$ ). The reach length was on average 56 m.

Table 2.1 Characteristics of riparian study sites alongside headwater streams under differing forestry management conditions in Malcolm Knapp Research Forest, British Columbia.

<b>Treatment</b>	<b>Reference</b>			<b>No Buffer</b>			<b>Buffer</b>			<b>Mean ± SD</b>
Site	Mayfly	Mike	Upper East	E10NB	E20NB	K34NB	E10B	K10B	K34B	
Stream bankfull width (m)	0.88	1.97	4.14	0.72	2.15	1.17	1.91	1.38	1.32	1.74 ± 1.03
Catchment area (ha)	5.4	39.4	37.0	3.4	13.9	2.6	6.3	23.4	3.3	8.8 ± 8.3
Riparian class	NA	NA	NA	S6	S6	S6	S3	S6	S4	
Buffer width (m)	NA	NA	NA	NA	NA	NA	11.0	16.2	11.8	13.0 ± 2.8
Elevation (m)	339	267	311	369	295	325	387	387	334	335 ± 41.1
Reach length (m)	66	72	54	56	34	49	102	21	47	56 ± 23
Bank slope (°)	24	7	29	12	13	6	3	10	13	13 ± 8
Stream slope (°)	15	5	7	12	5	7	1	8	9	8 ± 4
Forest harvest year	NA	NA	NA	2015	2016	2016	2015	2014	2016	
Humus form	Leptomoder	Rhizomull	Vermimull	Vermimull	Rhizomull	Rhizomull	Hydro-sphagnomor	Rhizomull	Vermimull	
Soil texture (A horizon)	Sandy loam	Silt	Silty loam	Sandy loam	Silty clay loam	Sandy loam	Sandy loam	Sandy loam	Silty clay loam	

## 2.3 Results

### 2.3.1 Environmental variables

Mean daily air temperature was, on average, lowest at the reference sites, intermediate at the buffer sites, and highest at the no buffer sites, with a mean of  $14.5 \pm 2.0$  °C,  $14.8 \pm 2.2$  °C, and  $15.3 \pm 2.6$  °C (mean  $\pm$  *SD*), respectively (June to September; Figure 2.5). The daily maximum temperature was also lowest at the reference sites, intermediate at the buffer sites, and highest at the no buffer sites, with an average daily maximum of  $10.7 \pm 6.3$  °C,  $16.3 \pm 6.0$  °C, and  $20.2 \pm 6.7$  °C, respectively (Figure 2.6). Similarly, the temperature range was greater at the no buffer sites than the reference and buffer sites, indicating greater daily temperature fluctuations at the clear-cut riparian zones. The mean daily temperature range was  $3.6 \pm 2.1$  °C,  $7.5 \pm 4.6$  °C, and  $11.0 \pm 6.5$  °C for the reference, buffer, and no buffer sites, respectively.

Mean soil temperature followed a similar trend, with the lowest mean soil temperature at the reference sites ( $13.6 \pm 1.5$  °C), intermediate at the buffer sites ( $14.4 \pm 1.3$  °C), and highest at the no buffer sites ( $14.9 \pm 1.3$  °C) (Figure 2.7). The seven-day running maximum soil temperature was  $14.9 \pm 1.2$  °C,  $16.3 \pm 1.1$  °C, and  $16.9 \pm 1.2$  °C at the reference, buffer, and no buffer sites, respectively (Figure 2.8). Mean soil temperature was similar at the groundwater discharge (DIS) areas ( $14.1 \pm 1.6$  °C) compared to the ND areas ( $14.5 \pm 1.5$  °C).

Mean soil moisture (measured as volumetric water content) was highest at no buffer sites. The mean soil moisture from June to September was  $43.3 \pm 14.4$  %,  $45.5 \pm 16.7$  %,  $50.4 \pm 14.3$  % at the reference, buffer, and no buffer sites, respectively (Figure 2.9). In terms of local groundwater

conditions, mean soil moisture was significantly higher in the DIS areas  $55.4 \pm 11.4$  % compared to the ND areas  $41.6 \pm 15.1$  %, across all treatments (Figure 2.9, Table A.2).

Mean depth to the groundwater table was the lowest at the no buffer sites, and was significantly lower than the buffer and reference sites (Figure 2.10, Table A.3). The mean depth to the groundwater table from June to September was  $28.7 \pm 9.6$  cm,  $26.2 \pm 12.7$  cm, and  $15.9 \pm 8.9$  cm at the reference, buffer, and no buffer sites, respectively. In terms of local groundwater conditions, mean depth to the groundwater table was significantly lower at the DIS areas ( $20.0 \pm 12.6$  cm) compared to the ND areas ( $27.4 \pm 10.1$  cm), across all treatments. There was no statistically significant difference in daily average soil temperature and soil moisture between treatments according to the LME (Table A.3).

### **2.3.2 Carbon dioxide**

Mean soil CO<sub>2</sub> efflux ( $\text{mg CO}_2\text{-C m}^{-2} \text{ h}^{-1}$ ) for the reference, buffer, and no buffer sites for the entire sampling period (June to September) was  $65.7 \pm 29.9$ ,  $76.0 \pm 39.1$ ,  $71.5 \pm 40.9$ , respectively (Figure 2.11). Based on the linear mixed effects (LME) model, CO<sub>2</sub> emissions were not significantly different between treatments (Table 2.2). However, over the sampling period, CO<sub>2</sub> emissions were, on average, 1.16 times higher at the buffer sites and 1.09 times higher at the no buffer sites compared to the reference sites, respectively (Figure 2.11). Mean soil CO<sub>2</sub>-C emissions peaked in the middle of the growing season, with  $85.9 \pm 38.5$  and  $83.6 \pm 42.0$   $\text{mg CO}_2\text{-C m}^{-2} \text{ h}^{-1}$ , in July and August, respectively (Figure 2.12). Mean soil CO<sub>2</sub> emissions were the lowest in the spring followed by the autumn, with  $53.1 \pm 24.78$  and  $56.9 \pm 33.9$   $\text{mg CO}_2\text{-C m}^{-2} \text{ h}^{-1}$  measured in June and September, respectively. Carbon dioxide fluxes were not significantly

different between local groundwater conditions (Table 2.3). On average, over the study period CO<sub>2</sub> efflux was  $64.9 \pm 37.6$  and  $74.9 \pm 36.3$  mg CO<sub>2</sub>-C m<sup>-2</sup> h<sup>-1</sup> at the DIS and ND areas, respectively (Figure 2.11). Soil temperature, soil moisture, and depth to the groundwater table were significant predictors of CO<sub>2</sub> fluxes according to the LME models, with a marginal r<sup>2</sup> of 0.16, 0.11, and 0.06, respectively (Table 2.3, Figure 2.13). For every one *SD* increase in soil temperature, CO<sub>2</sub> fluxes increased by 13.34 mg. For every one *SD* increase in soil moisture, CO<sub>2</sub> fluxes decreased by 7.68 mg. For every one *SD* increase in depth to the groundwater table, CO<sub>2</sub> fluxes decreased by 7.84 mg.

### 2.3.3 Methane

Mean soil CH<sub>4</sub> fluxes ( $\mu\text{g CH}_4\text{-C m}^{-2} \text{ h}^{-1}$ ) for the reference, buffer, and no buffer sites for the entire sampling period (June to September) were  $-26.3 \pm 17.7$ ,  $-19.7 \pm 21.6$ , and  $-9.1 \pm 22.2$ , respectively (Figure 2.14). Therefore, on average, all of the treatments were a net CH<sub>4</sub> sink over the study period (Figure 2.15). Based on the LME model, CH<sub>4</sub> fluxes were significantly higher at the no buffer sites than at the reference sites (Table 2.2). Methane uptake was on average 1.26 times higher at the buffer sites and 3.71 times higher at the no buffer sites, compared to the reference sites, respectively (Figure 2.14). Methane fluxes were significantly different between local groundwater conditions, with CH<sub>4</sub> uptake being significantly lower in the DIS areas (Table 2.3, Figure 2.14). Methane gas flux was  $-11.2 \pm 22.5$   $\mu\text{g CH}_4\text{-C m}^{-2} \text{ h}^{-1}$  at the DIS areas compared to  $-24.4 \pm 19.2$   $\mu\text{g CH}_4\text{-C m}^{-2} \text{ h}^{-1}$  at the ND sites, on average, for the entire study period. Soil moisture and depth to groundwater were significant predictors of CH<sub>4</sub> fluxes according to the LME models, with a marginal r<sup>2</sup> of 0.37 and 0.46 respectively (Table 2.3, Figure 2.16). For every

one *SD* increase in soil moisture, CH<sub>4</sub> fluxes increased by 5.88 µg. For every one *SD* increase in depth to the groundwater table, CH<sub>4</sub> fluxes decreased by 7.84 µg.

#### **2.3.4 Nitrous oxide**

Mean soil N<sub>2</sub>O fluxes (µg N<sub>2</sub>O-N m<sup>-2</sup> h<sup>-1</sup>) for the reference, buffer, and no buffer sites for the entire sampling period (June to September) were 3.6 ± 2.6, 2.1 ± 2.4, and 1.7 ± 1.6, respectively (Figure 2.17). According to the LME model, there was a treatment effect on N<sub>2</sub>O fluxes, with significantly higher fluxes at the reference sites compared to the no buffer sites (Table 2.2). Over the sampling period, N<sub>2</sub>O fluxes were, on average 1.70 times lower at the buffer sites and 2.05 times lower at the no buffer sites, compared to the reference sites, respectively (Figure 2.17). Additionally, mean soil N<sub>2</sub>O fluxes were the highest in the spring, and gradually declined throughout the summer to the fall, with the highest monthly mean (4.1 ± 2.9 µg N<sub>2</sub>O-N m<sup>-2</sup> h<sup>-1</sup>) and lowest monthly mean (1.6 ± 2.2 µg N<sub>2</sub>O-N m<sup>-2</sup> h<sup>-1</sup>) measured in June and September, respectively (Figure 2.18). Nitrous oxide fluxes were not significantly different between local groundwater conditions (Table 2.3). On average over the study period N<sub>2</sub>O efflux was 2.5 ± 2.2 and 2.4 ± 2.5 µg N<sub>2</sub>O-N m<sup>-2</sup> h<sup>-1</sup> at the DIS and ND areas, respectively (Figure 2.17). None of the environmental variables (i.e. soil moisture, soil temperature, and depth to the groundwater table) were significant predictors of N<sub>2</sub>O fluxes (Table 2.3, Figure 2.19).

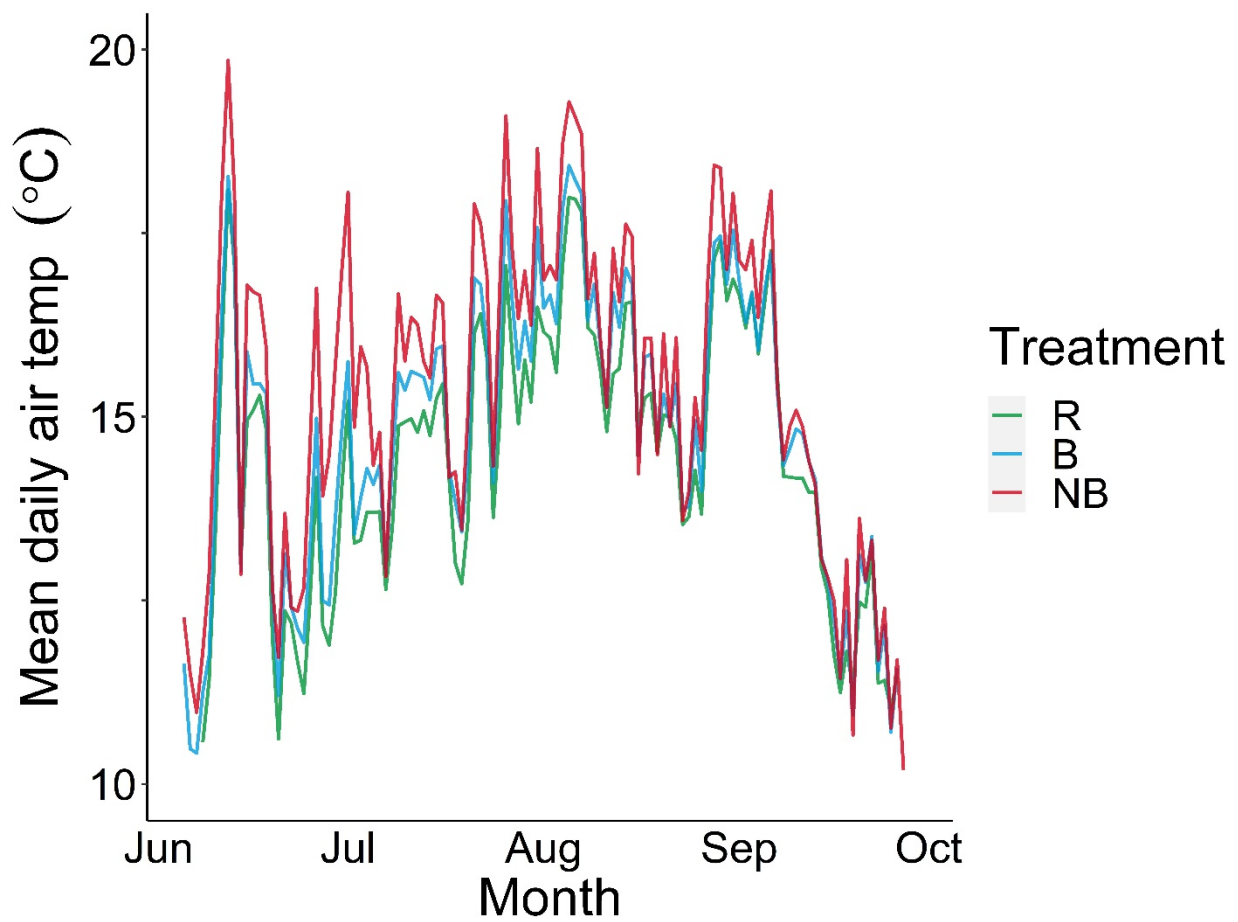


Figure 2.5 Mean daily air temperature in the riparian zone of headwater streams across reference (R, n = 3), buffer (B, n = 3), and no buffer (NB, n = 3) treatments from June to October 2019.

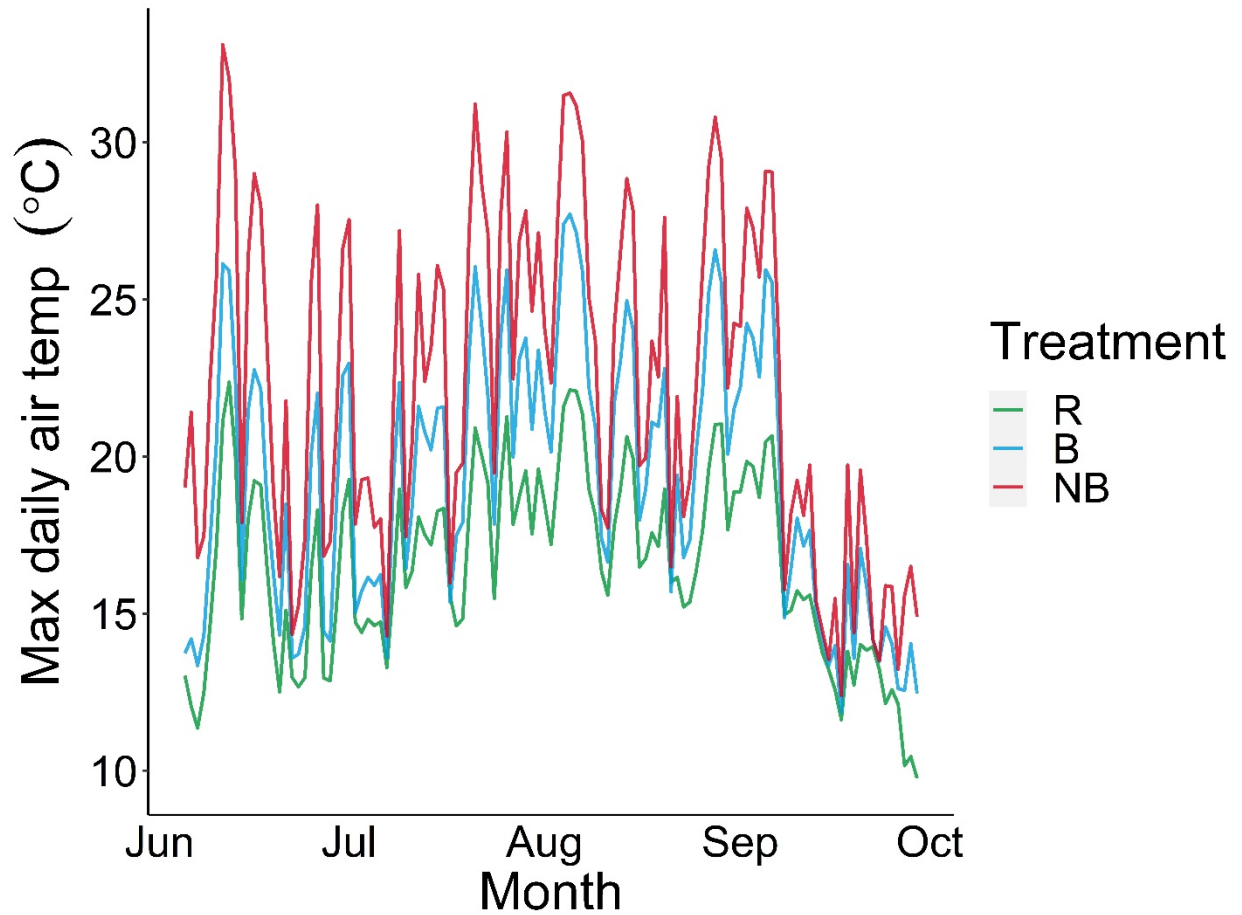


Figure 2.6 Maximum daily air temperature in the riparian zone of headwater streams across reference (R, n = 3), buffer (B, n = 3), and no buffer (NB, n = 3) treatments from June to October 2019.

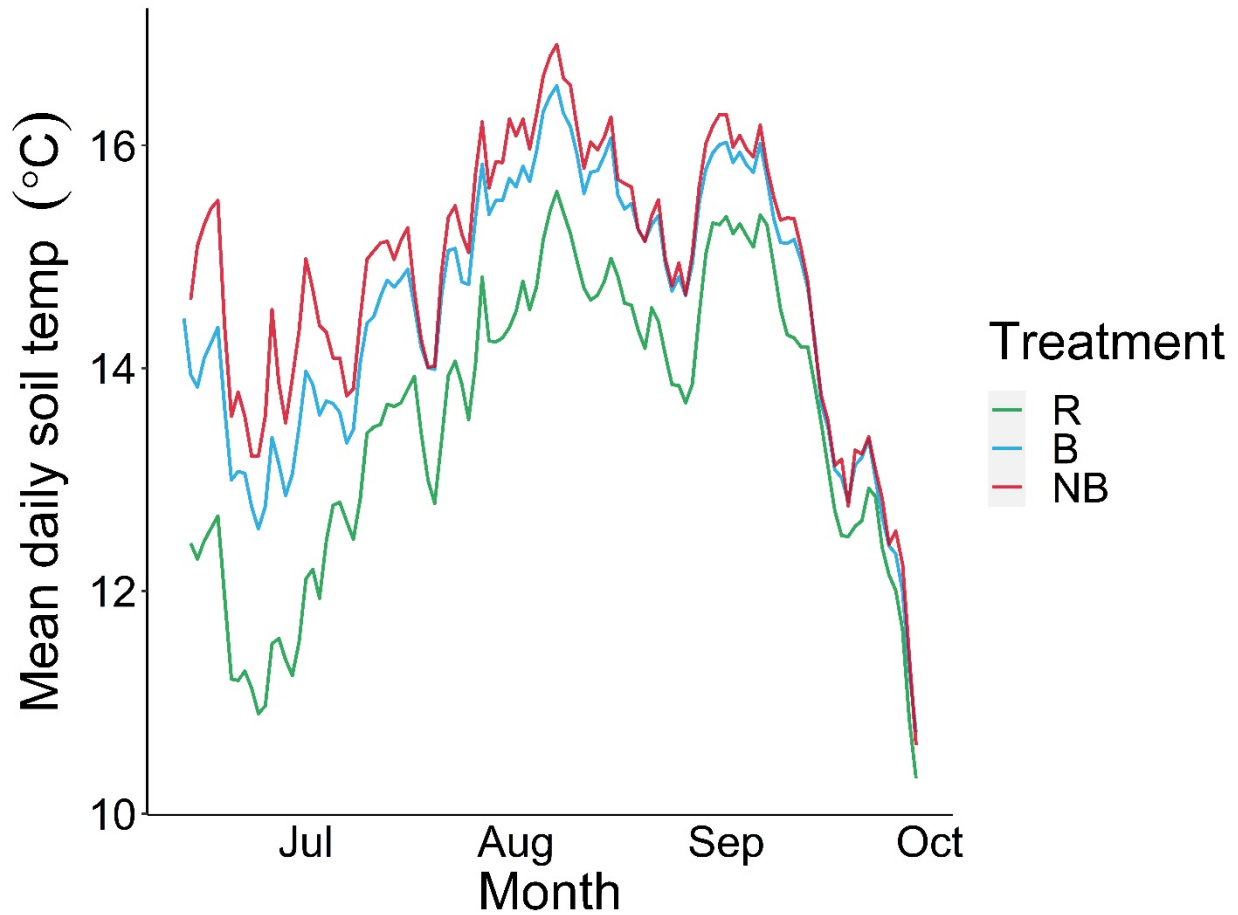


Figure 2.7 Mean daily soil temperature ~10 cm below the soil surface in the riparian zone of headwater streams in the Pacific coastal rainforest of British Columbia across reference (R, n = 3), buffer (B, n = 3), and no buffer (NB, n = 3) treatments from June to October 2019.

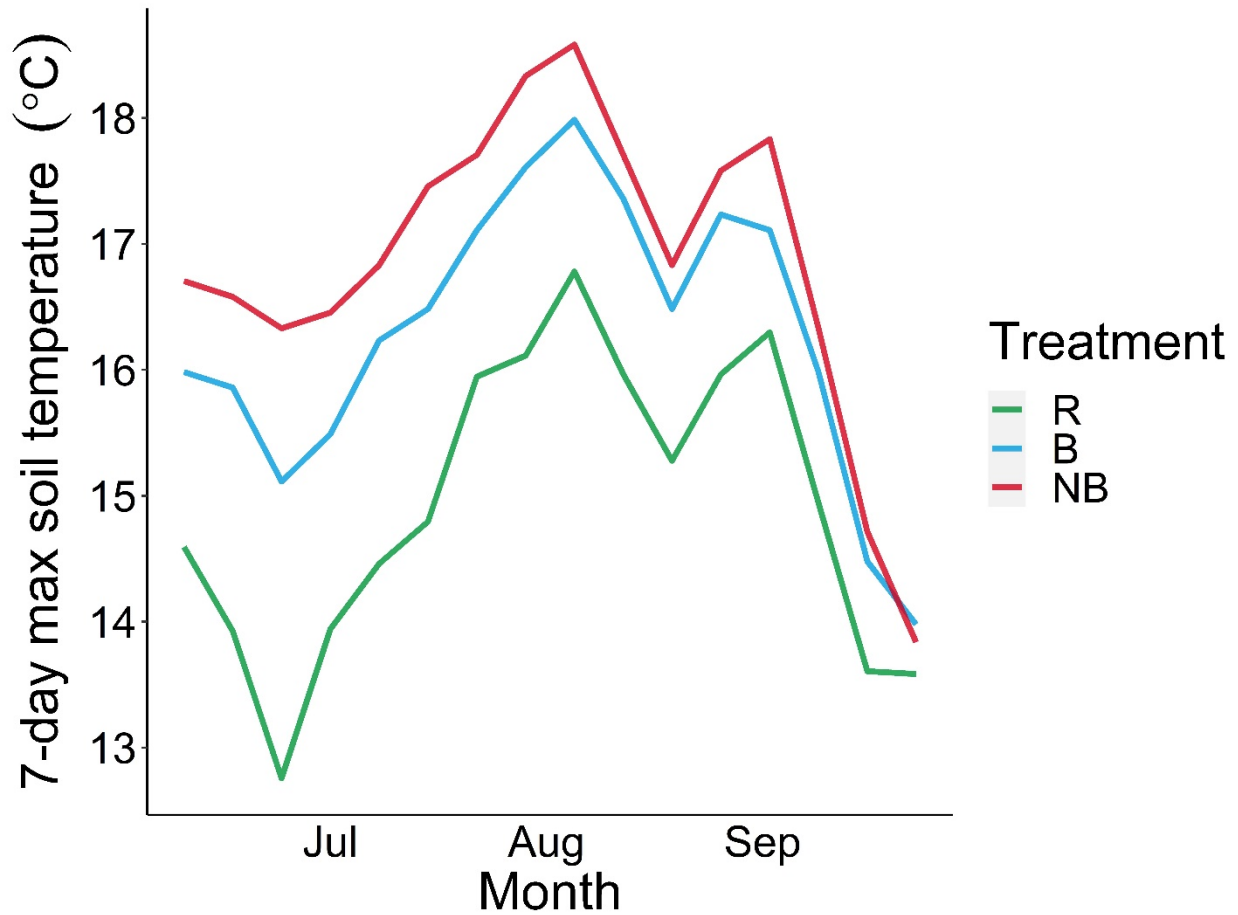


Figure 2.8 Seven-day running maximum soil temperature measured ~ 10 cm below the soil surface in the riparian zone of nine headwater streams in the Pacific coastal rainforest of British Columbia, averaged across three sites per treatment (R, Reference; B, Buffer; NB, No Buffer) from June to October 2019.

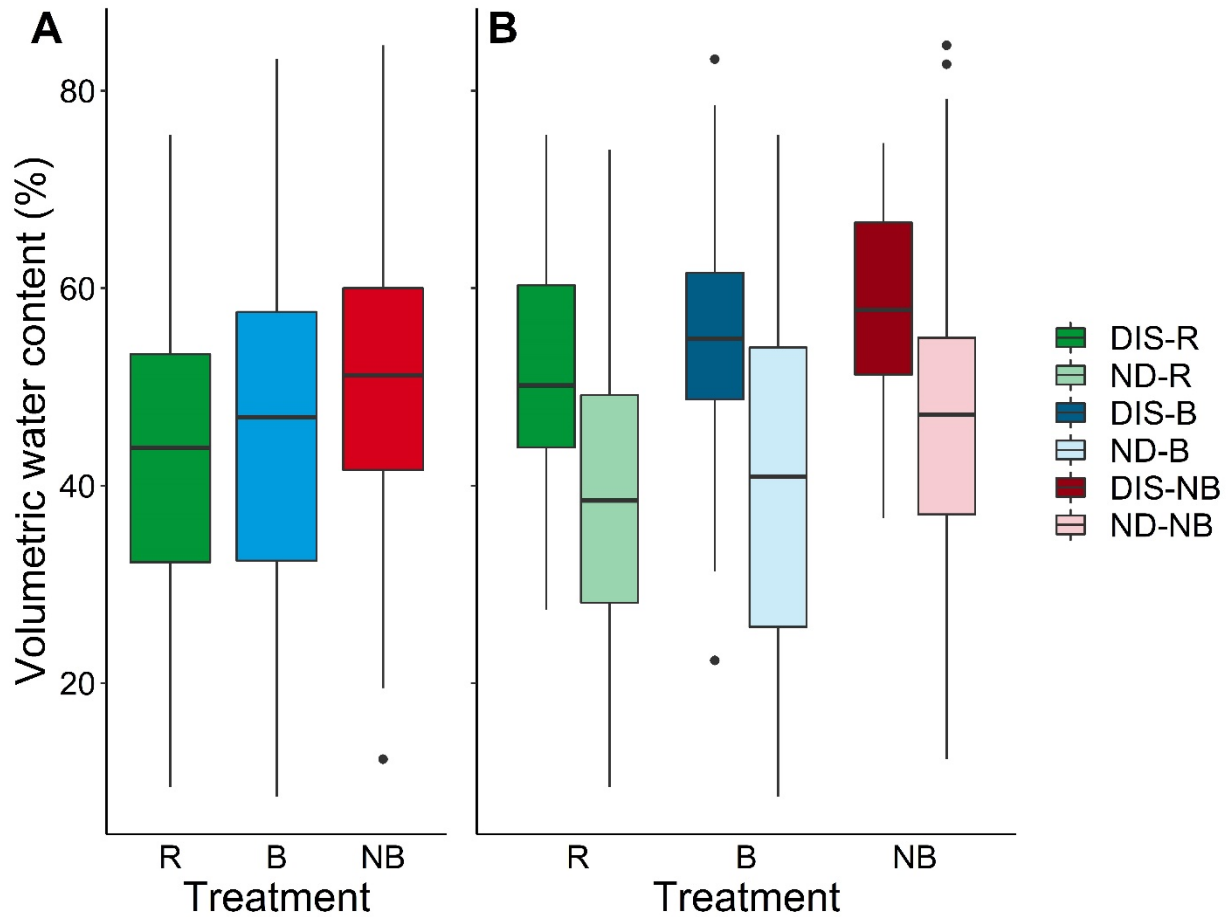


Figure 2.9 Mean soil moisture in the riparian zone of headwater streams in the Pacific coastal rainforest of British Columbia across reference (R,  $n = 3$ ), buffer (B,  $n = 3$ ), and no buffer (NB,  $n = 3$ ) treatments as well as in groundwater discharge (DIS) areas and in non-groundwater discharge (ND) areas from June to October 2019. Boxplots display the median, 25<sup>th</sup> and 75<sup>th</sup> percentiles, whiskers (1.5 times the IQR), and individual outliers (dots), for this and all subsequent boxplots.

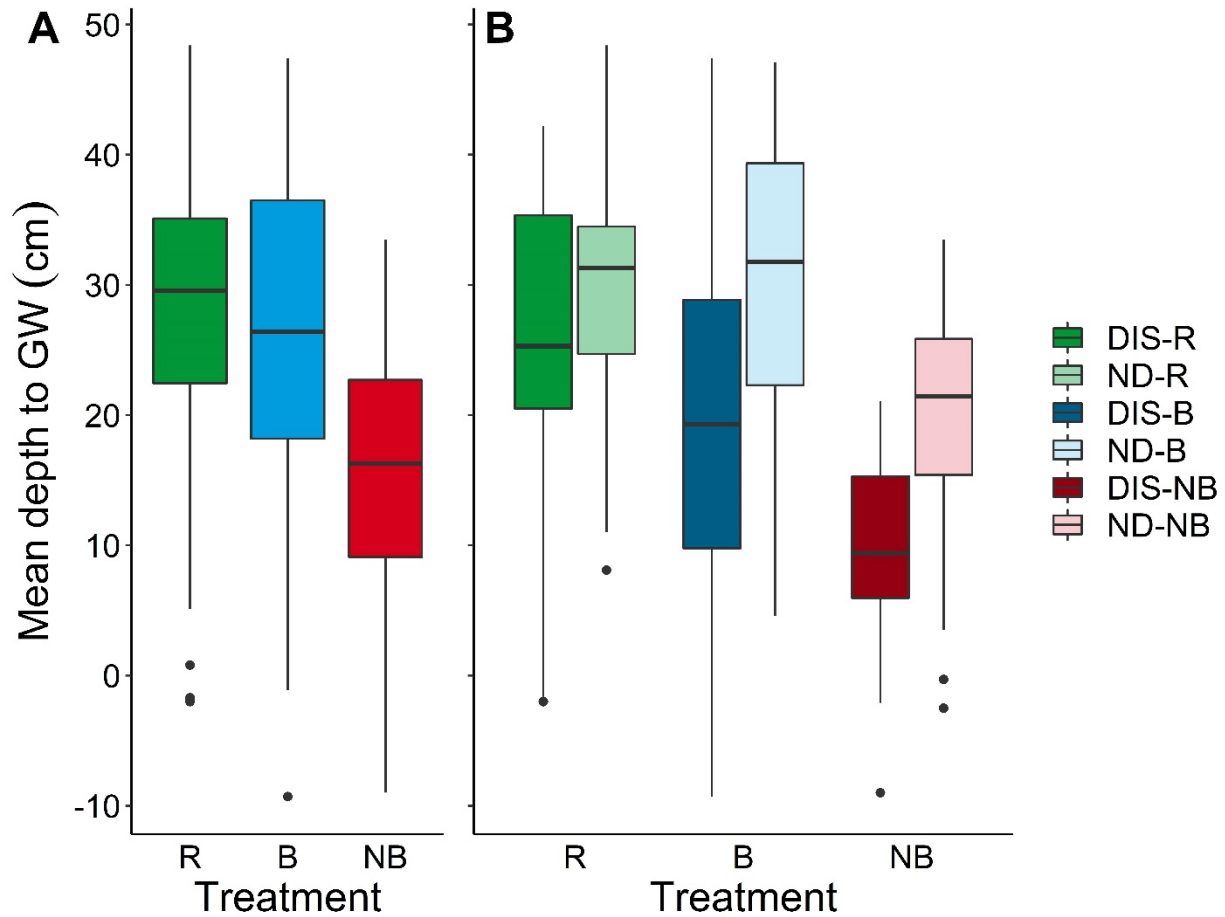


Figure 2.10 Mean depth to the groundwater table (cm) in the riparian zone of headwater streams in the Pacific coastal rainforest of British Columbia across reference (R, n = 3), buffer (B, n = 3), and no buffer (NB, n = 3) treatments as well as in groundwater discharge areas (DIS) and in non-groundwater discharge areas (ND) from June to October 2019.

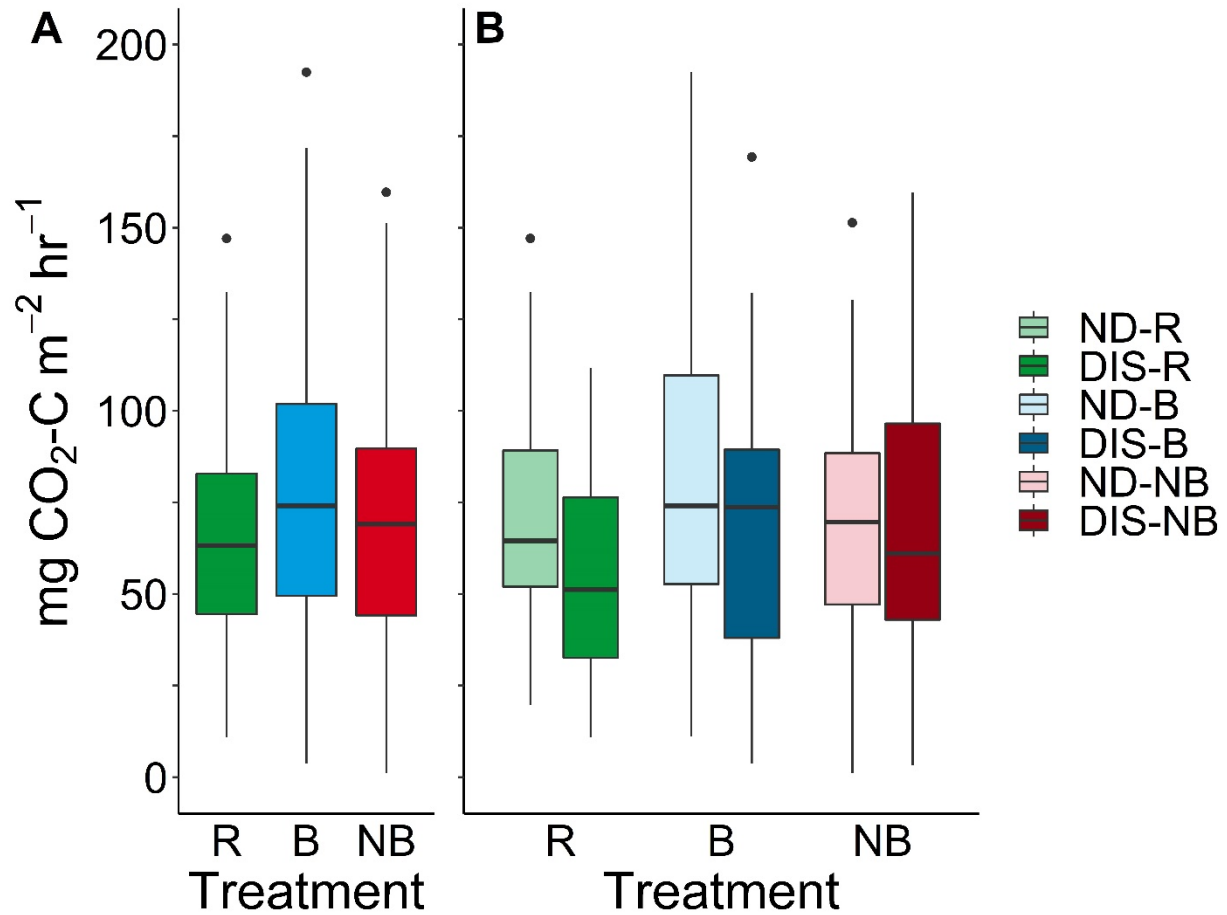


Figure 2.11 Riparian forest soil carbon dioxide emission rates from reference (R; n = 3), buffer (B; n = 3), and no buffer (NB; n = 3) treatments, in panel A, and from groundwater discharge (DIS) and non-groundwater discharge (ND) areas, in panel B, alongside headwater streams in the Pacific coastal temperate rainforest of British Columbia in 2019 (June - October).

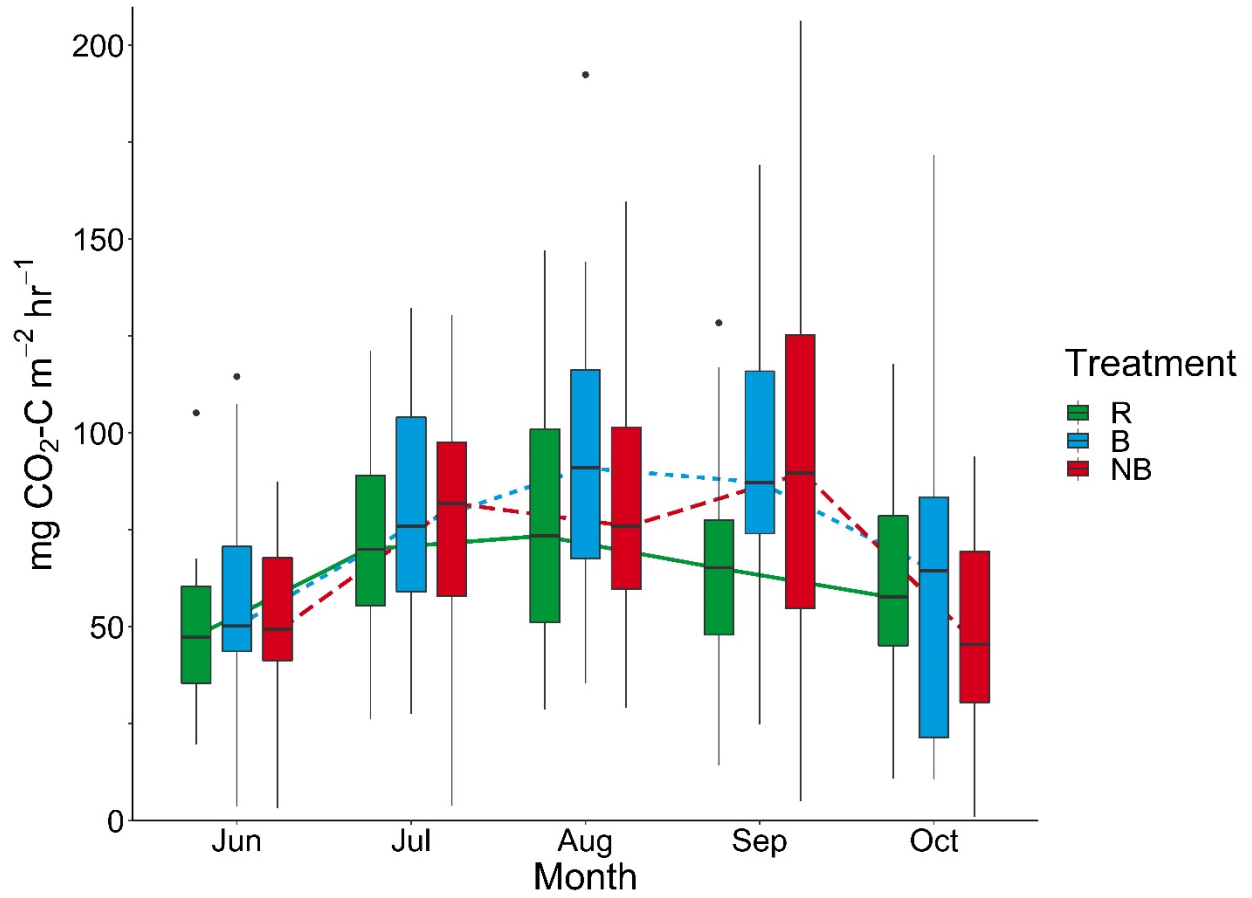


Figure 2.12 Riparian forest soil carbon dioxide emission rates from reference (R; n = 3), buffer (B; n = 3), and no buffer (NB; n = 3) treatments alongside headwater streams in the Pacific coastal temperate rainforest of British Columbia across five sampling periods from June to October, 2019.

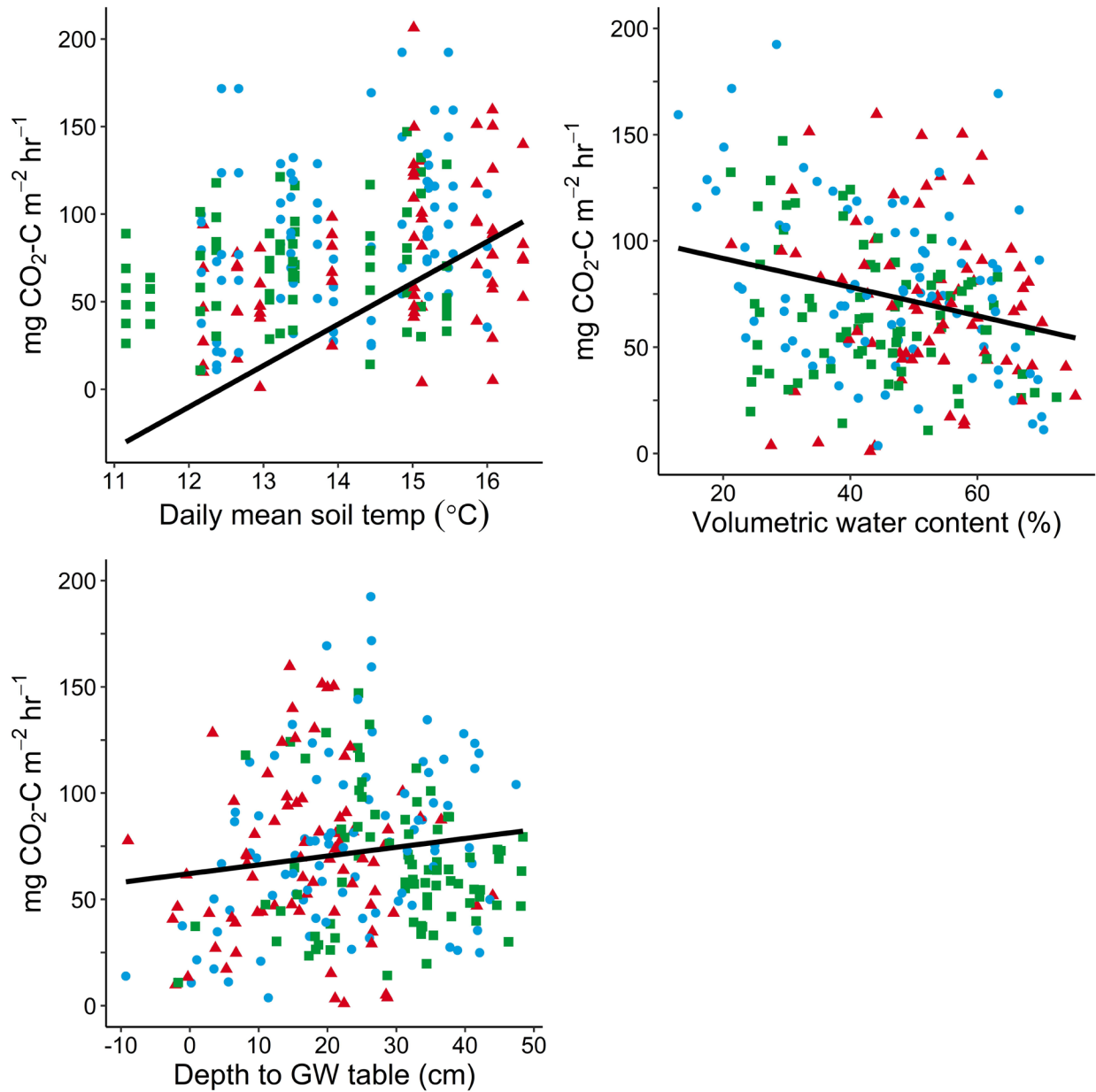


Figure 2.13 Relationships between carbon dioxide gas fluxes and the environmental variables of daily mean soil temperature, mean soil moisture, and depth to groundwater table, by treatment. Trend lines are based on LME models accounting for autocorrelation in the relationship between the two variables for reference (R, in green), buffer (B, in blue), and no buffer (NB, in red) treatments.

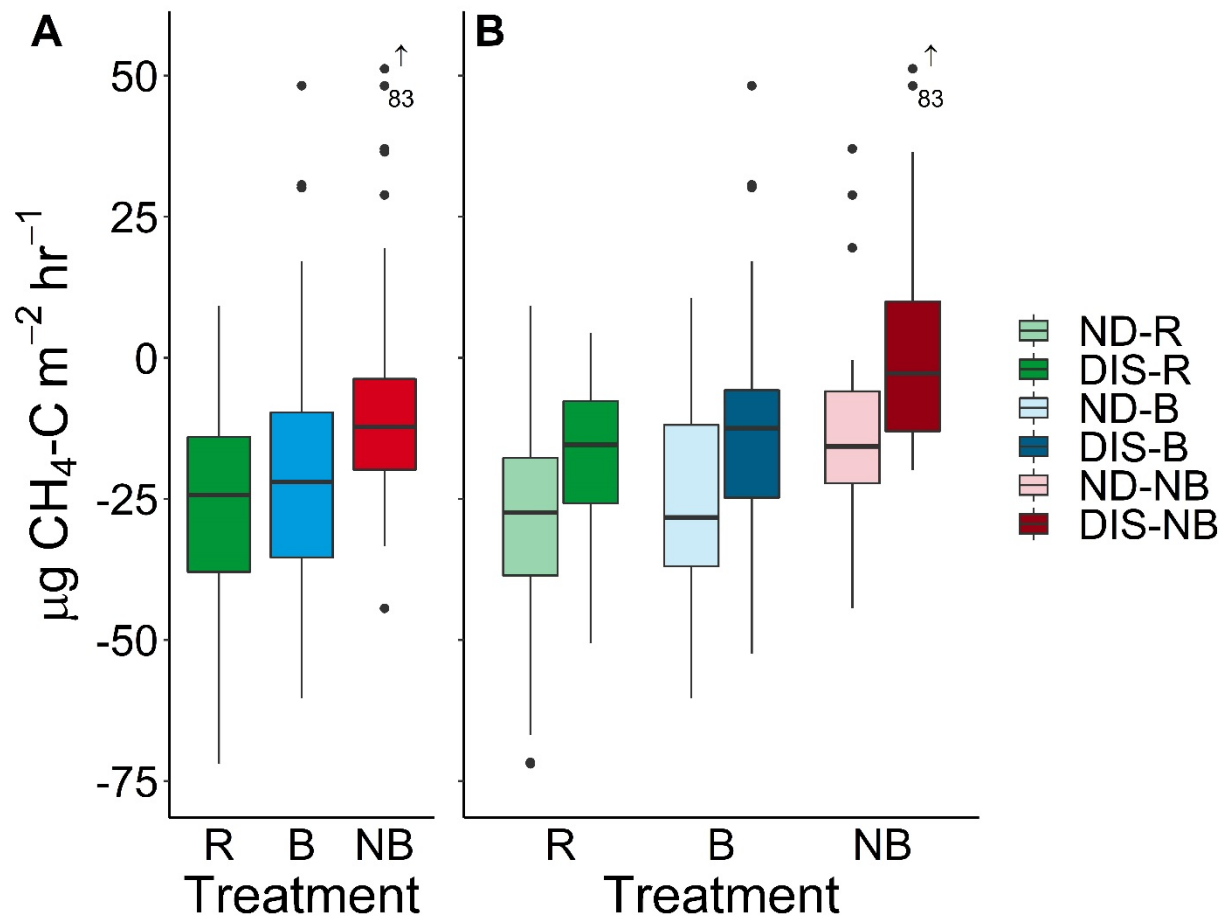


Figure 2.14 Riparian forest soil methane flux rates from reference (R; n = 3), buffer (B; n = 3), and no buffer (NB; n = 3) treatments, in panel A, and from groundwater discharge (DIS) and non-groundwater discharge (ND) areas, in panel B, alongside headwater streams in the Pacific coastal temperate rainforest of British Columbia in 2019 (June - September).

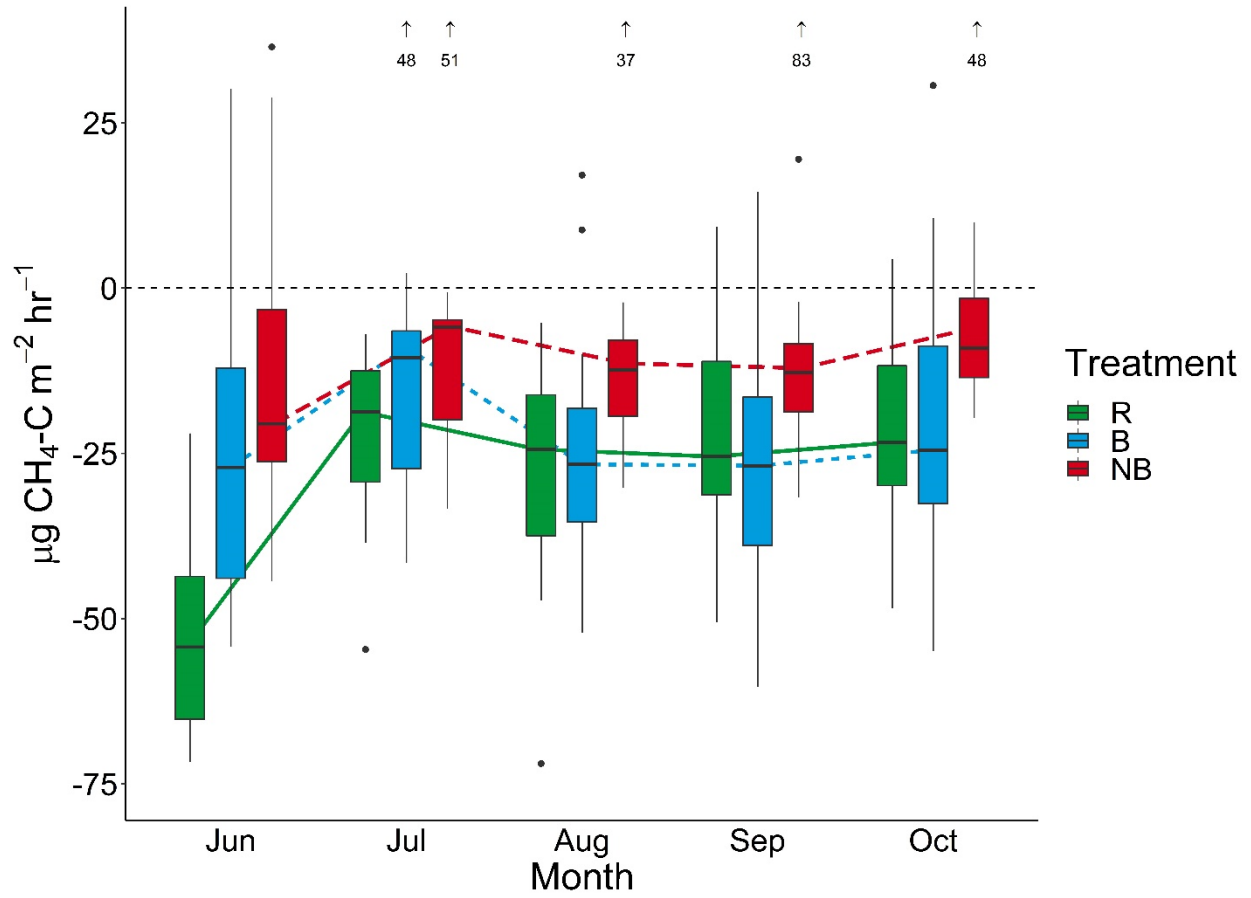


Figure 2.15 Riparian forest soil methane flux rates from reference (R; n = 3), buffer (B; n = 3), and no buffer (NB; n = 3) treatments alongside headwater streams in the Pacific coastal temperate rainforest of British Columbia across five sampling periods from June to September 2019.

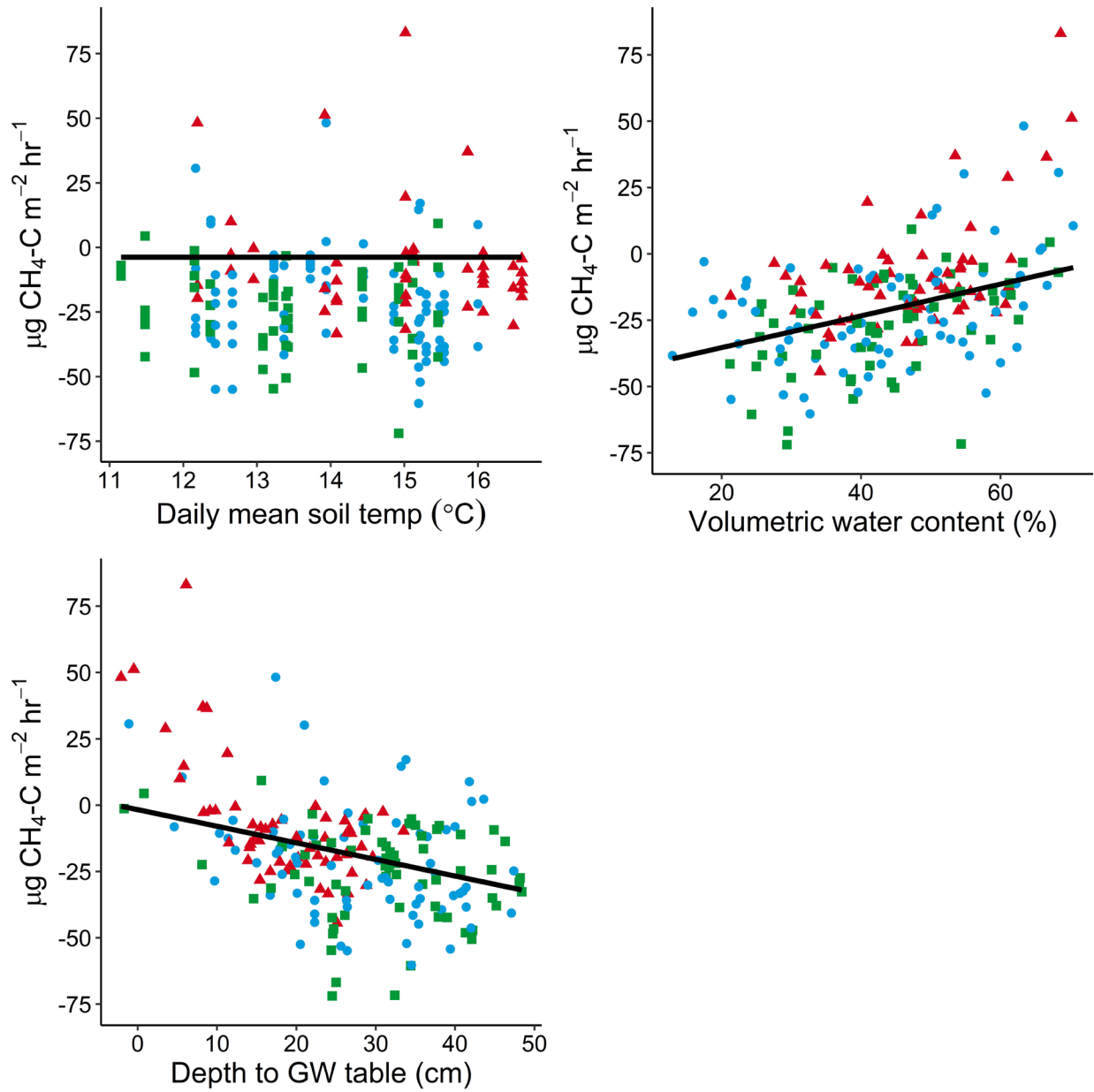


Figure 2.16 Relationships between methane gas fluxes and the environmental variables of daily mean soil temperature, mean soil moisture, and depth to groundwater table, by treatment. Trend lines are based on LME models accounting for autocorrelation in the relationship between the two variables for reference (R), buffer (B), and no buffer (NB) treatments.

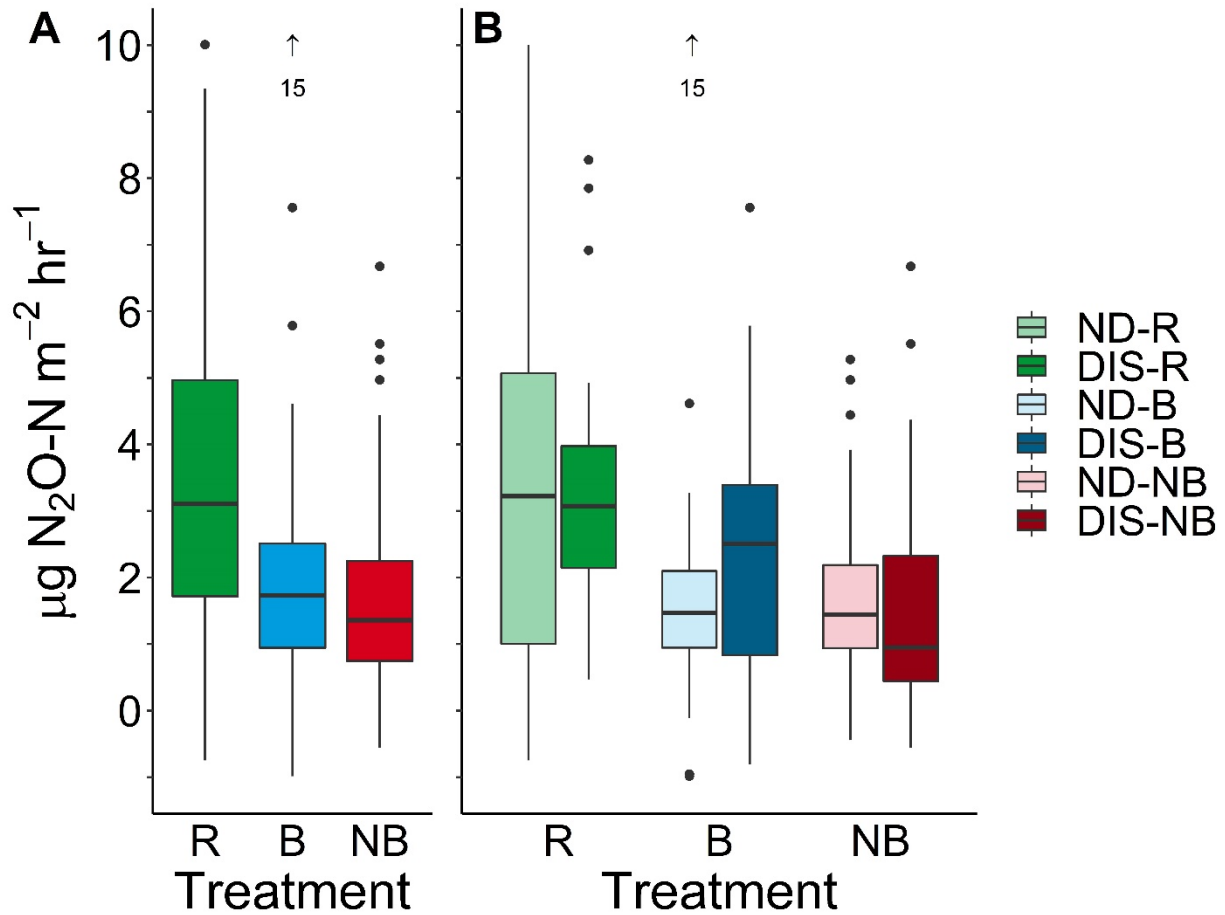


Figure 2.17 Riparian forest soil nitrous oxide flux rates from reference (R; n = 3), buffer (B; n = 3), and no buffer (NB; n = 3) treatments, in panel A, and from groundwater discharge (DIS) and non-groundwater discharge (ND) areas, in panel B, alongside headwater streams in the Pacific coastal temperate rainforest of British Columbia in 2019 (June - September).

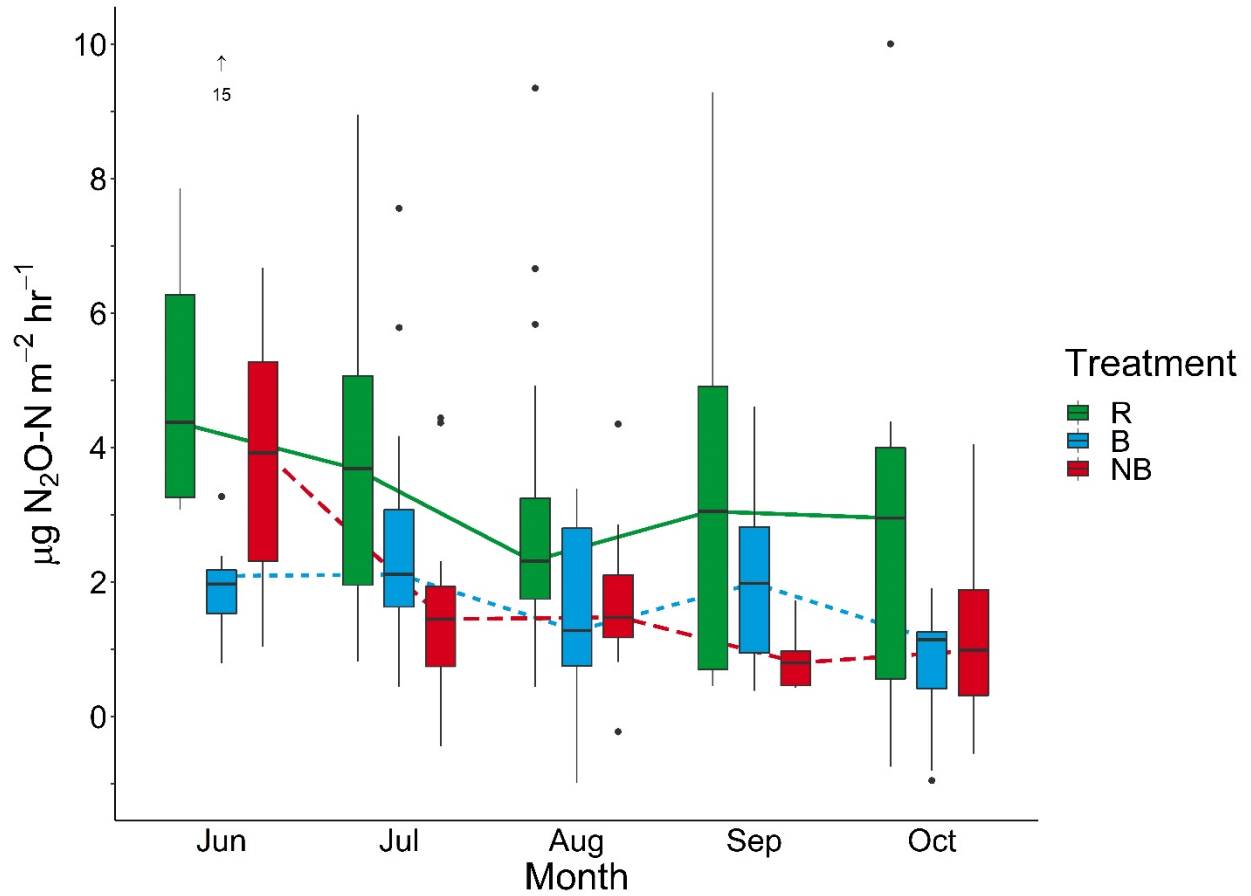


Figure 2.18 Riparian forest soil nitrous oxide flux rates from reference (R; n = 3), buffer (B; n = 3), and no buffer (NB; n = 3) treatments alongside headwater streams in the Pacific coastal temperate rainforest of British Columbia across five sampling periods from June to September 2019.

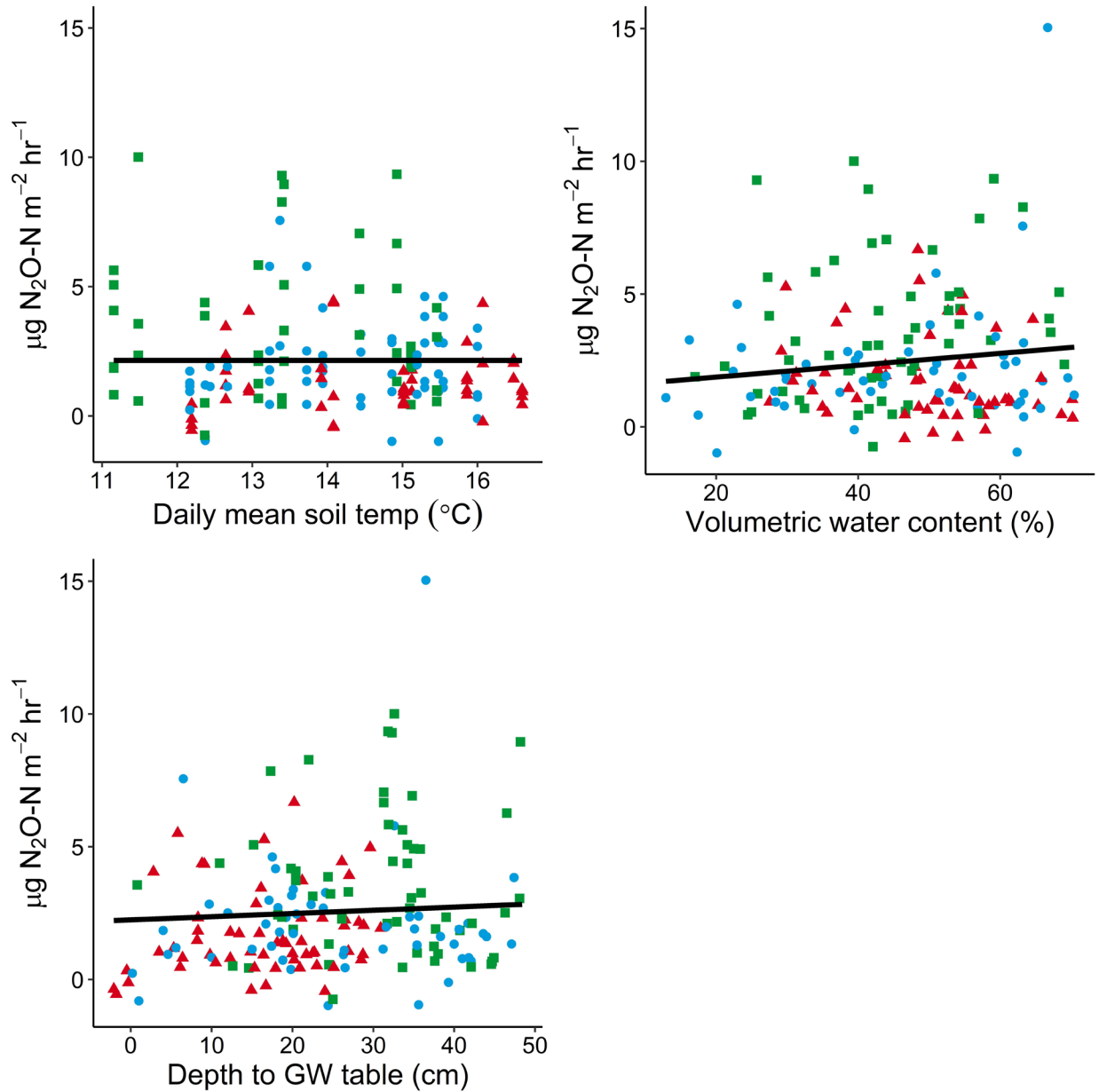


Figure 2.19 Relationships between nitrous oxide gas fluxes and the environmental variables of daily mean soil temperature, mean soil moisture, and depth to groundwater table, by treatment. Trend lines are based on LME models accounting for autocorrelation in the relationship between the two variables for reference (R), buffer (B), and no buffer (NB) treatments. Grey bands represent 95% confidence intervals of the relations.

Table 2.2 Pairwise difference between Treatment levels (reference, R; buffer B; and no buffer NB) using Tukey’s HSD *post hoc* test for the linear mixed effects models explaining the dynamics of carbon dioxide, methane, and nitrous oxide fluxes, respectively. All models included the autocorrelation term “AR1(Week + 0 | Site/Chamber)”. Bolded comparison indicates a significant effect at  $p < 0.05$ .

<b>Model</b>	<b>Comparison</b>	<b>Est.</b>	<b>SE</b>	<b><i>p</i></b>
CO <sub>2</sub> ~ Treatment	R - B	-8.65	11.2	0.72
	R - NB	-1.86	11.4	0.99
	B - NB	6.79	11.4	0.82
CH <sub>4</sub> ~ Treatment	R - B	-6.65	6.82	0.59
	<b>R - NB</b>	<b>-22.35</b>	<b>6.96</b>	<b>&lt; 0.01</b>
	B - NB	-15.71	6.97	0.07
N <sub>2</sub> O ~ Treatment	R - B	0.33	0.14	0.06
	<b>R - NB</b>	<b>0.39</b>	<b>0.14</b>	<b>0.02</b>
	B - NB	0.06	0.14	0.90

Table 2.3 Summarized output of linear mixed effects models explaining the dynamics of carbon dioxide, methane, and nitrous oxide fluxes, respectively. All models included the autocorrelation term “AR1(Week + 0 | Site/Chamber)”. Bolded models indicate a significant effect at  $p < 0.05$ . When comparing groundwater discharge (DIS) and non-groundwater discharge (ND) areas, note that ND is the reference level in the DIS\_ND term.

<b>Model</b>	<b>Est.</b>	<b>SE</b>	<b><i>p</i></b>
CO <sub>2</sub> ~ DIS_ND	-2.86	7.27	0.69
<b>CH<sub>4</sub> ~ DIS_ND</b>	<b>20.36</b>	<b>4.98</b>	<b>&lt; 0.001</b>
N <sub>2</sub> O ~ DIS_ND	0.08	0.09	0.42
<b>CO<sub>2</sub> ~ Soil temperature</b>	<b>13.34</b>	<b>2.15</b>	<b>&lt; 0.001</b>
CH <sub>4</sub> ~ Soil temperature	-2.13	1.31	0.10
N <sub>2</sub> O ~ Soil temperature	-0.01	0.04	0.72
<b>CO<sub>2</sub> ~ Soil moisture</b>	<b>-7.68</b>	<b>2.83</b>	<b>&lt; 0.01</b>
<b>CH<sub>4</sub> ~ Soil moisture</b>	<b>5.88</b>	<b>1.84</b>	<b>&lt; 0.01</b>
N <sub>2</sub> O ~ Soil moisture	0.04	0.05	0.39
<b>CO<sub>2</sub> ~ Depth to GW</b>	<b>6.17</b>	<b>2.84</b>	<b>0.03</b>
<b>CH<sub>4</sub> ~ Depth to GW</b>	<b>-7.84</b>	<b>1.77</b>	<b>&lt; 0.001</b>
N <sub>2</sub> O ~ Depth to GW	0.03	0.05	0.58

## 2.4 Discussion

In general, there were differences between treatments for the measured environmental characteristics. Firstly, mean and maximum daily air and soil temperatures were highest at the no buffer sites, intermediate at the buffer sites, and lowest at the reference sites, indicating the effect of increased incoming solar radiation from reduced shading due to the decline in canopy cover following harvest (Moore, Spittlehouse, & Story, 2005). Additionally, the groundwater level was on average closer to the surface in the no buffer sites compared to the buffer and reference sites, demonstrating that the reduction in transpiration due to forest harvest may cause a rise in the water table (Smerdon, Redding, & Beckers, 2009). This trend was reflected in volumetric soil moisture content, which was also highest in the no buffer sites, intermediate at the buffer sites, and lowest at the reference sites. Across treatments, the groundwater discharge (DIS) areas were generally wetter than the non-groundwater discharge (ND) areas, with shallower groundwater tables and higher soil moisture. These conditions occur because upland-originating groundwater converges and discharges in a depression in the topography of the riparian zone (Kuglerová et al., 2014b).

All of the measured GHG flux rates fell within the range of reported values for GHG emissions from riparian soils (Soosaar et al., 2011). For the sampling period, the riparian forest soils examined in this study were a net sink for CH<sub>4</sub>, and a net source for CO<sub>2</sub> and N<sub>2</sub>O. The reference sites had significantly higher N<sub>2</sub>O emissions and significantly lower CH<sub>4</sub> emissions than the no buffer sites. There were no significant treatment differences for CO<sub>2</sub> fluxes, although they were generally highest at no buffer sites. Carbon dioxide emissions showed a seasonal trend, with a peak in efflux in the middle of the summer, while CH<sub>4</sub> and N<sub>2</sub>O fluxes did not demonstrate any

distinct seasonal patterns during the study period (June to September). When examining annual data (see Chapter 2), N<sub>2</sub>O fluxes exhibit a similar seasonal trend to CO<sub>2</sub>, at the reference sites. Methane fluxes were significantly higher in the DIS areas compared to the ND areas, reflecting the higher soil moisture and resulting anaerobic conditions required for methanogenesis. There were no significant differences in CO<sub>2</sub> and N<sub>2</sub>O emissions between local groundwater conditions. Soil temperature, soil moisture, and depth to the groundwater table were significant predictors of CO<sub>2</sub> emissions. Soil moisture and depth to the groundwater table were significant predictors of CH<sub>4</sub> fluxes. None of the measured environmental variables were significant predictors of N<sub>2</sub>O fluxes.

#### **2.4.1 Effects of forest harvest**

Methane fluxes were significantly higher at the no buffer sites compared to the reference sites, and soil moisture and depth to the groundwater table were significant predictors of CH<sub>4</sub> fluxes. As such, these CH<sub>4</sub> results are in line with my Water Table Hypothesis, wherein forest harvest reduces catchment-wide transpiration rates, causing an increase in soil moisture due to higher water table levels (Gundersen et al., 2010), creating anaerobic conditions that promote methanogenesis. However, contrary to my hypothesis, maintaining a riparian buffer appears to have a buffering-effect on this phenomenon, as the buffer sites maintained CH<sub>4</sub> flux rates that were not significantly different from the reference sites. There was no statistically significant difference between treatments for CO<sub>2</sub> fluxes, therefore those results did not support my hypotheses. On the other hand, N<sub>2</sub>O fluxes were significantly higher at the reference sites compared to the no buffer sites. None of the measured environmental variables (i.e. soil moisture, depth to groundwater, and soil temperature) were significant predictors of N<sub>2</sub>O fluxes,

ruling out the Water Table and Soil Temperature hypotheses. The N<sub>2</sub>O results are in line with the Disturbance Hypothesis, where I predicted that the lowest GHG emissions would be observed at the no buffer sites compared to the buffer and reference sites, due to disturbance of soil microbial activity by forest harvest in the riparian zone. Although I did not directly measure a metric of disturbance (e.g. soil erosion, soil compaction, microbial biomass), a large body of literature shows evidence of soil ecosystem disturbance following forest harvest (Elliot, Page-Dumroese, & Robichaud, 2018; Hartmann et al., 2012; Lewandowski et al., 2019).

Clear-cutting has inconsistent effects on CO<sub>2</sub> emission rates (Striegl & Wickland, 1998; Ullah, Frasier, Pelletier, & Moore, 2009), with studies reporting a decline (Striegl & Wickland, 1998), an increase (Lavoie et al., 2013; Paul-Limoges et al., 2015), or no change (Kähkönen et al., 2002) in CO<sub>2</sub> emissions following harvest. In this study, there was no significant difference in CO<sub>2</sub> emission rates between treatments, although CO<sub>2</sub> emissions were highest at the buffer sites. This lack of a significant treatment difference may have been because the no buffer and buffer ecosystems have already recovered from the disturbance of forest harvest after three to five years. Perhaps if this study was conducted sooner post-harvest, there would have been greater differences in CO<sub>2</sub> fluxes between the treatments. For example, in the first three to four months after clear-cutting, CO<sub>2</sub> emissions were higher in the clear-cut than in the control plots of a Chinese fir and evergreen broadleaved forest (Guo et al., 2010). This initial increase of CO<sub>2</sub> emissions may be because clear-cutting provides substrate and stimulates microbial activity via increased temperatures (Guo et al., 2010). Another possible explanation of my CO<sub>2</sub> results may be due to the distinct conditions in riparian forests compared to upland forests, where the aforementioned studies were conducted. Riparian zone soils have high moisture levels due to

shallow water tables and a strong groundwater influence (Goodrick et al., 2016). Therefore, the rise in temperature following forest harvest that can explain the rise in CO<sub>2</sub> following harvest in upland forests (Lavoie et al., 2013), may be buffered by the generally moister and cooler soils of riparian forests (Clinton et al., 2010), resulting in a less distinct rise in CO<sub>2</sub> emissions following harvest in riparian forests compared to upland forests.

The results of my study were in line with other studies, which have also found that clear-cutting increased CH<sub>4</sub> efflux from the soil (Kähkönen et al., 2002; Wu et al., 2011). This rise can be attributed to higher average summer soil temperatures, greater soil moisture, and higher dissolved organic carbon concentrations in clear-cuts (Ullah et al., 2009; Wu et al., 2011). Forest harvest results in soil compaction, reduced transpiration, and a rise in the groundwater table, all of which promote waterlogging and anaerobic conditions (Christiansen et al., 2017; Gundersen et al., 2010). In my study, soil moisture and depth to the groundwater table were significant predictors of CH<sub>4</sub> fluxes, while temperature was not. In line with my results, CH<sub>4</sub> uptake was three times lower following clear-cutting in a temperate spruce forest in southern Germany (Wu et al., 2011). In another study, clear-cutting turned a spruce forest soil in Finland from a sink to a source of CH<sub>4</sub>, with a 40% decrease in CH<sub>4</sub> consumption rates (Kähkönen et al., 2002). The lower CH<sub>4</sub> uptake following forest harvest may be explained by the harmful impacts of soil disturbance on methanotrophic bacteria, resulting in the inhibition of CH<sub>4</sub>-oxidation (Le Mer & Roger, 2001; Wu et al., 2011). Alternatively, the anaerobic conditions created by higher soil moisture concentrations following forest harvest can promote the production of CH<sub>4</sub> (Wu et al., 2011). A clear-cut wetland in Québec, Canada produced 131 times more CH<sub>4</sub> than the undisturbed wetland soil, likely due to higher soil temperature and soil moisture in the clear-cut

(Ullah et al., 2009). In my study, the no buffer sites still were a net sink, albeit a weak sink, of CH<sub>4</sub> over the growing season. This is likely because unlike many wetlands, most riparian soils do not have consistently anoxic soils, which promote methanogenesis (Dalal & Allen, 2008). Given that there was no significant difference in CH<sub>4</sub> flux rates between the buffer and reference sites, it appears that riparian buffers may be effective in preserving soil ecosystem conditions contributing to CH<sub>4</sub> fluxes. Consequently, riparian buffer ones may be effective strategy for forest managers interested in maintaining GHG balance in riparian zone soils.

Given that forests are typically sources of N<sub>2</sub>O (Dalal & Allen, 2008), the lower N<sub>2</sub>O fluxes in the no buffer compared to the reference sites is a departure from undisturbed ecosystem function. The cycling of nitrogen is critical to ecosystem functioning of forests. Nitrogen is a critical nutrient for plant growth, and most temperate forests are considered nitrogen limited (Gundersen, 1991). It has been reported specifically for Malcolm Knapp Research Forest, where this study was conducted, that the forest soils are nitrogen and phosphorus limited (Feller, 1977). Conversely, an excess of nitrogen in forest soils can cause nutritional imbalances, leaching of nutrients and soil acidification (Gundersen, 1991). Therefore, the nitrogen cycle in forest soils requires a fine balance that is evidently impacted by forest harvest in the riparian zone.

The lower N<sub>2</sub>O emissions in the no buffer sites compared to undisturbed riparian zones was a surprising result because many other studies have reported an increase in N<sub>2</sub>O emissions following forest harvest. Typically, forest harvest can increase soil moisture and mobilize soil nitrogen, promoting N<sub>2</sub>O emissions from logged forest sites (Kreutzweiser et al., 2008). Higher N<sub>2</sub>O emissions were seen following forest harvest in the taiga region of eastern Siberia, Russia (Takakai et al., 2008). Additionally, N<sub>2</sub>O emissions were 2.7 times higher in clear-cut than in

mature black spruce forest soil in Québec, Canada (Ullah et al., 2009). However, these studies were not conducted in riparian forests, which have unique conditions such as shallow water tables, high soil organic matter quality and quantity, and high soil nitrogen availability, unlike most upland forests (Knoepp & Clinton, 2009; Vidon et al., 2018). Although I did not compare soil nutrient and carbon concentrations, soil moisture was found to be highest at the no buffer sites, likely due to the high water table when compared to the reference sites. Nitrous oxide emissions peak at intermediate soil moisture (Gundersen et al., 2010; Jungkunst, Flessa, Scherber, & Fiedler, 2008), which may explain the increase in N<sub>2</sub>O emissions following harvest in upland forests but not riparian forests. A greenhouse microcosm study found that mean N<sub>2</sub>O emissions peaked at an intermediate groundwater table level of -20 cm, and emissions were reduced by 18% when the groundwater table was at -40 cm or -5 cm (Jungkunst et al., 2008). These results follow the conceptual theory that the highest N<sub>2</sub>O fluxes occur at intermediately high water-filled pore-space (Davidson, Keller, Erickson, Verchot, & Veldkamp, 2000). Nitrous oxide is primarily produced from nitrification at low and moderate soil moistures, and denitrification becomes more important when the soil moisture content is greater than 60% water-filled pore space due a decrease in oxygen supply (Ruser et al., 2006). Forest harvest may increase soil moisture levels to about 60% in upland forests, where soil moisture levels are generally lower than in riparian zones, resulting in greater emissions following clear-cutting. However, in riparian zones, where soil moisture is already typically high due to the interaction with the surface and groundwater (Moore et al., 2005), forest harvest may increase the soil moisture levels much higher than 60%, at which N<sub>2</sub>O emissions are typically low (Jungkunst et al., 2008). This is evidenced by the relatively shallow mean groundwater table level (15.9 cm) at the no buffer sites in my study. The groundwater table is closer to the soil surface at the no buffer

sites in my study than the level that promotes peak N<sub>2</sub>O emissions as reported by Jungkunst et al. (2008). Additionally, there could have been a confounding effect of soil temperature, where at high moisture levels (typically observed in the winter) there is also low soil temperature, which has been shown to limit denitrifying activity (Maag & Vinther, 1996).

The unexpectedly low N<sub>2</sub>O fluxes at the no buffer sites could alternatively be explained by the mechanical soil disturbance in the riparian zone caused by forest harvest, as hypothesized in my Disturbance Hypothesis. The disruption of the structure and function of microbial communities responsible for nitrification and denitrification could contribute to the comparatively low N<sub>2</sub>O fluxes at the no buffer sites (Tan, Chang, & Kabzems, 2005). Meanwhile, N<sub>2</sub>O fluxes at the buffer sites were not significantly different from the reference sites, thus riparian buffers may be effective in preserving soil ecosystem conditions contributing to N<sub>2</sub>O fluxes. Disruption of the soil surface and death of tree roots was attributed to a decline in soil CO<sub>2</sub> emissions following the clear-cutting of a jack pine stand in Saskatchewan (Striegl & Wickland, 1998). Moreover, soil compaction as a result of forest harvest has been found to reduce net nitrification rates in the forest floor and mineral soil as well as reduce the soil microbial biomass nitrogen (Tan et al., 2005).

None of the measured environmental variables (i.e. soil temperature, soil moisture, and depth to the groundwater table) were significant drivers of N<sub>2</sub>O fluxes. Thus, perhaps some environmental variables not measured in this study could explain some of the unexplained treatment differences. For instance, soil nitrogen concentrations are an important driver of N<sub>2</sub>O fluxes (Christiansen & Gundersen, 2011). Thus, there may have been lower soil nitrogen

concentrations in the no buffer sites than in the reference sites. Some forest plants, notably alder, can fix organic nitrogen from atmospheric nitrogen, increasing soil nitrogen availability (Kreutzweiser et al., 2008). It is possible that the reference sites had more nitrogen-fixing plants that resulted in higher soil nitrogen levels and subsequently higher N<sub>2</sub>O fluxes. Given the reduction in litterfall following forest harvest (Moroni & Zhu, 2012), even if the reference sites did not have more nitrogen-fixing species, the reduced nitrogen inputs from the lack of fallen tree litter could have contributed to the trend of higher soil N<sub>2</sub>O emissions at reference sites observed in this study.

As hypothesized, soil moisture, soil temperature, and depth to the groundwater table were important drivers of GHG fluxes. Soil moisture and depth to the groundwater table were the dominant drivers of CH<sub>4</sub> fluxes. Methane is produced under anaerobic conditions and is consumed under aerobic conditions, thus soil moisture is a key factor in the dynamics of CH<sub>4</sub> fluxes from soils (Christiansen et al., 2012; Oertel et al., 2016). The shallow water tables and high soil organic matter content in riparian zones have the potential to contribute significant amounts of CH<sub>4</sub> to the atmosphere (Vidon et al., 2018). However, in this study, the riparian soils were on average a weak methane sink. Soil temperature, soil moisture, and depth to the groundwater table were significant predictors of CO<sub>2</sub> fluxes. This is consistent with the large body of literature on the drivers of soil respiration (Luo & Zhou, 2006). Soil respiration usually increases exponentially with temperature, reaches a maximum, and then declines (Luo & Zhou, 2006). Temperature controls many aspects of soil respiration from the activity of cellular enzymes, to root growth and microbial activity (Luo & Zhou, 2006). Soil moisture is another well-established driver of soil CO<sub>2</sub> emissions, with the common conceptual relationship where

soil respiration is low under dry conditions, reaches a maximum at intermediate soil levels, and decreases at high soil moisture content where anaerobic conditions depress aerobic microbial activity (Luo & Zhou, 2006). The interactive effects of these two variables on soil respiration is a key knowledge gap (Meyer et al., 2018), thus our research provides valuable information to help understand the effects of these factors on soil respiration in the unique riparian environment. Conversely, depth to the groundwater table was not a significant predictor of CO<sub>2</sub> fluxes, even though soil moisture was. This is likely because other factors contributing to soil moisture, such as precipitation, play an important role. The importance of precipitation events is evidenced by research on the pulsing effect whereby soil respiration increases within minutes of the onset of rainfall, driven by the renewed mineralization and availability of easily decomposable materials for the metabolism of reactivated microbes (Luo & Zhou, 2006).

#### **2.4.2 Effects of local groundwater conditions**

I hypothesized that due to the higher soil moisture at DIS areas, the emission of anaerobically produced CH<sub>4</sub> and N<sub>2</sub>O would be higher than at ND areas. There were no significant differences between the DIS and ND areas for CO<sub>2</sub> and N<sub>2</sub>O emissions, although ND areas generally had higher CO<sub>2</sub> emissions on average and DIS areas generally had higher N<sub>2</sub>O emissions on average. However, the CH<sub>4</sub> flux results supported my hypothesis that groundwater discharge conditions control the spatial occurrence and magnitude of fluxes. Methane uptake was significantly lower in the DIS sites compared to the ND sites. This means that DIS sites were more likely to be CH<sub>4</sub> sources, while ND sites were more likely to be CH<sub>4</sub> sinks. Similar results were found in riparian zones in central Indiana, where a topographic depression in the riparian forest accounted for 78% of annual CH<sub>4</sub> emissions, despite only covering <8% of the total land area (Jacinthe et al., 2015).

Additionally, GHG fluxes from flowing stream waters have been found to peak downstream of DIS areas, due to their lateral gas inputs from riparian soils (Lupon et al., 2019). Given that methane fluxes were highest in DIS areas at no buffer sites, the results of my study provide additional support for the use of hydrologically adapted buffers, which provide more protection for wet areas, such as DIS areas, in the riparian zone (Tiwari et al., 2016). The variable buffer width adapted to site-specific hydrological conditions can protect biogeochemical and ecological functions as well as provide economic savings when compared to fixed width buffers (Tiwari et al., 2016).

Counter to my hypothesis, I did not see statistically significantly higher N<sub>2</sub>O emissions in DIS areas, although emissions were on average slightly higher in these areas. This result may have been observed because the DIS areas had soil moisture levels that were higher than the optimal soil volumetric water content for N<sub>2</sub>O production (Christiansen et al., 2012). Nitrous oxide emissions are highest at intermediate moisture levels, with peak N<sub>2</sub>O efflux measured at 40 to 60 % volumetric soil water content in a temperate deciduous forest soil (Christiansen et al., 2012). The mean volumetric soil water content at the DIS areas in this study was 55.4%, thus the moisture conditions would often be higher than those ideal for N<sub>2</sub>O production.

### **2.4.3 Conclusions**

In conclusion, my work shows that forest harvest and local groundwater conditions influence GHG emissions from riparian forest soils alongside headwater streams. The riparian forests investigated in this study were a net sink for CH<sub>4</sub>, and a net source for CO<sub>2</sub> and N<sub>2</sub>O. There were no treatment differences for CO<sub>2</sub> fluxes. Methane emissions were significantly higher at the no

buffer sites than the reference sites, which was in line with the body of literature on forestry impacts on CH<sub>4</sub> fluxes; and N<sub>2</sub>O emissions were significantly higher at the reference sites than at the no buffer sites, which did not align with many studies of upland forest harvest. My results were consistent with the assertion that soil temperature, soil moisture, and depth to the groundwater table regulate CO<sub>2</sub> fluxes, and soil moisture and depth to the groundwater table regulate CH<sub>4</sub> fluxes. In addition, I observed that local groundwater conditions play an important role in driving CH<sub>4</sub> fluxes, with significantly higher emissions in DIS than ND areas.

Considering that neither soil moisture, soil temperature, nor depth to the groundwater table explained N<sub>2</sub>O emissions, other controlling variables such as soil nutrient concentrations should be explored. Moreover, given that the treatment effects on N<sub>2</sub>O fluxes followed my Disturbance Hypothesis, measuring some metric of soil disturbance of the microbial community, such as microbial biomass carbon, would help to provide additional support for this assertion. It would also be interesting to examine riparian soil GHG fluxes sooner after harvest, to see if there are greater effects on CO<sub>2</sub>. The results of this research provide important information for GHG budgets, by observing GHG fluxes in riparian forests, which are often not considered separately from upland forests, despite their unique conditions. Moreover, my results demonstrate that riparian buffers may be effective in protecting soil ecosystem functions contributing to CH<sub>4</sub> and N<sub>2</sub>O fluxes, which may be useful to forest managers interested in managing riparian buffer zones for GHG balance and climate change mitigation.

## **Chapter 3: Temporal and micro-topographical variations in greenhouse gas fluxes from riparian forest soils along headwater streams**

### **3.1 Introduction**

Soils play an important role in the carbon cycle, and subsequently climate change, as the Earth's soils contain three times more carbon than the atmosphere (Lal, Negassa, & Lorenz, 2015).

Depending on the conditions of the ecosystem, soils can sequester carbon or be sources of greenhouse gases (GHGs) to the atmosphere (Oertel et al., 2016). Improving our understanding of the controls on the rates of GHG fluxes to the atmosphere is important for reducing uncertainty in global estimates of carbon cycling to help mitigate climate change (Oertel et al., 2016; Sun et al., 2013).

Greenhouse gas fluxes from soils are primarily biogenic in origin, i.e., produced by living organisms in the soil. The production of three important gases emitted from soils—carbon dioxide (CO<sub>2</sub>), methane (CH<sub>4</sub>), and nitrous oxide (N<sub>2</sub>O)—is strongly controlled by soil temperature and soil moisture (Luo & Zhou, 2006). Carbon dioxide emissions consist of the combined emissions from root respiration (autotrophic respiration) and microbial decomposition of organic matter (heterotrophic respiration) (Luo & Zhou, 2006). As such, CO<sub>2</sub> emissions are also affected by substrate availability (Luo & Zhou, 2006). Methane is produced by methanogens in anaerobic conditions, and consumed by methanotrophs in aerobic conditions (Oertel et al., 2016). Besides low-oxygen conditions and soil temperature, soil pH and substrate availability impact the microbial community contributing to CH<sub>4</sub> exchange (Serrano-Silva et al., 2014).

Nitrous oxide is primarily produced by denitrification under anaerobic conditions, in addition to nitrification under aerobic conditions (Oertel et al., 2016). Other important factors influencing these processes are nitrogen deposition and fertilization, as well as soil pH (Dalal & Allen, 2008).

While several studies have evaluated GHG fluxes from forests (as summarized in Dalal and Allen [2008] and Oertel et al. [2016]), studies on GHG emissions from the riparian areas of forests remain limited (Goodrick et al., 2016; Soosaar et al., 2011). Moreover, the majority of riparian GHG flux research is conducted in the riparian zone of wetlands, not streams (Audet et al., 2013; Nag et al., 2017), or if the focus is on streams they are in an agricultural buffer context (Fisher, Jacinthe, Vidon, Liu, & Baker, 2014; Skinner et al., 2014). Moreover, many of these studies only focus on CO<sub>2</sub>, neglecting CH<sub>4</sub> and N<sub>2</sub>O (Tufekcioglu et al., 2001). Because of the unique conditions of riparian ecosystems, the drivers of gas fluxes may differ from those in non-riparian areas (Goodrick et al., 2016).

The ecosystem for this study, the riparian zones of headwater streams in southwestern British Columbia, was chosen for its unique conditions and ecological importance. Riparian zones, that is, the three dimensional zones of direct interaction between terrestrial and aquatic ecosystems (Gregory et al., 1991), are important for nutrient cycling (Hinshaw & Dahlgren, 2016), biodiversity (Ramey & Richardson, 2017), and carbon sequestration (Hazlett et al., 2005). Carbon storage generally increases with wetter conditions where decomposition of organic matter is limited by oxygen, thus decreasing soil respiration (Gundersen et al., 2010). Due to the typically moist conditions as a result of the influence of surface and belowground water, riparian

zones can sequester more carbon than many upland forests (Gundersen et al., 2010). Conversely, due to their shallow and fluctuating water tables (Goodrick et al., 2016), hydromorphic (wet) soils (Gundersen et al., 2010), and high soil organic matter content, riparian zones have the potential to contribute significant amounts of CH<sub>4</sub> and N<sub>2</sub>O to the atmosphere (Vidon et al., 2018). Small streams occur at a high density in forested landscapes of the Pacific Northwest, with about 2.5 small streams per square kilometer (Richardson, Naiman, Swanson, & Hibbs, 2005). As such, the extent and unique conditions of riparian zones are relevant to climate change, since CH<sub>4</sub> and N<sub>2</sub>O are GHGs with high global warming potentials (Christiansen et al., 2012). Given that riparian zones may be hotspots of GHG fluxes to the atmosphere, it is critical to improve our understanding of the magnitudes, as well as the spatial and temporal variability, of GHG fluxes in these systems. Soil moisture and soil temperature have a strong influence on the ecosystem processes driving GHG emissions, thus it is perhaps not surprising that seasonal variation can impact gas fluxes (Sun et al., 2013). For example, CO<sub>2</sub> emissions are expected to peak during time periods when daily air temperatures are highest (Sun et al., 2013). Nitrous oxide emissions have also been found to peak in warmer summer months, with lower emissions in autumn to the following spring (De Carlo et al., 2019). In addition, freeze-thaw cycles can enhance N<sub>2</sub>O emissions in winter months by releasing nutrients for microbial metabolism through disaggregation of soil particles (De Carlo et al., 2019; Oertel et al., 2016). Improving our understanding of these seasonal dynamics of GHG fluxes in riparian zones of headwater streams will contribute to informing more accurate carbon budgets for these understudied ecosystems (Sun et al., 2013).

Landscape features that dictate soil characteristics, such as local microtopography and hydrogeomorphic setting, can be important for predicting riparian GHG emissions as they may affect the spatial distribution of soil moisture, nutrients, and organic matter, thus consequently affecting the intensity of GHG emissions (Jacinthe & Vidon, 2017; Soosaar et al., 2011). Local groundwater discharge conditions may create particularly important micro-site variation in the riparian zones of streams. Groundwater discharge (DIS) areas, or discrete riparian inflow points, are the result of upland-originating groundwater converging and discharging in a depression in the riparian zone (Kuglerová et al., 2014b). Soil conditions at DIS areas have been found to have higher base cation and nitrogen concentrations, soil moisture, and pH levels when compared to surrounding non-groundwater discharge (ND) areas (Giesler et al., 1998), resulting in hotspots of riparian plant species richness (Kuglerová et al., 2014b). These soil conditions may also influence the processes controlling soil GHG fluxes. For instance, a topographic depression in a riparian forest accounted for 78% of annual CH<sub>4</sub> emissions, despite only covering <8% of the total land area (Jacinthe et al., 2015). Additionally, recent evidence suggests that in-stream GHG fluxes peak downstream of DIS areas, likely from lateral gas inputs from riparian soils (Lupon et al., 2019). However, it is uncertain if similar trends will be observed alongside headwater streams in coastal British Columbia. The wet climate in the region and the close connectivity of headwater riparian zones with groundwater (Moore et al., 2005; Richardson, 2019) may reduce the distinct conditions between DIS and ND areas.

In this study, I evaluated the spatial and temporal variation of soil GHG fluxes from the forested riparian zone of two relatively undisturbed headwater streams in the Pacific coastal temperate rainforest. The objectives were (1) to quantify the effects of local riparian groundwater

conditions on soil GHG flux rates, and (2) to examine the effects of temporal variation on GHG fluxes from riparian soils. I hypothesized that DIS areas, will have higher soil moisture from groundwater influence compared to ND areas, resulting in greater anaerobically produced CH<sub>4</sub> and N<sub>2</sub>O emissions, and lower aerobically produced CO<sub>2</sub> emissions. I further hypothesized that riparian soil GHG fluxes would have significant temporal variation associated with seasonal changes in soil temperature and soil moisture, with peak gas emissions occurring in the warmest and/or wettest season or month.

### **3.2 Methods**

For the site description, experimental design, soil sampling and analysis, and greenhouse gas sampling and analysis please refer to the Methods section (2.2) in Chapter 2. Any deviations from those methods are described below. For the spatial and temporal analysis of GHG fluxes from riparian soils alongside headwater streams in this Chapter, I focused on two relatively undisturbed stream sites (Mike Ck. and Upper East Ck.), as a subset of the nine sites observed in Chapter 2. The reduction in sites was due to the time and cost involved in annual GHG sampling. Sampling occurred on a weekly basis from May to September 2019, and on an approximately monthly basis from October 2019 to May 2020. In all figures, weekly flux rate values are averaged to a monthly value. Soil moisture and depth to the groundwater table were measured at each of the six chambers at each site at each gas sampling occasion. Soil temperature was measured continuously throughout the study period using four ibutton dataloggers per site. Two ibuttons were buried a few metres from the most upstream and downstream chamber at Upper East Ck. and Mike Ck., respectively; one at 0.5 m and the other at 1.5 m from the bank full stream width to coordinate with a parallel study. The remaining two ibuttons were buried beside

two chambers (one in a DIS and one in a ND area) at each site, no more than 0.5 from the chamber. Due to user error, the latter two ibuttons only recorded until November 2019, as reflected in Figure 3.1 of the Results section. Soil temperature measurements for the period of January 12 to January 22, 2020 were excluded from analysis due to data logger malfunction during this period. The data was divided into seasons using the days of the spring and fall equinox, and summer and winter solstice.

Quality control measures as well as Cook's Distance statistical test to identify influential outliers resulted in the removal of 11% of flux rate data points for CO<sub>2</sub>, 7% for CH<sub>4</sub>, and 27% for N<sub>2</sub>O. For statistical analysis, all of the models met the assumptions of normality, and did not need to be transformed. Annual GHG emission rates were calculated from the sum of weekly average emission rates. Weeks with missing data were interpolated from previous and subsequent weeks' data. I acknowledge that my statistical models are pseudoreplicated as I only examined two streams, thus limiting statistical inference and universality of the results. As such, the results should be considered as a case study. However, we can still glean important information, particularly as the dynamics of GHG fluxes from riparian areas of headwater streams is an understudied area of research.

### **3.3 Results**

#### **3.3.1 Environmental variables**

The mean annual soil temperature for the Mike Ck. and Upper East Ck. sites was  $8.6 \pm 4.4$  °C and  $8.2 \pm 4.7$  °C, respectively (Figure A.1). The highest daily average temperature was 17.0 °C

in August at Mike Ck., and the lowest daily average temperature was 0.7 °C in March at Upper East Ck. (excluding the 10-day period in January, which was possibly even colder). When averaged across the two sites, mean daily soil temperature was 14.3 °C in the summer,  $7.7 \pm 2.8$  in the fall,  $7.3 \pm 3.1$  in the spring, and 3.8 °C in the winter. In the summer, mean daily soil temperature was  $14.6 \pm 1.3$  °C at a subset of the DIS areas and  $14.0 \pm 1.1$  °C at a subset of the ND areas (Figure 3.1). For a summary of weekly maximum and minimum values for soil temperature, soil moisture, and depth to the groundwater table refer to Table A.4 in the Appendix.

The mean annual soil moisture at the Mike Ck. and Upper East Ck. sites was  $52.5 \pm 11.8\%$  and  $44.0 \pm 12.5\%$ , respectively (Figure 3.2). The highest measured mean soil moisture was 76.0% in December at Upper East Ck., and the lowest mean soil moisture was 5.6% in May at Mike Ck.. When averaged across the two sites, mean soil moisture was  $55.4 \pm 10.2\%$  in the winter,  $51.9 \pm 11.5$  in the fall,  $49.4 \pm 12.4\%$  in the spring, and  $46.8 \pm 13.4 \%$  in the summer. Annual mean soil moisture was 1.16 times higher at the DIS areas ( $54.3 \pm 9.5\%$ ) than at the ND areas ( $46.8 \pm 13.6\%$ ).

The mean annual depth to the groundwater table for Mike Ck. and Upper East Ck. was  $27.1 \pm 8.1$  cm and  $26.7 \pm 12.5$  cm, respectively (Figure 3.3). The highest water table depth was 2 cm above the ground surface (flooding) on a rainy day in June at a DIS area at Mike Ck. The water table was deeper than what the well could measure on 35% of sampling occasions, which occurred most often (48%) in the summer. When averaged across the two sites, the mean depth to the groundwater table was  $28.8 \pm 8.2$  cm in the spring, closely followed by  $28.4 \pm 8.3$  cm in the

summer and  $27.5 \pm 9.5$  cm in the winter. The shallowest mean seasonal depth to the groundwater table was  $22.1 \pm 11.8$  cm in the fall. On average over the year, the water table was closer to the soil surface at the DIS areas ( $26.2 \pm 9.8$  cm) compared to the ND areas ( $27.5 \pm 9.5$  cm). In the fall, the season with the shallowest mean groundwater table level, the groundwater table was closer to the soil surface in the DIS ( $20.1 \pm 12.4$  cm) areas compared to the ND ( $23.2 \pm 11.6$  cm) areas. However, in the spring, the season with the deepest mean groundwater table level the mean levels in the DIS ( $28.9 \pm 6.6$  cm) and ND ( $28.7 \pm 9.2$  cm) areas were more similar.

### **3.3.2 Spatial and temporal variation in greenhouse gas fluxes**

None of the greenhouse gas flux rates were significantly different between DIS and ND areas GHG (Table 3.1). In addition, there were no statistically significant differences in the environmental variables of soil temperature, soil moisture, and depth to groundwater between the DIS and ND areas (Table A.5). Although on average soil moisture and soil temperature were higher, and the depth to the groundwater table was lower in the DIS areas (Table 3.2). On average, CO<sub>2</sub> emission rates ( $\text{mg CO}_2\text{-C m}^{-2} \text{ h}^{-1}$ ) were 1.35 times lower in DIS areas ( $48.8 \pm 27.5$ ) compared to the ND areas ( $65.7 \pm 35.8$ ). Methane uptake rates ( $\mu\text{g CH}_4\text{-C m}^{-2} \text{ h}^{-1}$ ) were 1.71 times lower in DIS ( $-17.0 \pm 11.7$ ) areas compared to the ND ( $-29.1 \pm 19.3$ ) areas (Figure 3.4, Figure 3.5). There was no difference in the N<sub>2</sub>O average annual flux ( $\mu\text{g N}_2\text{O-N m}^{-2} \text{ h}^{-1}$ ) between the DIS ( $2.7 \pm 2.8$ ) and ND ( $2.7 \pm 2.8$ ) areas (Figure 3.6).

On average, CO<sub>2</sub> fluxes ( $\text{mg CO}_2\text{-C m}^{-2} \text{ h}^{-1}$ ) were 2.73 times higher in the summer ( $75.6 \pm 33.1$ ) than in the winter ( $27.7 \pm 21.8$ ), with intermediate levels in the fall ( $48.5 \pm 28.3$ ) and spring ( $56.7 \pm 27.7$ ) (Figure 3.4). In terms of cumulative annual CO<sub>2</sub> emissions, 40% were emitted in the

summer, 26% in the spring, 20% in the fall, and 14% in the winter. In the summer, CO<sub>2</sub> emissions (mg CO<sub>2</sub>-C m<sup>-2</sup> h<sup>-1</sup>) ranged from 8.2 to 154.6. In the spring, CO<sub>2</sub> emissions ranged from 11.0 to 130.4 mg CO<sub>2</sub>-C m<sup>-2</sup> h<sup>-1</sup>. In the fall, CO<sub>2</sub> emissions ranged from 7.9 to 117.9 mg CO<sub>2</sub>-C m<sup>-2</sup> h<sup>-1</sup>. In the winter, CO<sub>2</sub> emissions ranged from 3.3 to 90.9 mg CO<sub>2</sub>-C m<sup>-2</sup> h<sup>-1</sup>. The cumulative annual CO<sub>2</sub> emissions were 419.4 g CO<sub>2</sub>-C m<sup>-2</sup> yr<sup>-1</sup> (Figure 3.2).

Average CH<sub>4</sub> uptake rates (μg CH<sub>4</sub>-C m<sup>-2</sup> h<sup>-1</sup>) were 1.53 times higher in the spring (-31.1 ± 23.8) than in the fall (-20.3 ± 15.8), with intermediate levels in the summer (-25.0 ± 15.5) and winter (-22.3 ± 22.5) (Figure 3.5). The largest percent of annual CH<sub>4</sub> fluxes were taken up in the winter (30%), followed by 28% in the summer, 25% in the spring, and 17% in the fall. In the winter, CH<sub>4</sub> fluxes (μg CH<sub>4</sub>-C m<sup>-2</sup> h<sup>-1</sup>) ranged from -72.6 to 0.04. In the summer, CH<sub>4</sub> fluxes ranged from -71.9 to 9.3 μg CH<sub>4</sub>-C m<sup>-2</sup> h<sup>-1</sup>. In the spring, CH<sub>4</sub> fluxes ranged from -71.7 to 18.2 μg CH<sub>4</sub>-C m<sup>-2</sup> h<sup>-1</sup>. In the fall, CH<sub>4</sub> fluxes ranged from -61.7 to 6.3 μg CH<sub>4</sub>-C m<sup>-2</sup> h<sup>-1</sup> (Figure 3.3). The cumulative annual CH<sub>4</sub> fluxes were -206.5 mg CH<sub>4</sub>-C m<sup>-2</sup> yr<sup>-1</sup>.

Nitrous oxide fluxes (μg N<sub>2</sub>O-N m<sup>-2</sup> h<sup>-1</sup>) were lower in the winter (-0.02 ± 4.1) than in the spring (3.0 ± 2.2), summer (3.9 ± 2.3), and fall (2.0 ± 1.7) (Figure 3.6). In terms of cumulative annual N<sub>2</sub>O emissions, 53% were emitted in the summer, 33% in the spring, 20% in the fall, and -6% in the winter. In the summer, N<sub>2</sub>O fluxes (μg N<sub>2</sub>O-N m<sup>-2</sup> h<sup>-1</sup>) ranged from 0.44 to 9.35. In the spring, N<sub>2</sub>O fluxes ranged from 0.11 to 7.9 μg N<sub>2</sub>O-N m<sup>-2</sup> h<sup>-1</sup>. In the fall, N<sub>2</sub>O fluxes ranged from -0.75 to 6.14 μg N<sub>2</sub>O-N m<sup>-2</sup> h<sup>-1</sup>. In the winter, N<sub>2</sub>O fluxes ranged from -7.0 to 8.5 μg N<sub>2</sub>O-N m<sup>-2</sup> h<sup>-1</sup> (Figure 3.4). Cumulative annual N<sub>2</sub>O emissions were 17.1 mg N<sub>2</sub>O-N m<sup>-2</sup> yr<sup>-1</sup>.

According to the LME models, soil temperature was a significant predictor of CO<sub>2</sub> and N<sub>2</sub>O fluxes, where a one *SD* increase in soil temperature resulted in 18.4 mg increase in CO<sub>2</sub> emissions and a 1.4 µg increase in N<sub>2</sub>O fluxes (Figure 3.7 and 3.9, Table 3.1). The marginal r<sup>2</sup> values for the soil temperature models for CO<sub>2</sub> and N<sub>2</sub>O were 0.78 and 0.67, respectively. Soil moisture was a significant term in the model explaining CH<sub>4</sub> and N<sub>2</sub>O fluxes (Figure 3.8 and 3.9, Table 3.1). For a one *SD* increase in soil moisture, CH<sub>4</sub> fluxes increased by 4.0 µg, and N<sub>2</sub>O fluxes increased by 1.1 µg. The marginal r<sup>2</sup> values for the soil moisture models for CH<sub>4</sub> and N<sub>2</sub>O were 0.14 and 0.23, respectively. Additionally, depth to the groundwater table were significant terms in the model explaining N<sub>2</sub>O fluxes, with a marginal r<sup>2</sup> of 0.14 (Figure 3.9, Table 3.1). For every one *SD* increase in depth to the groundwater table, N<sub>2</sub>O fluxes increased by 0.5 µg.

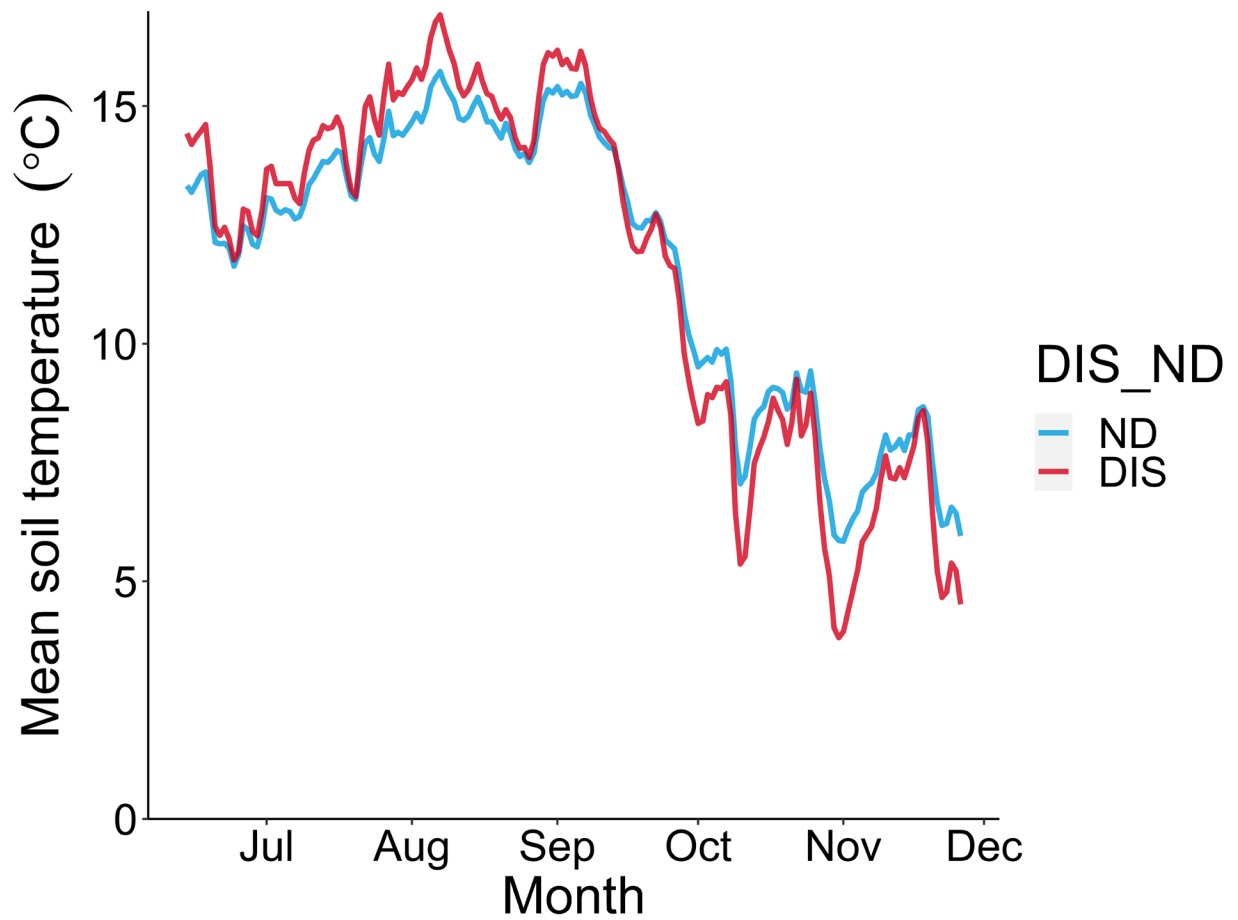


Figure 3.1 Mean daily soil temperature measured ~10 cm below the soil surface in the riparian zone of two headwater streams in groundwater discharge (DIS, in blue) and non-groundwater discharge (ND, in red) conditions from June 2019 to November 2019. See Figure A.1 in Appendix B for mean soil temperature by site for the entire study period.

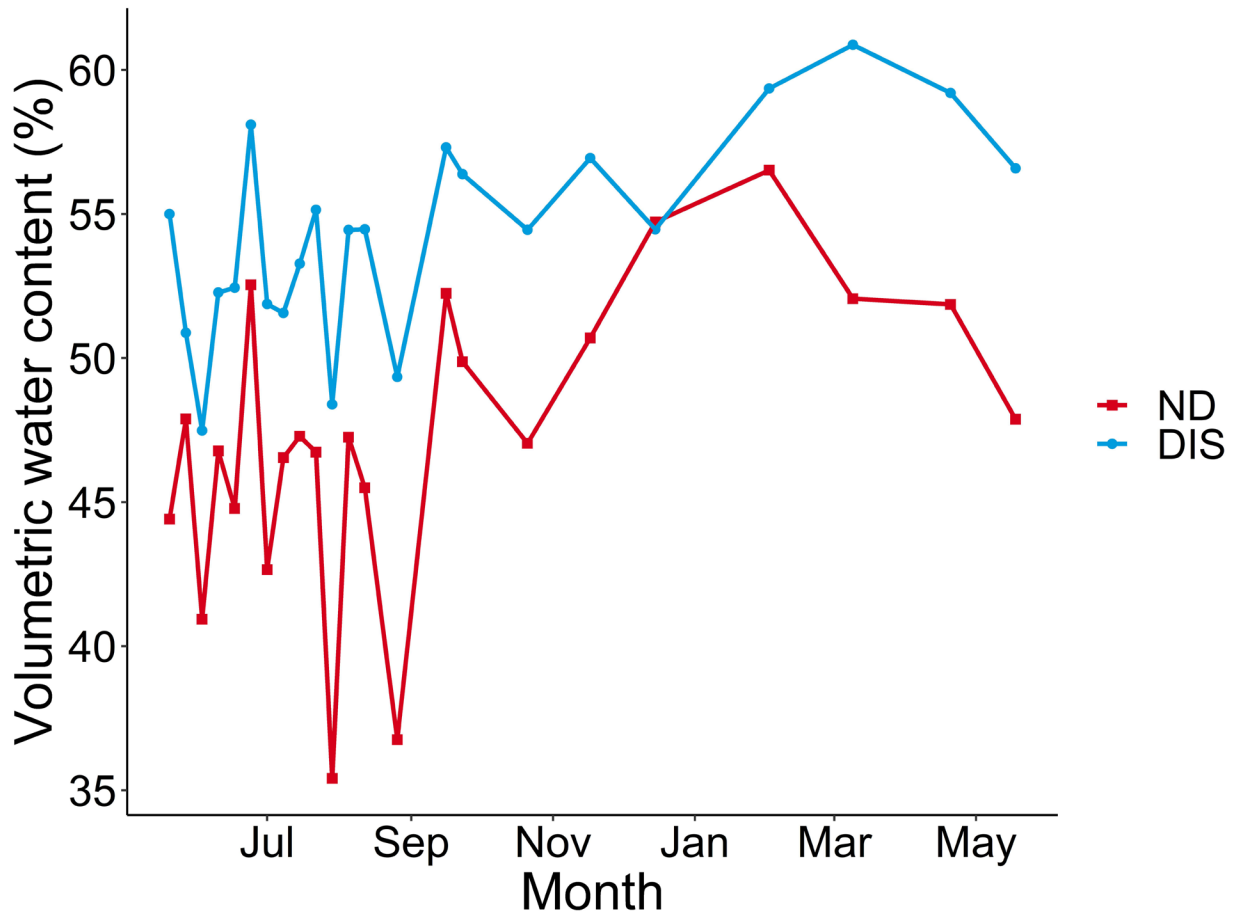


Figure 3.2 Mean volumetric soil water content (%) in groundwater discharge (DIS) and non-groundwater discharge (ND) areas of riparian soils alongside along two headwater streams in southwestern British Columbia from May 2019 to May 2020. Lines connecting the points are for visual effect only and are not meant to indicate continuous measurements.

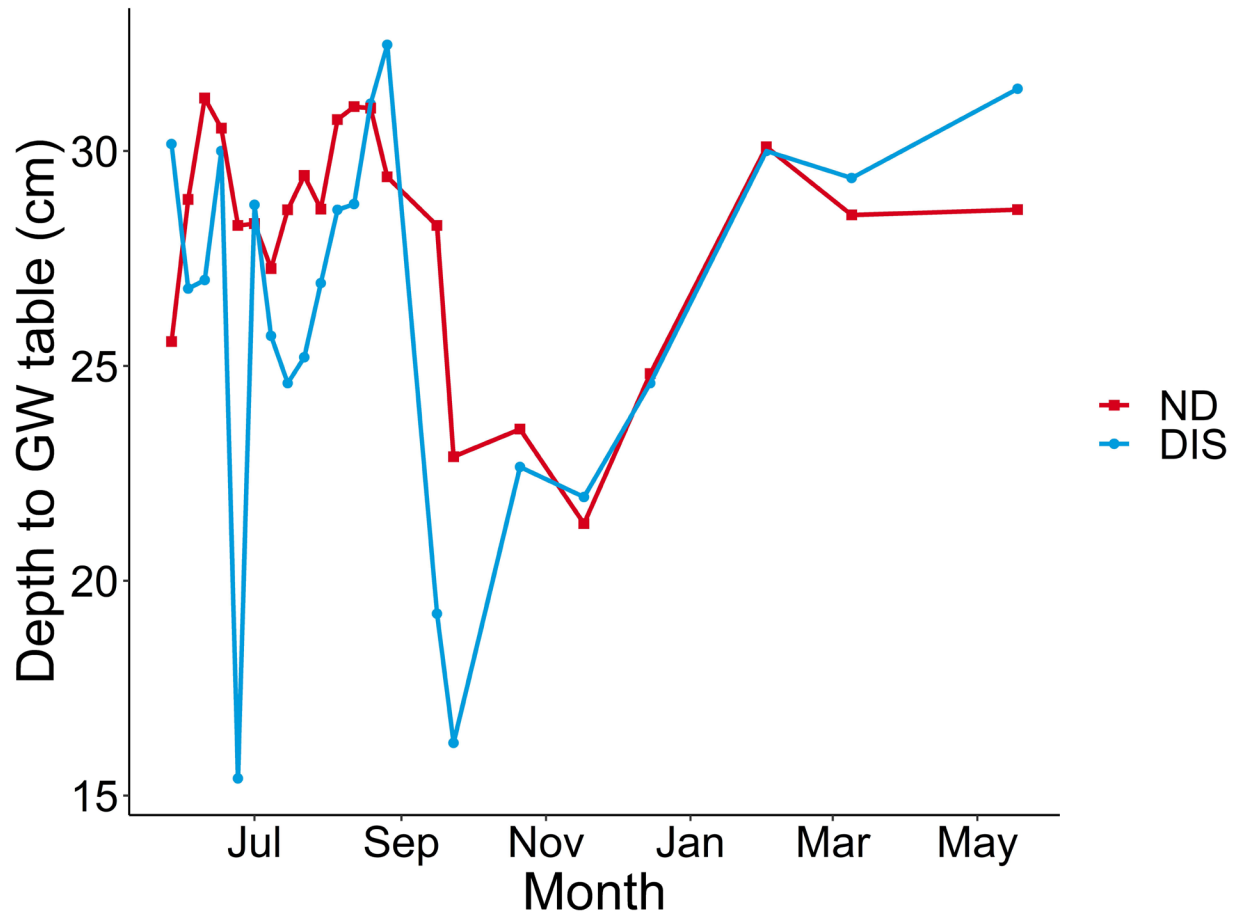


Figure 3.3 Mean depth to the groundwater table (cm) in groundwater discharge (DIS) and non-groundwater discharge (ND) areas of riparian soils alongside along two headwater streams in southwestern British Columbia from May 2019 to May 2020. Lines connecting the points are for visual effect only and are not meant to indicate continuous measurements.

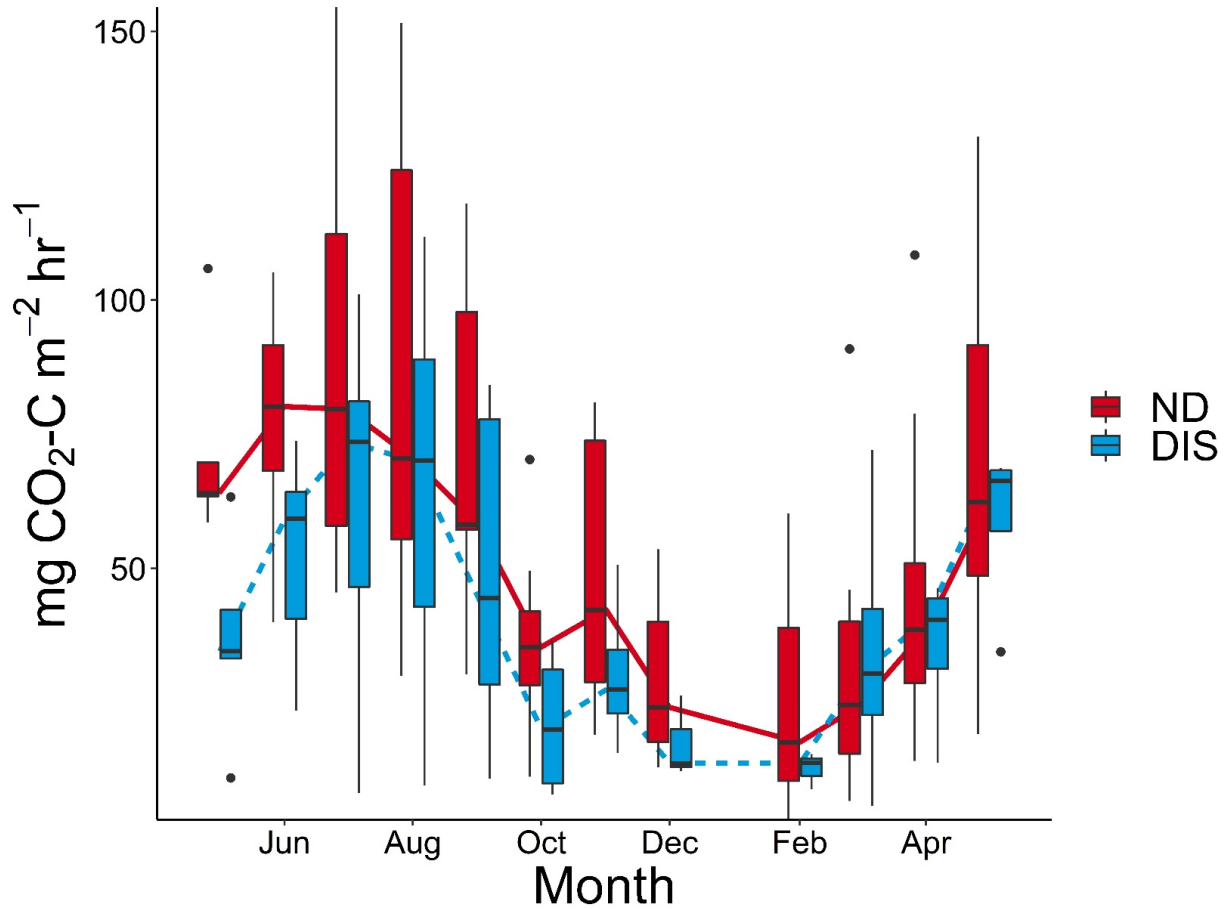


Figure 3.4 Riparian forest soil carbon dioxide emission rates ( $\text{mg CO}_2\text{-C m}^{-2} \text{ h}^{-1}$ ) from groundwater discharge (DIS) and non-groundwater discharge (ND) areas of forested riparian areas alongside two headwater streams in the Pacific coastal temperate rainforest of British Columbia from May 2019 to May 2020. Boxplots display the median, 25<sup>th</sup> and 75<sup>th</sup> percentiles, whiskers (1.5 times the IQR), and individual outliers (dots), for this and all subsequent boxplots.

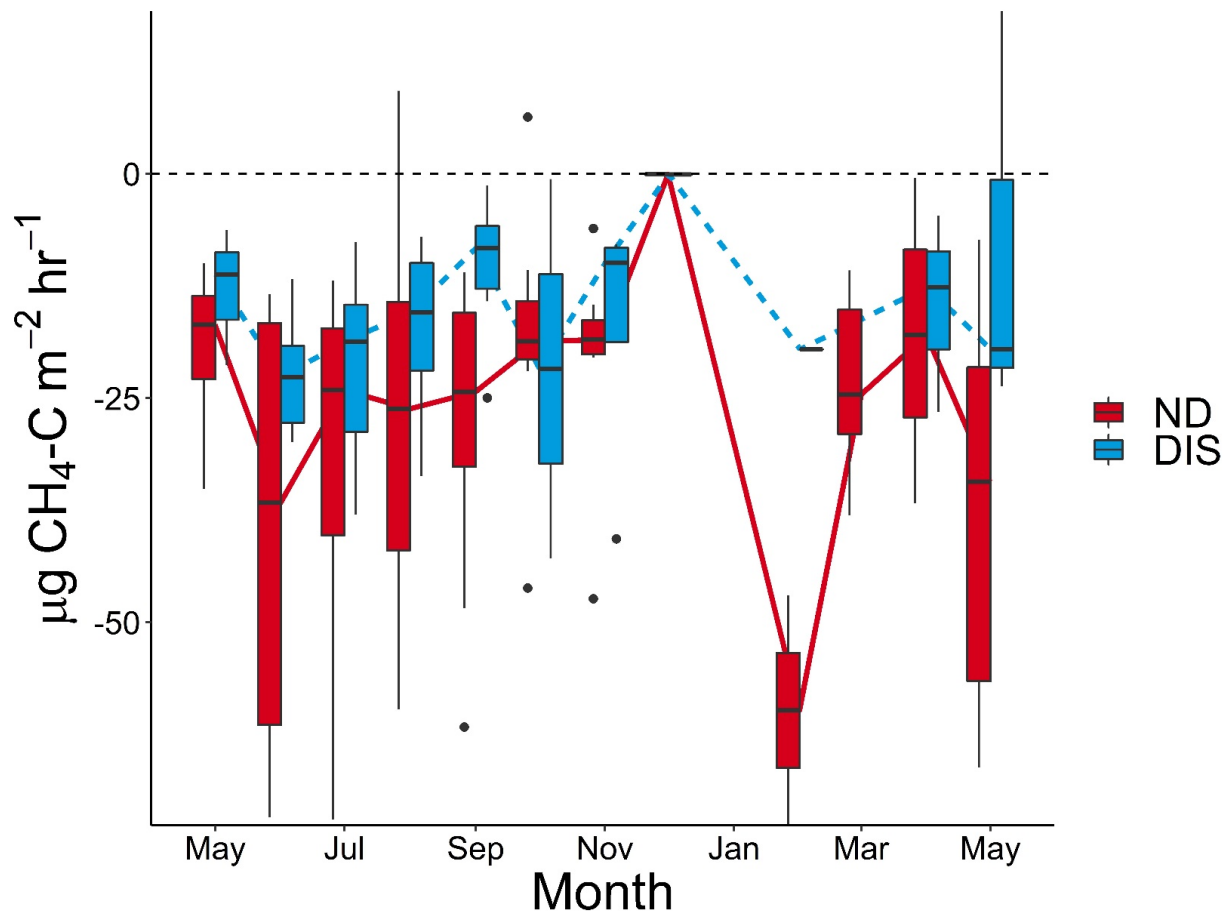


Figure 3.5 Riparian forest soil methane emission rates ( $\mu\text{g CH}_4\text{-C m}^{-2} \text{ h}^{-1}$ ) from groundwater discharge (DIS) and non-groundwater discharge (ND) areas of forested riparian zones alongside two headwater streams in the Pacific coastal temperate rainforest of British Columbia from May 2019 to May 2020.

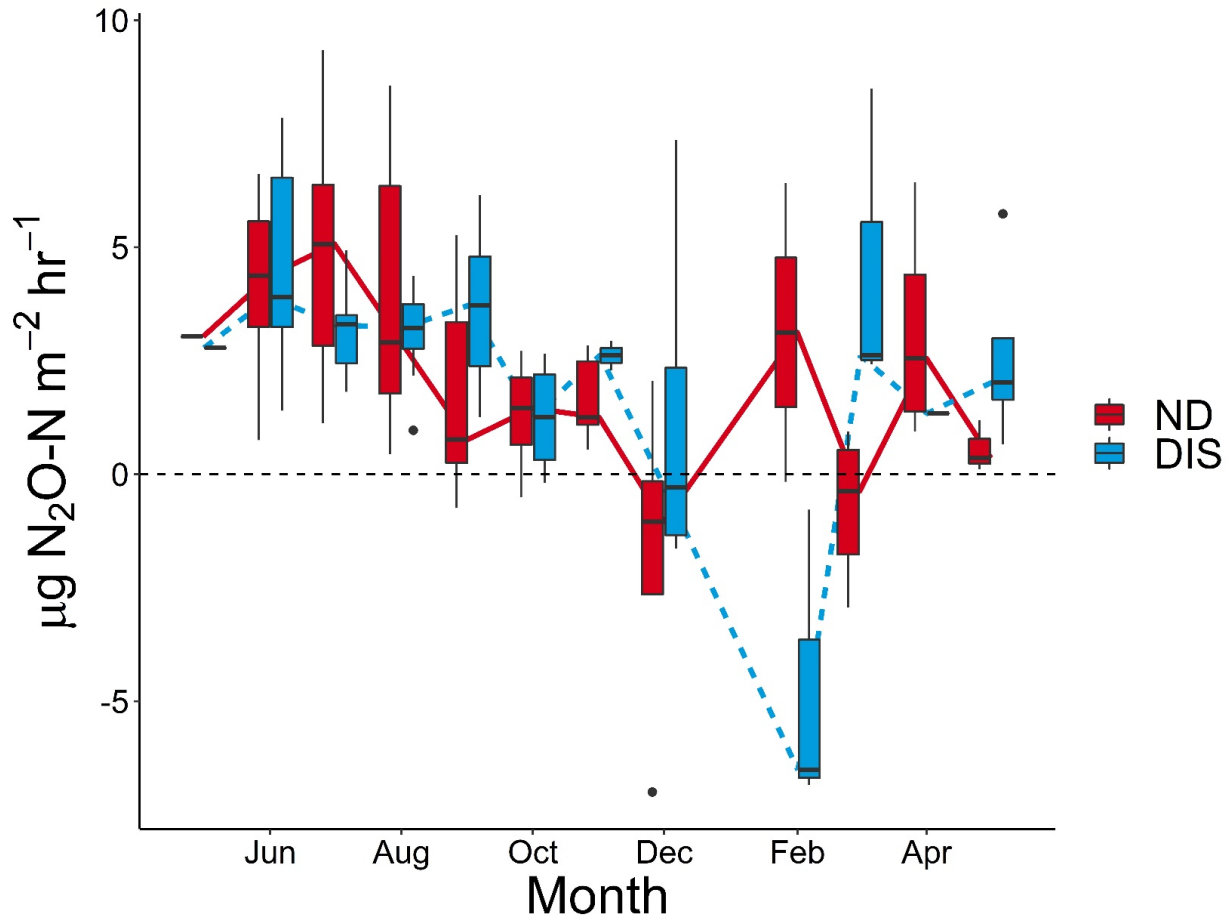


Figure 3.6 Riparian forest soil nitrous oxide emission rates ( $\mu\text{g N}_2\text{O-N m}^{-2} \text{ h}^{-1}$ ) from groundwater discharge (DIS) and non-groundwater discharge (ND) areas of forested riparian zones alongside two headwater streams in the Pacific coastal temperate rainforest of British Columbia from May 2019 to May 2020.

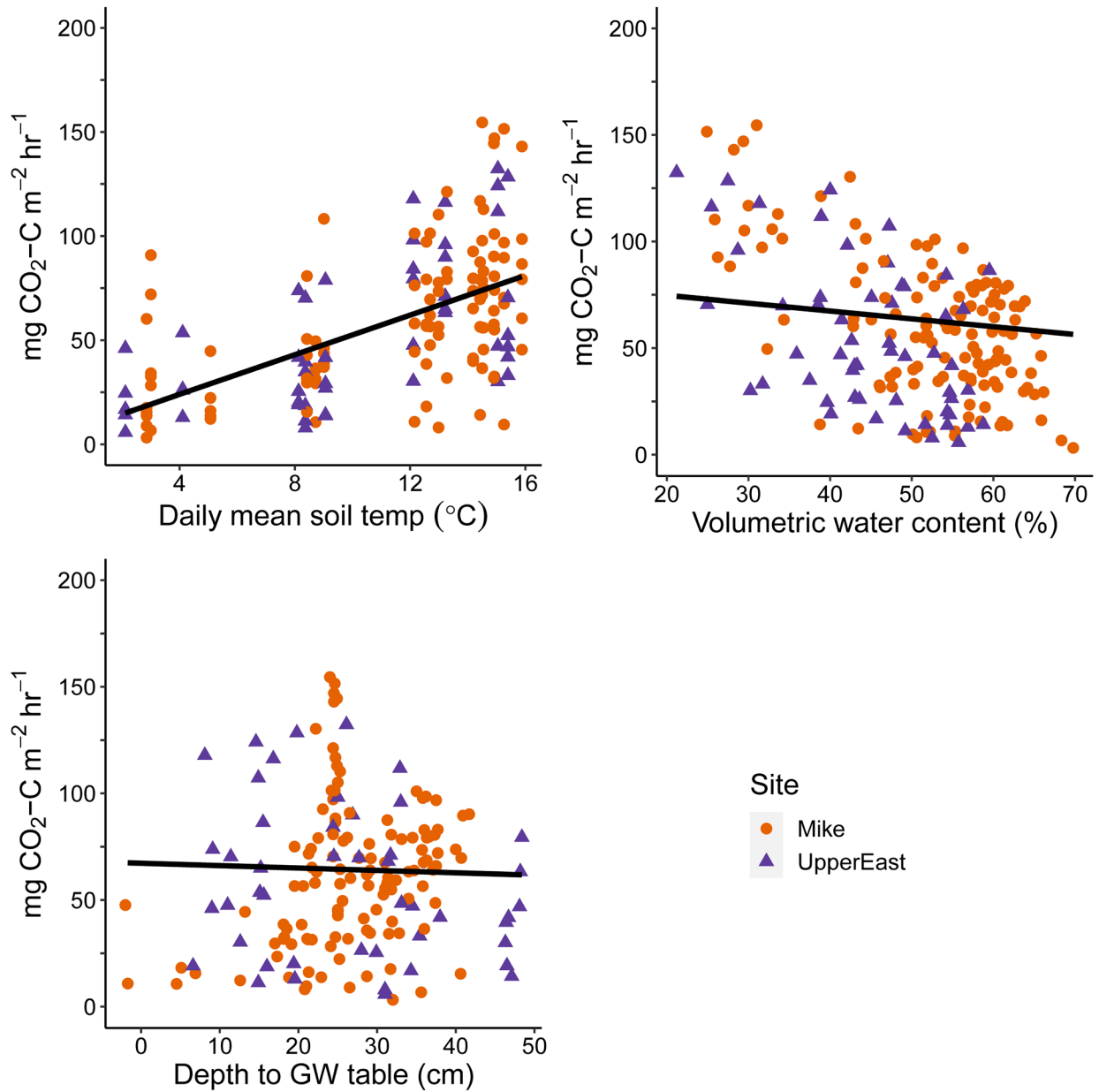


Figure 3.7 Relationships between carbon dioxide gas fluxes and the environmental variables of daily mean soil temperature, mean soil moisture, and depth to groundwater table, by site. Trend lines are based on LME models accounting for autocorrelation in the relationship between the two variables for Mike Ck. and Upper East Ck..

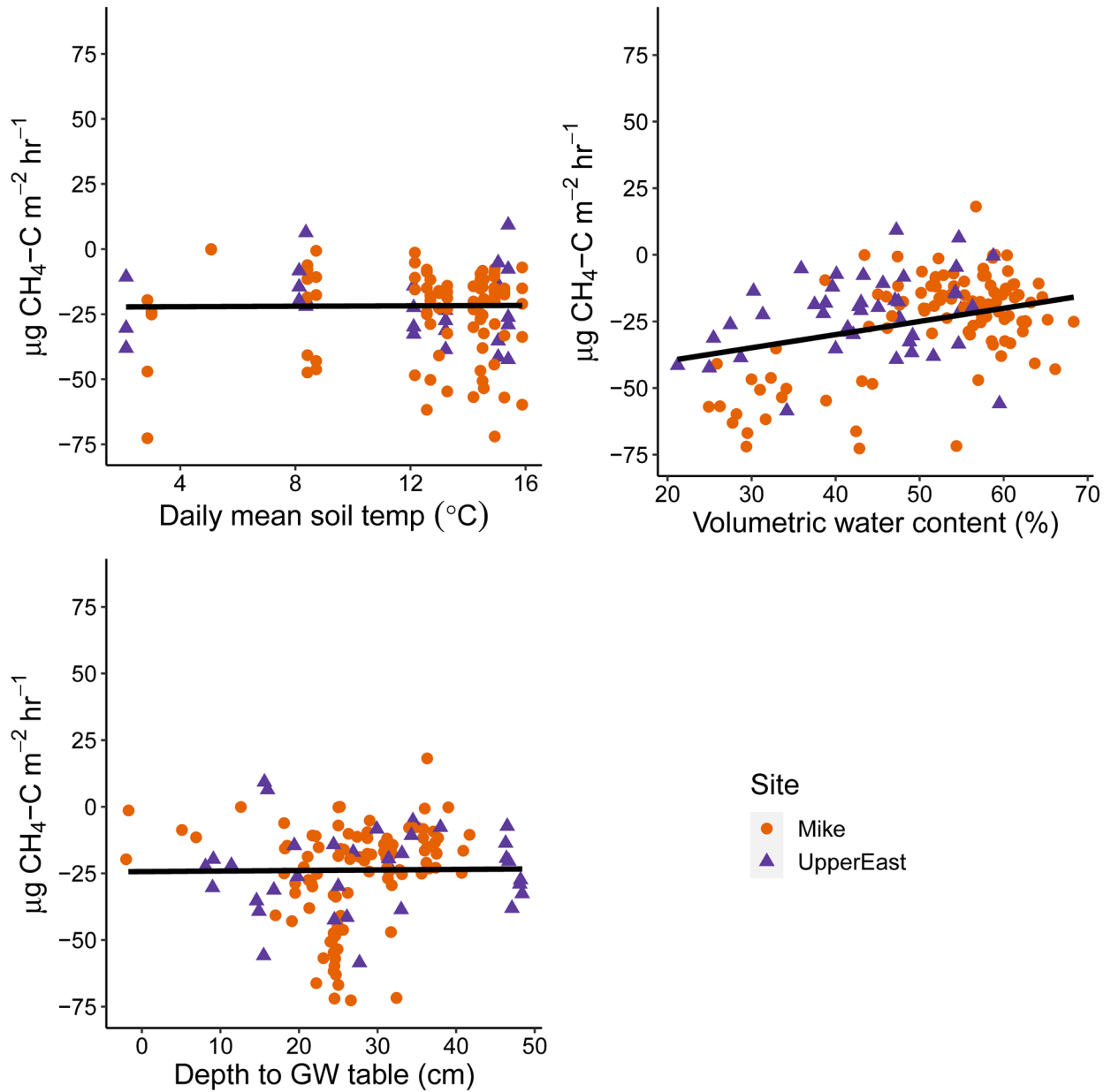


Figure 3.8 Relationships between methane gas fluxes and the environmental variables of daily mean soil temperature, mean soil moisture, and depth to groundwater table, by site. Trend lines are based on LME models accounting for autocorrelation in the relationship between the two variables for Mike Ck. and Upper East Ck..

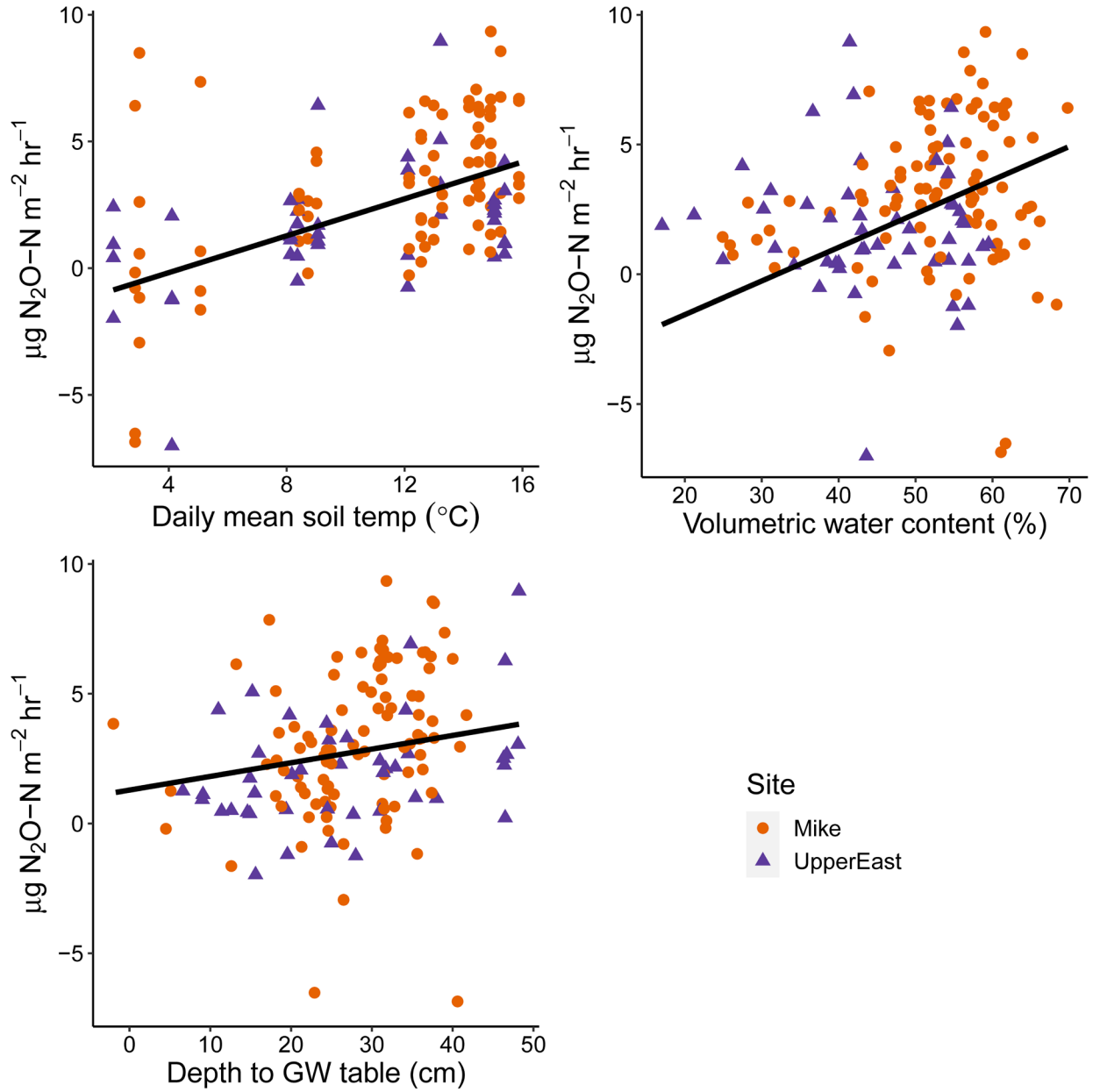


Figure 3.9 Relationships between nitrous oxide gas fluxes and the environmental variables of daily mean soil temperature, mean soil moisture, and depth to groundwater table, by site. Trend lines are based on LME models accounting for autocorrelation in the relationship between the two variables for Mike Ck. and Upper East Ck..

Table 3.1 Summarized output of linear mixed effects model explaining the dynamics of annual carbon dioxide, methane, and nitrous oxide fluxes. All models included the autocorrelation term “AR1(Week + 0 | Site/Chamber)”. Bolded models indicate a significant effect at  $p < 0.05$ . Note that ND is the reference level in the DIS\_ND term.

<b>Model</b>	<b>Est.</b>	<b>SE</b>	<b><i>p</i></b>
CO <sub>2</sub> ~ DIS_ND	-20.48	12.50	0.10
CH <sub>4</sub> ~ DIS_ND	11.73	7.11	0.10
N <sub>2</sub> O ~ DIS_ND	-0.06	0.49	0.91
<b>CO<sub>2</sub> ~ Soil temperature</b>	<b>18.42</b>	<b>2.70</b>	<b>&lt; 0.001</b>
CH <sub>4</sub> ~ Soil temperature	0.14	1.30	0.91
<b>N<sub>2</sub>O ~ Soil temperature</b>	<b>1.43</b>	<b>0.25</b>	<b>&lt; 0.001</b>
CO <sub>2</sub> ~ Soil moisture	-2.77	2.74	0.31
<b>CH<sub>4</sub> ~ Soil moisture</b>	<b>3.96</b>	<b>1.92</b>	<b>0.04</b>
<b>N<sub>2</sub>O ~ Soil moisture</b>	<b>1.07</b>	<b>0.22</b>	<b>&lt; 0.001</b>
CO <sub>2</sub> ~ Depth to GW	-1.14	2.31	0.62
CH <sub>4</sub> ~ Depth to GW	0.20	1.69	0.90
<b>N<sub>2</sub>O ~ Depth to GW</b>	<b>0.53</b>	<b>0.22</b>	<b>0.02</b>

### 3.4 Discussion

The riparian forest soils alongside two headwater streams in southwestern British Columbia were on average a CO<sub>2</sub> and N<sub>2</sub>O source, and a CH<sub>4</sub> sink. The majority of natural (i.e. unmanaged) ecosystems are net sinks for CO<sub>2</sub>, tundra and wetlands are large sources of CH<sub>4</sub>, and significant N<sub>2</sub>O emissions come from tropical and temperate forests (Dalal & Allen, 2008). Soils play a very important role in these greenhouse gas flux estimates, as soil denitrification is the main source of ecosystem N<sub>2</sub>O emissions and CH<sub>4</sub> is primarily produced by methanogens inhabiting anoxic environments in soils, sediments, and wetlands (Dalal & Allen, 2008). Ecosystem respiration includes CO<sub>2</sub> emissions from plant foliage, stems, and branches in addition to soil respiration, which can account for 55 to 85% of ecosystem respiration (Knohl, Sørensen, Kutsch, Göckede, & Buchmann, 2008). Greenhouse gas flux rates vary across ecosystem types reflecting the characteristics and conditions in those ecosystems (Luo & Zhou, 2006). The cumulative annual (hereafter referred to as annual) CO<sub>2</sub> emission rate from soils in this study (4,194 kg CO<sub>2</sub>-C ha<sup>-1</sup> yr<sup>-1</sup>) was higher than the average for soils in the tundra (600), deserts (2,240), boreal forests (3,220), and wetlands (4,130), but was lower than the average for temperate grasslands (4,420), tropical savannas (6,290), temperate forests (6,640), and tropical forests (9,665) (Luo & Zhou, 2006). My observed emission rates were more similar to wetlands and boreal forests than to temperate forests, likely because the annual mean air temperature and precipitation rates in my study region are cooler (9.7°C) and higher (2,131 mm) than in most temperate forests (10 °C, 1,125 mm) (Levy, 2020).

When compared to annual CH<sub>4</sub> fluxes reported by studies in other ecosystems, the CH<sub>4</sub> uptake rate from riparian soils alongside headwater streams (-2.1 kg CH<sub>4</sub>-C ha<sup>-1</sup> yr<sup>-1</sup>) was lower than the

average for temperate grasslands (-3.2), temperate forests (-4.8), and tropical forests (-6.6), but higher than the average for tropical savannas (-0.8), boreal forests (-1.9), and deserts (-2.1), (Dalal & Allen, 2008). The tundra (10.1) and wetlands (168.9) were on average net sources of CH<sub>4</sub> (kg CH<sub>4</sub>-C ha<sup>-1</sup> yr<sup>-1</sup>) (Dalal & Allen, 2008). It is interesting to note that although riparian areas tend to have shallow water tables and higher soil moisture levels than upland ecosystems (Vidon et al., 2018); the riparian CH<sub>4</sub> flux rates in this study were more similar to reported values for forests than wetlands.

The observed annual N<sub>2</sub>O flux rate from riparian soils in my study was 0.2 kg N<sub>2</sub>O-N ha<sup>-1</sup> yr<sup>-1</sup>. This N<sub>2</sub>O flux rate (kg N<sub>2</sub>O-N ha<sup>-1</sup> yr<sup>-1</sup>) was lower than the average for other ecosystems, including boreal forests (0.4), deserts (0.5), tundra (0.5), temperate grasslands (0.6), tropical savannas (1.0), wetlands (1.4), temperate forests (1.6), and tropical forests (4.8) (Dalal & Allen, 2008). Given the low annual flux rate that I measured, I may have underestimated N<sub>2</sub>O flux due to the difficulty in capturing N<sub>2</sub>O flux rates given their high spatial and temporal variability, limitations in measurement equipment, and the methodology used to quantify emissions and exclude outliers (Kroon, Hensen, Van den Bulk, Jongejan, & Vermeulen, 2008). However, there were a few studies that reported similarly low annual N<sub>2</sub>O flux rates (kg N<sub>2</sub>O-N ha<sup>-1</sup> yr<sup>-1</sup>), including a temperate forest in Japan (0.2) (Morishita et al., 2007), a boreal forest in Finland (0.04) (Pihlatie et al., 2007), and a swamp forest in Indonesia (0.3) (Furukawa, Inubushi, Ali, Itang, & Tsuruta, 2005).

After comparing the flux rates observed in my study to other ecosystems, I will now compare my flux rates to those reported from other riparian ecosystems. It is expected that the distinctive

conditions in riparian zones, including shallow water tables, high soil organic matter content, and greater total nitrogen concentrations, create the potential to contribute significant amounts of anaerobically produced methane and nitrous oxide to the atmosphere, when compared to upland areas within forest types (Knoepp & Clinton, 2009; Vidon, Welsh, & Hassanzadeh, 2018). For example, in a Mediterranean riparian forest, CO<sub>2</sub> emissions were highest near the hillslope, while N<sub>2</sub>O emissions were highest adjacent to the stream channel (Poblador, Lupon, Sabaté, & Sabater, 2017). Conversely, soil CO<sub>2</sub> concentrations were higher in the riparian zone than the hillslope in central Montana, USA (Pacific, McGlynn, Riveros-Iregui, Welsch, & Epstein, 2008). Their results were explained by the intermediate levels of soil water content (40 to 60%) in the riparian zone soils, which promotes soil respiration, compared to lower values in the hillslope (Pacific et al., 2008). Although I did not measure hillslope GHG efflux in my study, when examining upland forests in the Pacific Northwest, similarly disparate trends can be found. A Douglas-fir stand near Campbell River on Vancouver Island, BC measured an annual CO<sub>2</sub> emission rate (8,530 kg CO<sub>2</sub>-C ha<sup>-1</sup> yr<sup>-1</sup>) more than double that in the riparian forests in my study (4,194 kg CO<sub>2</sub>-C ha<sup>-1</sup> yr<sup>-1</sup>) and a much lower annual N<sub>2</sub>O emission rate (70 g N<sub>2</sub>O-N ha<sup>-1</sup> yr<sup>-1</sup>) than measured in my riparian forest soils (171 g N<sub>2</sub>O-N ha<sup>-1</sup> yr<sup>-1</sup>). These results are in line with the suggestion that conditions in the riparian zone may create hotspots for potent, anaerobically produced, GHG fluxes. However, when comparing my annual riparian flux rates (4,194 kg CO<sub>2</sub>-C ha<sup>-1</sup> yr<sup>-1</sup>, -2.1 kg CH<sub>4</sub>-C ha<sup>-1</sup> yr<sup>-1</sup>, 171 g N<sub>2</sub>O-N ha<sup>-1</sup> yr<sup>-1</sup>) to those of a Douglas-fir upland forest in Oregon (6,826 kg CO<sub>2</sub>-C ha<sup>-1</sup> yr<sup>-1</sup>, -4.1 kg CH<sub>4</sub>-C ha<sup>-1</sup> yr<sup>-1</sup>, 329 g N<sub>2</sub>O-N ha<sup>-1</sup> yr<sup>-1</sup>), the upland CO<sub>2</sub> and N<sub>2</sub>O flux rates and CH<sub>4</sub> uptake rates were all generally higher (Shrestha, Strahm, Sucre, Holub, & Meehan, 2014). The higher flux rates in the managed upland forest may be due to a history of fertilizer additions, as nutrient additions have been found to increase CO<sub>2</sub> and N<sub>2</sub>O

emissions (Jassal, Black, Trofymow, Roy, & Nestic, 2010; Shrestha et al., 2014). Alternatively, their values may have been disproportionately influenced by an event resulting in emission peaks (e.g. rainstorm) as they only measured on four occasions throughout the year, once per season (Shrestha et al., 2014). Due to the site-specific nature of GHG fluxes, a study of the riparian-hillslope gradient in GHG fluxes alongside headwater streams in my study area would be needed to more definitively conclude whether or not the riparian soils are a hotspot for GHG fluxes when compared to adjacent upland forests.

The annual emission rates were comparable to, but generally lower than, other reported emission rates from riparian soils. Annual CO<sub>2</sub> emissions from riparian grass buffers in an agricultural landscape in central Iowa, USA were more than twice as high (12,200 kg CO<sub>2</sub>-C ha<sup>-1</sup> yr<sup>-1</sup>) as the annual CO<sub>2</sub> emissions that I measured (4,194 kg CO<sub>2</sub>-C ha<sup>-1</sup> yr<sup>-1</sup>) (Tufekcioglu et al., 2001). The comparatively higher rates in the central Iowa study are likely due to the nutrient rich run-off from the adjacent crop fields (Tufekcioglu et al., 2001), which has been shown to stimulate CO<sub>2</sub> emissions, likely due to increased root growth (Jassal et al., 2010). Annual CO<sub>2</sub> emissions from a Mediterranean riparian forest soil were also higher (27,860 kg CO<sub>2</sub>-C ha<sup>-1</sup> yr<sup>-1</sup>) than I measured, likely due to the warmer climate in Spain (Poblador et al., 2017). Studies have shown that high soil temperatures can sustain high CO<sub>2</sub> emission rates in riparian soils, provided there is adequate soil moisture (e.g. above 17% in a Mediterranean riparian soil) (Chang et al., 2014). Similar to other riparian zones, the riparian soils I measured were a net CH<sub>4</sub> sink (-2.1 kg CH<sub>4</sub>-C ha<sup>-1</sup> yr<sup>-1</sup>). My observed flux rate fell within the range of annual CH<sub>4</sub> flux rates of -1.2 and 10.2 kg CH<sub>4</sub>-C ha<sup>-1</sup> yr<sup>-1</sup> observed in occasionally-flooded and flood-protected forested riparian zones, respectively, in Indiana, USA (Jacinthe, 2015); while the frequently flooded riparian zone was a

net CH<sub>4</sub> source (2.6 kg CH<sub>4</sub>-C ha<sup>-1</sup> yr<sup>-1</sup>) (Jacinthe, 2015). A non-flooded riparian grassland in an agricultural landscape in central Indiana was a net CH<sub>4</sub> sink (-1.1 kg CH<sub>4</sub>-C ha<sup>-2</sup> yr<sup>-1</sup>), likely due to subsurface tile drains which improve soil drainage and reduce anoxic conditions (Jacinthe et al., 2015). I observed annual N<sub>2</sub>O emissions of 171 g N<sub>2</sub>O-N ha<sup>-1</sup> yr<sup>-1</sup> in the forested riparian soils alongside headwater streams. Annual N<sub>2</sub>O emissions in an undisturbed riparian zone in southern Ontario were more than twice as high at 517 g N<sub>2</sub>O-N ha<sup>-1</sup> yr<sup>-1</sup> (De Carlo et al., 2019). The presence of nutrient-enriched runoff from the surrounding agricultural landscape likely contributed to the higher N<sub>2</sub>O emissions observed in southern Ontario than in my study (De Carlo et al., 2019). A much higher annual emission rate of 3,066 g N<sub>2</sub>O-N ha<sup>-2</sup> yr<sup>-1</sup> was reported from a Mediterranean riparian forest soil, likely due to higher mean soil temperature (11.5 °C, from February to November, compared to 8.4 °C annually in my study) stimulating soil respiration (Poblador et al., 2017).

There are very few studies of GHG emissions that are explicitly reported for the riparian zones of headwater streams (Chang et al., 2014; Leith et al., 2015). Often stream order, stream width, or catchment size are not reported, so the designation of a headwater stream cannot be determined (Richardson & Danehy, 2007). This apparent lack of studies alongside headwater streams represents a regrettable gap in the literature, given the ubiquity of headwater streams across the landscape (Richardson & Danehy, 2007). One study monitored CO<sub>2</sub> concentrations in wells across a hillslope riparian transect of a headwater stream in Sweden (Leith et al., 2015). They found that CO<sub>2</sub> concentrations (ppmv) were on average higher in the riparian zone than at the corresponding depth in the hillslope, likely due to enhanced productivity in the riparian zone and greater mobilization of CO<sub>2</sub> due to the generally wetter conditions found in riparian zones (Leith

et al., 2015). Nevertheless, they did not directly measure GHG efflux from the soil, which is controlled by different conditions than pore-water GHG concentrations.

Some studies have considered GHG emissions from headwater streams (Duvert, Butman, Marx, Ribolzi, & Hutley, 2018; Lupon et al., 2019; Schade, Bailio, & McDowell, 2016). Historically, GHG emissions from freshwater systems were not considered as sizeable components of the global carbon cycle due to the small area they cover (Cole et al., 2007). However, net carbon fluxes in aquatic systems actually tend to be greater per unit area than surrounding terrestrial ecosystems (Cole et al., 2007). Recent evidence suggests that headwater streams in particular may have a disproportionately large contribution to global riverine carbon efflux due to their long cumulative length, high turbulence, and strong coupling with adjacent terrestrial environments (Duvert et al., 2018; Raymond et al., 2013). Terrestrially derived CO<sub>2</sub> is produced in riparian soils and transported to streams via lateral groundwater inputs (Hotchkiss et al., 2015). Terrestrially derived CO<sub>2</sub> dominates emissions from small and headwater streams, due to their close connectivity with the adjacent terrestrial landscape (Hotchkiss et al., 2015). Stream efflux measured at an experimental stream in Malcolm Knapp Research Forest, where my research was also conducted, was on average 90 kg CO<sub>2</sub>-C ha<sup>-1</sup> d<sup>-1</sup> over 70 days (Atwood, Hammill, & Richardson, 2014). This estimate of stream efflux is higher than the average I observed from nearby riparian soils over a full year (11.5 kg CO<sub>2</sub>-C ha<sup>-1</sup> d<sup>-1</sup>). What is more, GHG fluxes from streams has been found to peak downstream of DIS areas, due to their lateral dissolved gas inputs from riparian soils (Lupon et al., 2019). Therefore, having a better understanding of riparian GHG emissions alongside headwater streams will also help to inform global freshwater GHG and carbon budgets.

### 3.4.1 Spatial variation in greenhouse gas fluxes

My results did not indisputably support my hypothesis that groundwater discharge (DIS) areas would have higher soil moisture from groundwater influence compared to non-groundwater discharge (ND) areas, resulting in greater anaerobically produced CH<sub>4</sub> and N<sub>2</sub>O emissions and lower aerobically produced CO<sub>2</sub> emissions. None of the GHG flux rates were statistically significantly different between the DIS and ND areas. Nevertheless, there were several pieces of evidence that did provide some indication of support for the mechanisms underlying my hypothesis. Firstly, the water table and soil moisture were on average 1.05 and 1.16 times higher, respectively, at the DIS sites compared to the ND sites. These conditions are likely a result of upland-originating groundwater converging and discharging in a depression in the topography of the riparian zone (Kuglerová et al., 2014b). Moreover, although not statistically significant, CH<sub>4</sub> uptake and CO<sub>2</sub> emission rates were on average 1.71 and 1.35 times lower, respectively, at the DIS areas, as my hypothesis predicted. In contrast with other studies, mean N<sub>2</sub>O emission rates were virtually the same in DIS and ND areas. Other studies have found variations in GHG emission rates based on a gradient of soil water content in the riparian zone. For instance, CO<sub>2</sub> efflux peaked in areas of deep groundwater (-358 cm mean depth to the groundwater table) near the hillslope, while N<sub>2</sub>O emissions were highest in wet areas adjacent to the stream channel (-54 cm mean depth to the groundwater table) in a Mediterranean riparian forest soil (Poblador et al., 2017). Additionally, in a central Indiana watershed, a topographic depression in a riparian forest accounted for 78% of annual CH<sub>4</sub> emissions, despite only covering <8% of the total land area (Jacinthe et al., 2015). Depending on the local conditions, CO<sub>2</sub> emissions may not always be limited in riparian zones. Soil CO<sub>2</sub> concentrations were higher in the riparian zone compared to

the adjacent hillslope in a subalpine catchment in Montana, likely due to limiting soil water content farther from the riparian zone (~20%), compared to in the riparian zone (~40-60%) (Pacific et al., 2008).

The lack of significant difference in flux rates between the DIS and ND areas, may be because the soil moisture is already relatively high in the riparian zone of headwater streams in southwestern British Columbia, due to the wet climate and interaction with the stream channel (Moore et al., 2005). To illustrate, the mean depth to the groundwater table in the riparian zone in my study was 27 cm, compared to 54 cm in a headwater catchment in Spain (Poblador et al., 2017). Therefore, the additional moisture in the DIS areas may not play as important of a role in predicting GHG emissions as it might in a different, more arid landscape. For example, in central Indiana, the topographical depressions only covered <8% of the land area, but accounted for 78% of annual CH<sub>4</sub> emissions (Jacinthe et al., 2015). The climate in their study region was warmer and drier than in ours, with 10°C and 1040 mm mean annual air temperature and precipitation in central Indiana compared to 9.7°C and 2131 mm, respectively, at the Malcolm Knapp Research Forest.

In contrast to the results of this chapter, in Chapter 2 I found that CH<sub>4</sub> fluxes were statistically significantly higher in DIS areas. Chapter 2 considered streams running through harvested forest stands (with and without a buffer) in addition to the reference streams examined in this Chapter. Therefore, although CH<sub>4</sub> fluxes may not be statistically significantly higher in the DIS areas of relatively undisturbed riparian zones, the DIS areas are greater sources of CH<sub>4</sub> than ND areas under disturbed ecosystem conditions, such as forest harvest. An explanation for this

phenomenon could be that forest harvest causes generally drier surface soil due to increased evaporation from the solar radiation coming in to the riparian zone (Moore et al., 2005). At the same time clear-cutting causes a rise in the water table due to reduced catchment-wide transpiration rates (Bliss & Comerford, 2002), resulting in drier ND areas and wetter DIS areas in clear-cut compared to undisturbed riparian zones. In Chapter 2, I observed on average, 1.10 times higher soil temperatures and 1.16 times higher soil moisture levels at the clear-cut than the reference sites. Thus, the difference in soil moisture conditions between the DIS and ND areas are more pronounced in a clear-cut than in an undisturbed riparian zone.

### **3.4.2 Temporal variation in greenhouse gas fluxes**

Given that GHG fluxes are strongly controlled by environmental factors that often fluctuate throughout the year, I hypothesized that GHG fluxes would have significant temporal variation associated with seasonal changes in soil temperature, groundwater level, and soil moisture, with peak gas emissions occurring in the wettest and/or warmest months. My CO<sub>2</sub> results supported this hypothesis, as CO<sub>2</sub> emissions were 2.73 times higher in the summer than in the winter, and they were significantly controlled by soil temperature. This trend in CO<sub>2</sub> emissions is in line with the well-established, positive, exponential relationship between soil respiration and temperature, which reaches a maximum, and then declines (Luo & Zhou, 2006). Soil moisture was a significant driver of CH<sub>4</sub> fluxes, which were highest the spring. Given that methane is produced under anaerobic conditions and consumed under aerobic conditions, soil moisture is a key factor in the dynamics of CH<sub>4</sub> fluxes from soils (Christiansen et al., 2012; Oertel et al., 2016). Both soil temperature, soil moisture and depth to the groundwater table were significant drivers of N<sub>2</sub>O emissions, which peaked in the summer, further supporting my hypothesis. Nitrous oxide fluxes

have been found to peak at intermediate levels of soil moisture (Christiansen et al., 2012), and to have a positive relationship with flooding of the groundwater table (Mander et al., 2015).

My results were in line with other temporal studies of riparian GHG flux rates. Carbon dioxide emission rates showed a strong seasonal pattern, with peak rates in the spring and summer, and lowest rates in the fall and winter, significantly related to soil temperature, in a riparian floodplain forest in Indiana, USA (Jacinthe, 2015). In the same study, pulses of CH<sub>4</sub> emissions were observed following riparian flooding events in the spring (Jacinthe, 2015). Soil temperature, soil moisture, and soil nitrogen levels were significantly related to N<sub>2</sub>O emissions, with peak N<sub>2</sub>O emissions observed in the summer from a riparian forest in southern Ontario, Canada (De Carlo et al., 2019). In northern Thailand, N<sub>2</sub>O flux rates were higher in the wet season than in the dry season in a tropical riparian ecosystem (Kachenchart et al., 2012). There, variations in N<sub>2</sub>O emissions were strongly positively correlated with microbial biomass carbon, denitrification rates, and water-filled pore space (Kachenchart et al., 2012).

### **3.4.3 Conclusions**

In conclusion, my research showed that there are seasonal variations in GHG fluxes from riparian soils alongside headwater streams, influenced by changes in soil moisture and soil temperature. Although the summer months had peak emissions of CO<sub>2</sub> and N<sub>2</sub>O, the other seasons still had sizeable GHG contributions (e.g. 14% of CO<sub>2</sub> emissions were emitted in the winter months). However, the riparian soils were a N<sub>2</sub>O sink in the winter, compared to a source the remainder of the year. The riparian forest soils investigated in this study were a net sink for CH<sub>4</sub>, and a net source for CO<sub>2</sub> and N<sub>2</sub>O, similar to other riparian studies. In agreement with other studies, my results showed that soil temperature was a significant driver of CO<sub>2</sub> emissions, soil

moisture was a significant driver of methane fluxes, and soil temperature and soil moisture were significant drivers of N<sub>2</sub>O emissions. I further found that riparian micro-topography alongside two headwater streams in southwestern British Columbia does not have a statistically significant effect on soil GHG emissions, although there were on average higher CH<sub>4</sub> fluxes and lower CO<sub>2</sub> emissions in the DIS areas, as predicted.

Given the lack of significant difference between DIS and ND areas in my study, it would be interesting to see if there would be a more striking difference between these microtopographic areas in a more arid environment, such as in the interior of British Columbia. Additionally, given the strong terrestrial-aquatic coupling between headwater streams and their riparian zones (Richardson & Danehy, 2007), future studies could explore the relationship between riparian soil GHG emissions and stream GHG emissions. Another suggested domain for future research is examining the riparian-hillslope gradient of GHG fluxes alongside headwater streams in the Pacific Northwest to conclude whether or not the riparian soils are a hotspot for GHG fluxes when compared to adjacent upland forests. The results of this research further our understanding of the seasonal and spatial dynamics of GHG fluxes in riparian zones. This research contributes to greater accuracy in terrestrial GHG budgets (Hotchkiss et al., 2015; Sun et al., 2013), by measuring GHG fluxes in riparian forest soils alongside headwater streams, which to date have been understudied, despite their unique conditions and ubiquity across the global landscape.

## Chapter 4: Conclusions

### 4.1 Findings and limitations

Through this research, my aim was to address three objectives: 1) to quantify the effects of forest harvest practices on soil GHG flux rates and to determine the dominant driver(s) of gas fluxes, 2) to quantify the effects of riparian groundwater inflow conditions on GHG flux rates, and 3) to examine the effects of temporal variation on GHG fluxes from riparian soils. To summarize my results, I found that the sites with no buffers were generally warmer, wetter, and had shallower groundwater tables than buffer and reference sites. Additionally, there was no significant effect of treatment on CO<sub>2</sub> emissions, but there were significantly higher CH<sub>4</sub> fluxes in no buffer sites compared to reference sites and significantly higher N<sub>2</sub>O emissions in the reference treatment compared to the no buffer treatments. The CH<sub>4</sub> results followed my Water Table Hypothesis, as soil moisture and depth to the groundwater table were significant predictors of CH<sub>4</sub> fluxes. The N<sub>2</sub>O results were in line with my Disturbance Hypothesis where I predicted that that forest harvest in the riparian zone will disturb soil microbial activity and tree roots, resulting in reduced emission rates. There was no significant difference in CO<sub>2</sub> and N<sub>2</sub>O fluxes between DIS and ND areas in either Chapters 2 and 3, but CH<sub>4</sub> fluxes were significantly higher in DIS areas in Chapter 2 when data from all three treatments were considered. This result was in line with my hypothesis that DIS areas will have higher soil moisture and nutrients from groundwater influence compared to ND areas, resulting in greater anaerobically produced CH<sub>4</sub>. On average, CO<sub>2</sub> emissions were higher at the ND areas and N<sub>2</sub>O flux rates were very similar between DIS and ND areas across chapters. Seasonal trends in GHG emissions showed the highest flux rates in summer, spring, and summer for CO<sub>2</sub>, CH<sub>4</sub>, and N<sub>2</sub>O respectively. These results followed my

hypothesis that the peak GHG emission rates would occur in the warmest (summer) months. A considerable amount of GHGs was still emitted in the season with the lowest emission rates for CO<sub>2</sub> and CH<sub>4</sub>, with 14% of total annual CO<sub>2</sub> fluxes emitted in the winter and 17% of total annual CH<sub>4</sub> fluxes emitted in the fall. Conversely, the soils were a net source of N<sub>2</sub>O in the winter, but a N<sub>2</sub>O sink for the remainder of the year. In both Chapters 2 and 3, soil moisture and soil temperature were significant predictors of CO<sub>2</sub> fluxes and soil moisture was a significant predictor of CH<sub>4</sub> fluxes. Depth to the groundwater table was only a significant predictor of CH<sub>4</sub> fluxes in Chapter 2. Soil temperature and soil moisture were significant predictors of N<sub>2</sub>O emissions only when annual data from reference sites was considered in Chapter 3.

There were some limitations to this research, namely related to limited time and resources. Observing GHG fluxes from nine sites, with six collars per site, and with headspace samples over four time-points, was at the upward limit in terms of what two individuals could reasonably sample. Moreover, analyzing trace gas fluxes using gas chromatography is costly. However, due to the high spatial and temporal variability associated with GHG emissions from soils, increasing the number of samples at different replication levels would lead to increased statistical power (Kravchenko & Robertson, 2015). It also would have been beneficial to increase the sampling frequency in order to better capture some of the temporal variability, especially hot moments of N<sub>2</sub>O emissions (e.g. after precipitation events) (McClain et al., 2003). In addition, I had a high rate of removal of flux rate data points for N<sub>2</sub>O. By adding an additional headspace sample time-point, thereby increasing the headspace samples from four to five time-points, it would have likely reduced the number of removed flux rates data points. Moreover, I was lucky enough to be able to conduct my fieldwork in Malcolm Knapp Research Forest, which had many benefits including availability of detailed logging history, easy site access, security of research

equipment, high resolution digital elevation data, and a rich history of research. However, there were some limitations in finding suitable harvested sites that necessitated me to expand my site selection criteria to older cutblocks (up to five years post-harvest), as opposed to the more recent cutblocks that I was originally interested in observing.

## **4.2 Implications and future directions**

My study provides a good foundation of information about spatial and temporal trends in GHG emissions from riparian zones of headwater streams in southwestern British Columbia, and how prevailing forestry practices influence emission rates. There are still several outstanding research questions to address GHG emissions from riparian soils alongside headwater streams. For instance, future studies could consider other variables not measured in this study, such as soil nutrient concentrations (Christiansen & Gundersen, 2011) or microbial community composition and structure (Lewandowski et al., 2019), to explain variations in emissions. It would also be beneficial to understand the recovery trajectory of riparian soils following disturbance perpetrated by forest harvest by examining GHG fluxes on a regular (e.g. annual) basis following forest harvest, until pre-harvest levels are measured (if that ever occurs). To further investigate the effects of DIS areas on GHG fluxes from riparian streams, it would be interesting to see if there would be a more striking difference between these microtopographic zones in a more arid environment, such as in the interior of British Columbia. Moreover, future studies could explore the riparian-hillslope gradient of GHG fluxes headwater streams in the Pacific Northwest to conclude whether or not the riparian soils are a hotspot for GHG fluxes when compared to adjacent upland forests.

My research has implications for the fields of forestry, hydrology, soil science, and climate science. This research may be noteworthy to forest managers interested in managing their forests for GHG balance and climate change mitigation. My results demonstrate that the soil ecosystem processes contributing to CH<sub>4</sub> and N<sub>2</sub>O emissions are impacted by clear-cutting in the riparian zone up to three to five years following harvest, but a buffer zone with no harvest is effective in mitigating these effects. Additionally, my research provides support for hydrologically adapted buffers, with the lowest mean CH<sub>4</sub> uptake observed in the no buffer DIS zones. Hydrologically adapted buffers provide more protection for wet areas, such as DIS sites, in the riparian zone (Tiwari et al., 2016). In contrast to the traditional fixed-width buffers, variable buffer width adapted to site-specific hydrological conditions can protect biogeochemical and ecological functions as well as provide economic savings when compared to fixed width buffers (Tiwari et al., 2016). Now in addition to those benefits, my research shows that hydrologically adapted buffers may promote CH<sub>4</sub> uptake for climate change mitigation, by protecting DIS areas in the riparian zone. My research may also be of interest to hydrologists or freshwater biologists who are interested in quantifying biogeochemical cycles in riverine systems. Since headwater streams are tightly connected to their surrounding terrestrial environment (Richardson & Danehy, 2007), a large percentage of GHG emissions from the stream are produced in riparian soils and laterally transported via the shallow groundwater to the stream (Lupon et al., 2019). Thus, understanding the drivers and magnitudes of riparian soil GHG fluxes, is also important in understanding stream GHG fluxes. Additionally, my research has value for the field of soil science as it provides evidence for the relationships between soil characteristics (e.g. moisture and temperature) and GHG fluxes in an understudied ecosystem. My research also provides data to create more accurate and climate and ecosystem specific carbon and GHG budgets. Although

riparian zones are widespread across the global landscape, I found very few studies examining GHG fluxes from the riparian zones of small or headwater streams (Chang et al., 2014; Leith et al., 2015). Due to the distinctive conditions of riparian zones, with shallow and fluctuating water tables and high soil organic matter content (Vidon et al., 2018), particularly those of headwater streams, are likely to differ from upland soils, although more research is needed to demonstrate this.

My thesis provides new information about the biosphere-atmosphere exchange of GHGs in the riparian zone of headwater streams in southwestern British Columbia. It also adds to the understanding of where temperate riparian forests fit in the global distribution of flux rates across ecosystem types. I examined the effects of forestry, a dominant human disturbance for this ecosystem, as well as an in-depth temporal study of relatively undisturbed riparian conditions. Headwater streams can make up 80% of stream length in a given stream network (Richardson & Danehy, 2007), thus their riparian zones represent a considerable land area. Nevertheless, studies of GHG fluxes from the soils in headwater riparian zones remain limited (Chang et al., 2014; Leith et al., 2015), allowing this research to fill an important gap in the literature. By gaining a better understanding of seasonal and microtopographical trends in GHG emissions from riparian soils alongside headwater streams in this region, it can help inform more accurate regional and global GHG budgets and establish baseline flux rates to contrast with flux rates from disturbed riparian zones. Forestry is a leading disturbance to the riparian zones of headwater streams in the Pacific Northwest (Basiliko et al., 2009), therefore understanding the effects of forestry on GHG emissions from riparian soils alongside headwater streams is an information gap. Knowledge of the mechanisms by which forestry impacts GHG fluxes in the riparian zone alongside headwater

streams in the Pacific Northwest, can assist forest managers in developing region-specific strategies to minimize those impacts. Given the important role that soils play in climate change (Lal, 2004), this research also contributes to improved estimates of GHG budgets to help mitigate climate change. Increasing stocks of carbon in the soil and reducing emissions of GHGs to the atmosphere are important climate change mitigation strategies (Derrien et al., 2016). Learning more about the spatial and temporal drivers of GHG fluxes in these ecosystems can help inform more accurate GHG budgets to help mitigate climate change, particularly in the face of increasing anthropogenic disturbances.

## References

- Atwood, T. B., Hammill, E., & Richardson, J. S. (2014). Trophic-level dependent effects on CO<sub>2</sub> emissions from experimental stream ecosystems. *Global Change Biology*, 20(11), 3386-3396.
- Audet, J., Elsgaard, L., Kjaergaard, C., Larsen, S. E., & Hoffmann, C. C. (2013). Greenhouse gas emissions from a Danish riparian wetland before and after restoration. *Ecological Engineering*, 57, 170-182.
- Basiliko, N., Khan, A., Prescott, C. E., Roy, R., & Grayston, S. J. (2009). Soil greenhouse gas and nutrient dynamics in fertilized western Canadian plantation forests. *Canadian Journal of Forest Research*, 39(6), 1220-1235.
- Biggs, J., Von Fumetti, S., & Kelly-Quinn, M. (2017). The importance of small waterbodies for biodiversity and ecosystem services: Implications for policy makers. *Hydrobiologia*, 793(1), 3-39.
- Blevins, L. L., Prescott, C. E., & Van Niejenhuis, A. (2006). The roles of nitrogen and phosphorus in increasing productivity of western hemlock and western red cedar plantations on northern Vancouver Island. *Forest Ecology and Management*, 234(1-3), 116-122.
- Bliss, C., & Comerford, N. (2002). Forest harvesting influence on water table dynamics in a Florida flatwoods landscape. *Soil Science Society of America Journal*, 66(4), 1344-1349.
- Boucher, O., Friedlingstein, P., Collins, B., & Shine, K. P. (2009). The indirect global warming potential and global temperature change potential due to methane oxidation. *Environmental Research Letters*, 4(4), 044007.

- British Columbia Forest Service. (1995). *Riparian management area guidebook*. Victoria, B.C: Forest Service, British Columbia BC Environment.
- Brooks, M. E., Kristensen, K., van Benthem, K. J., Magnusson, A., Berg, C. W., Nielsen, A., . . . Bolker, B. M. (2017). glmmTMB balances speed and flexibility among packages for zero-inflated generalized linear mixed modeling. *The R Journal*, 9(2), 378–400.
- Burt, T., Pinay, G., Matheson, F., Haycock, N., Butturini, A., Clement, J., . . . Hillbricht-Ilkowska, A. (2002). Water table fluctuations in the riparian zone: Comparative results from a pan-European experiment. *Journal of Hydrology*, 265(1-4), 129-148.
- Canadian Agricultural Services Coordinating Committee. (1998). *The Canadian system of soil classification*. Ottawa: NRC Research Press.
- Capon, S. J., & Pettit, N. E. (2018). Turquoise is the new green: Restoring and enhancing riparian function in the Anthropocene. *Ecological Management & Restoration*, 19, 44-53.
- Carter, M. R., & Gregorich, E. G. (2008). *Soil sampling and methods of analysis* (2nd ed.). Boca Raton, FL: CRC Press.
- Chang, C., Sabaté i Jorba, S., Sperlich, D., Poblador Ibáñez, S., Sabater i Comas, F., & Gracia, C. (2014). Does soil moisture overrule temperature dependence of soil respiration in Mediterranean riparian forests? *Biogeosciences*, 2014, Vol.11, P.6173-6185,
- Chapin, F., Matson, P., Vitousek, P., & Chapin, M. (2011). Nutrient cycling. In Chapin, F., Matson, P., Mooney, H., Vitousek, P. (Ed.), *Principles of terrestrial ecosystem ecology* (2nd ed., pp. 197-223). New York: Springer.
- Christiansen, J., Riis., & Gundersen, P. (2011). Stand age and tree species affect N<sub>2</sub>O and CH<sub>4</sub> exchange from afforested soils. *Biogeosciences*, 8(9), 2535-2546.

- Christiansen, J. R., Levy-Booth, D., Prescott, C. E., & Grayston, S. J. (2016). Microbial and environmental controls of methane fluxes along a soil moisture gradient in a pacific coastal temperate rainforest. *Ecosystems*, *19*(7), 1255-1270.
- Christiansen, J. R., Levy-Booth, D., Prescott, C. E., & Grayston, S. J. (2017). Different soil moisture control of net methane oxidation and production in organic upland and wet forest soils of the pacific coastal rainforest in Canada. *Canadian Journal of Forest Research*, *47*(5), 628-635.
- Christiansen, J. R., Vesterdal, L., & Gundersen, P. (2012). Nitrous oxide and methane exchange in two small temperate forest catchments—effects of hydrological gradients and implications for global warming potentials of forest soils. *Biogeochemistry*, *107*(1-3), 437-454.
- Clinton, B. D., Vose, J. M., Knoepp, J. D., Elliott, K. J., Reynolds, B. C., & Zarnoch, S. J. (2010). Can structural and functional characteristics be used to identify riparian zone width in southern Appalachian headwater catchments? *Canadian Journal of Forest Research*, *40*(2), 235-253.
- Cole, J. J., Prairie, Y. T., Caraco, N. F., McDowell, W. H., Tranvik, L. J., Striegl, R. G., . . . Middelburg, J. J. (2007). Plumbing the global carbon cycle: Integrating inland waters into the terrestrial carbon budget. *Ecosystems*, *10*(1), 172-185.
- Collier, S. M., Ruark, M. D., Oates, L. G., Jokela, W. E., & Dell, C. J. (2014). Measurement of greenhouse gas flux from agricultural soils using static chambers. *JoVE (Journal of Visualized Experiments)*, (90), e52110.
- Conrad, R. (2007). Microbial ecology of methanogens and methanotrophs. *Advances in Agronomy*, *96*, 1-63.

- Dalal, R. C., & Allen, D. E. (2008). Greenhouse gas fluxes from natural ecosystems. *Australian Journal of Botany*, 56(5), 369-407.
- Dannenmann, M., Gasche, R., & Papen, H. (2007). Nitrogen turnover and N<sub>2</sub>O production in the forest floor of beech stands as influenced by forest management. *Journal of Plant Nutrition and Soil Science*, 170(1), 134-144.
- Davidson, E. A., Keller, M., Erickson, H. E., Verchot, L. V., & Veldkamp, E. (2000). Testing a conceptual model of soil emissions of nitrous and nitric oxides: Using two functions based on soil nitrogen availability and soil water content, the hole-in-the-pipe model characterizes a large fraction of the observed variation of nitric oxide and nitrous oxide emissions from soils. *Bioscience*, 50(8), 667-680.
- De Carlo, N., Oelbermann, M., & Gordon, A. (2019). Spatial and temporal variation in soil nitrous oxide emissions from a rehabilitated and undisturbed riparian forest. *Journal of Environmental Quality*, 48(3), 624-633.
- Derrien, D., Dignac, M., Basile-Doelsch, I., Barot, S., Cécillon, L., Chenu, C., . . . Guenet, B. (2016). Stocker du C dans les sols: Quels mécanismes, quelles pratiques agricoles, quels indicateurs. *Etude et gestion des sols*, 23, 193-223.
- Dosskey, M. G., Vidon, P., Gurwick, N. P., Allan, C. J., Duval, T. P., & Lowrance, R. (2010). The role of riparian vegetation in protecting and improving chemical water quality in streams<sup>1</sup>. *JAWRA Journal of the American Water Resources Association*, 46(2), 261-277.
- Duvert, C., Butman, D. E., Marx, A., Ribolzi, O., & Hutley, L. B. (2018). CO<sub>2</sub> evasion along streams driven by groundwater inputs and geomorphic controls. *Nature Geoscience*, 11(11), 813-818.

- Elliot, W. J., Page-Dumroese, D., & Robichaud, P. R. (2018). The effects of forest management on erosion and soil productivity. *Soil Quality and Soil Erosion*,
- Feller, M. (1977). Nutrient movement through western hemlock-western red cedar ecosystems in southwestern British Columbia. *Ecology*, 58(6), 1269-1283.
- Fisher, K., Jacinthe, P., Vidon, P., Liu, X., & Baker, M. (2014). Nitrous oxide emission from cropland and adjacent riparian buffers in contrasting hydrogeomorphic settings. *Journal of Environmental Quality*, 43(1), 338-348.
- Frey, B., Niklaus, P. A., Kremer, J., Luscher, P., & Zimmermann, S. (2011). Heavy-machinery traffic impacts methane emissions as well as methanogen abundance and community structure in oxic forest soils. *Applied and Environmental Microbiology*, 77(17), 6060-6068.
- Furukawa, Y., Inubushi, K., Ali, M., Itang, A., & Tsuruta, H. (2005). Effect of changing groundwater levels caused by land-use changes on greenhouse gas fluxes from tropical peat lands. *Nutrient Cycling in Agroecosystems*, 71(1), 81-91.
- Giesler, R., Högberg, M., & Högberg, P. (1998). Soil chemistry and plants in Fennoscandian boreal forest as exemplified by a local gradient. *Ecology*, 79(1), 119-137.
- Goodrick, I., Connor, S., Bird, M., & Nelson, P. (2016). Emission of CO<sub>2</sub> from tropical riparian forest soil is controlled by soil temperature, soil water content and depth to water table. *Soil Research*, 54(3), 311-320.
- Gregory, S. V., Swanson, F. J., McKee, W. A., & Cummins, K. W. (1991). An ecosystem perspective of riparian zones. *Bioscience*, 41(8), 540-551.
- Gundersen, P. (1991). Nitrogen deposition and the forest nitrogen cycle: Role of denitrification. *Forest Ecology and Management*, 44(1), 15-28.

- Gundersen, P., Laurén, A., Finér, L., Ring, E., Koivusalo, H., Sætersdal, M., . . . Laine, J. (2010). Environmental services provided from riparian forests in the Nordic countries. *Ambio*, 39(8), 555-566.
- Guo, J., Yang, Y., Chen, G., Xie, J., Gao, R., & Qian, W. (2010). Effects of clear-cutting and slash burning on soil respiration in Chinese fir and evergreen broadleaved forests in mid-subtropical China. *Plant and Soil*, 333(1-2), 249-261.
- Hartmann, M., Howes, C. G., VanInsberghe, D., Yu, H., Bachar, D., Christen, R., . . . Mohn, W. W. (2012). Significant and persistent impact of timber harvesting on soil microbial communities in northern coniferous forests. *The ISME Journal*, 6(12), 2199-2218.
- Hashimoto, S., & Suzuki, M. (2004). The impact of forest clear-cutting on soil temperature: A comparison between before and after cutting, and between clear-cut and control sites. *Journal of Forest Research*, 9(2), 125-132.
- Hazlett, P., Gordon, A., Sibley, P., & Buttle, J. (2005). Stand carbon stocks and soil carbon and nitrogen storage for riparian and upland forests of boreal lakes in northeastern Ontario. *Forest Ecology and Management*, 219(1), 56-68.
- Hinshaw, S. E., & Dahlgren, R. A. (2016). Nitrous oxide fluxes and dissolved N gases (N<sub>2</sub> and N<sub>2</sub>O) within riparian zones along the agriculturally impacted San Joaquin River. *Nutrient Cycling in Agroecosystems*, 105(2), 85-102.
- Hotchkiss, E., Hall Jr, R., Sponseller, R., Butman, D., Klaminder, J., Laudon, H., . . . Karlsson, J. (2015). Sources of and processes controlling CO<sub>2</sub> emissions change with the size of streams and rivers. *Nature Geoscience*, 8(9), 696-699.

- Hotta, N., Tanaka, N., Sawano, S., Kuraji, K., Shiraki, K., & Suzuki, M. (2010). Changes in groundwater level dynamics after low-impact forest harvesting in steep, small watersheds. *Journal of Hydrology*, 385(1-4), 120-131.
- Jacinthe, P. (2015). Carbon dioxide and methane fluxes in variably-flooded riparian forests. *Geoderma*, 241, 41-50.
- Jacinthe, P., & Vidon, P. (2017). Hydro-geomorphic controls of greenhouse gas fluxes in riparian buffers of the white river watershed, IN (USA). *Geoderma*, 301, 30-41.
- Jacinthe, P., Vidon, P., Fisher, K., Liu, X., & Baker, M. (2015). Soil methane and carbon dioxide fluxes from cropland and riparian buffers in different hydrogeomorphic settings. *Journal of Environmental Quality*, 44(4), 1080-1090.
- Jassal, R. S., Black, T. A., Trofymow, J., Roy, R., & Nesic, Z. (2010). Soil CO<sub>2</sub> and N<sub>2</sub>O flux dynamics in a nitrogen-fertilized Pacific Northwest Douglas-fir stand. *Geoderma*, 157(3-4), 118-125.
- Jungkunst, H. F., Flessa, H., Scherber, C., & Fiedler, S. (2008). Groundwater level controls CO<sub>2</sub>, N<sub>2</sub>O and CH<sub>4</sub> fluxes of three different hydromorphic soil types of a temperate forest ecosystem. *Soil Biology and Biochemistry*, 40(8), 2047-2054.
- Kachenchart, B., Jones, D. L., Gajaseeni, N., Edwards-Jones, G., & Limsakul, A. (2012). Seasonal nitrous oxide emissions from different land uses and their controlling factors in a tropical riparian ecosystem. *Agriculture, Ecosystems & Environment*, 158, 15-30.
- Kähkönen, M. A., Wittmann, C., Ilvesniemi, H., Westman, C. J., & Salkinoja-Salonen, M. S. (2002). Mineralization of detritus and oxidation of methane in acid boreal coniferous forest soils: Seasonal and vertical distribution and effects of clear-cut. *Soil Biology and Biochemistry*, 34(8), 1191-1200.

- Kellman, L., & Kavanaugh, K. (2008). Nitrous oxide dynamics in managed northern forest soil profiles: Is production offset by consumption? *Biogeochemistry*, *90*(2), 115-128.
- Klinka, K. (1976). *Ecosystem Units, their Classification, Interpretation and Mapping in the University of British Columbia Research Forest*. (Doctoral dissertation, The University of British Columbia).
- Klinka, K., Green, R. N., Trowbridge, R. L., & Lowe, L. E. (1981). *Taxonomic classification of humus forms in ecosystems of British Columbia*. Victoria, BC: BC Ministry of Forests.
- Klinka, K., Chourmouzis, C., & Varga, P. (2005). Site units of the University of British Columbia Malcolm Knapp Research forest. *Malcolm Knapp Research Forest, Maple Ridge, BC*.
- Knoepp, J. D., & Clinton, B. D. (2009). Riparian zones in southern Appalachian headwater catchments: Carbon and nitrogen responses to forest cutting. *Forest Ecology and Management*, *258*(10), 2282-2293.
- Knohl, A., Sørensen, A. R., Kutsch, W. L., Göckede, M., & Buchmann, N. (2008). Representative estimates of soil and ecosystem respiration in an old beech forest. *Plant and Soil*, *302*(1-2), 189-202.
- Kottek, M., Grieser, J., Beck, C., Rudolf, B., & Rubel, F. (2006). World map of the Köppen-Geiger climate classification updated. *Meteorologische Zeitschrift*, *15*(3), 259-263.
- Kravchenko, A., & Robertson, G. (2015). Statistical challenges in analyses of chamber-based soil CO<sub>2</sub> and N<sub>2</sub>O emissions data. *Soil Science Society of America Journal*, *79*(1), 200-211.
- Kreutzweiser, D. P., Hazlett, P. W., & Gunn, J. M. (2008). Logging impacts on the biogeochemistry of boreal forest soils and nutrient export to aquatic systems: A review. *Environmental Reviews*, *16*, 157-179.



[20temperature%20varies%20widely%20from,fairly%20evenly%20throughout%20the%20year.](#)

- Lewandowski, T. E., Forrester, J. A., Mladenoff, D. J., Marin-Spiotta, E., D'Amato, A. W., Palik, B. J., & Kolka, R. K. (2019). Long term effects of intensive biomass harvesting and compaction on the forest soil ecosystem. *Soil Biology and Biochemistry*, 137, 107572.
- Likens, G. E., Bormann, F. H., Johnson, N. M., Fisher, D., & Pierce, R. S. (1970). Effects of forest cutting and herbicide treatment on nutrient budgets in the Hubbard Brook watershed-ecosystem. *Ecological Monographs*, 40(1), 23-47.
- Luo, Y., & Zhou, X. (2006). *Soil respiration and the environment*. Amsterdam: Elsevier Academic Press.
- Lupon, A., Denfeld, B. A., Laudon, H., Leach, J., Karlsson, J., & Sponseller, R. A. (2019). Groundwater inflows control patterns and sources of greenhouse gas emissions from streams. *Limnology and Oceanography*, 64(4), 1545-1557.
- Maag, M., & Vinther, F. P. (1996). Nitrous oxide emission by nitrification and denitrification in different soil types and at different soil moisture contents and temperatures. *Applied Soil Ecology*, 4(1), 5-14.
- Mander, Ü, Maddison, M., Soosaar, K., Teemusk, A., Kanal, A., Uri, V., & Truu, J. (2015). The impact of a pulsing groundwater table on greenhouse gas emissions in riparian grey alder stands. *Environmental Science and Pollution Research*, 22(4), 2360-2371.
- Malcolm Knapp Research Forest [MKRF]. (2016). MKRF 1 m DEM [Data file].
- McClain, M. E., Boyer, E. W., Dent, C. L., Gergel, S. E., Grimm, N. B., Groffman, P. M., . . . Mayorga, E. (2003). Biogeochemical hot spots and hot moments at the interface of terrestrial and aquatic ecosystems. *Ecosystems*, 301-312.

- Meyer, N., Welp, G., & Amelung, W. (2018). The temperature sensitivity (Q<sub>10</sub>) of soil respiration: Controlling factors and spatial prediction at regional scale based on environmental soil classes. *Global Biogeochemical Cycles*, 32(2), 306-323.
- Moore, R. D., Spittlehouse, D. L., & Story, A. (2005). Riparian microclimate and stream temperature response to forest harvesting: A review 1. *JAWRA Journal of the American Water Resources Association*, 41(4), 813-834.
- Morishita, T., Sakata, T., Takahashi, M., Ishizuka, S., Mizoguchi, T., Inagaki, Y., . . . Yasuda, H. (2007). Methane uptake and nitrous oxide emission in Japanese forest soils and their relationship to soil and vegetation types. *Soil Science & Plant Nutrition*, 53(5), 678-691.
- Moroni, M., & Zhu, X. (2012). Litter-fall and decomposition in harvested and un-harvested boreal forests. *The Forestry Chronicle*, 88(5), 613-621.
- Munsell Color. (2010). *Munsell soil color charts: With genuine Munsell color chips*. Grand Rapids, MI: Munsell Color.
- Nag, S. K., Liu, R., & Lal, R. (2017). Emission of greenhouse gases and soil carbon sequestration in a riparian marsh wetland in central Ohio. *Environmental Monitoring and Assessment*, 189(11), 580.
- National Research Council. (2001). *Climate change science: An analysis of some key questions*. Washington, DC: National Academies Press. Retrieved from <https://doi.org/10.17226/10139>
- Natural Resources Canada [NRCAN]. (2018). *The state of Canada's forests: Annual report 2018*. (PDF, Online). Ottawa: Natural Resources Canada. Retrieved from <https://cfs.nrcan.gc.ca/publications/download-pdf/39336>
- Oelbermann, M., & Raimbault, B. A. (2015). Riparian land-use and rehabilitation: Impact on organic matter input and soil respiration. *Environmental Management*, 55(2), 496-507.

- Oertel, C., Matschullat, J., Zurba, K., Zimmermann, F., & Erasmi, S. (2016). Greenhouse gas emissions from soils—A review. *Chemie Der Erde-Geochemistry*, *76*(3), 327-352.
- Pacific, V. J., McGlynn, B. L., Riveros-Iregui, D. A., Welsch, D. L., & Epstein, H. E. (2008). Variability in soil respiration across riparian-hillslope transitions. *Biogeochemistry*, *91*(1), 51-70.
- Parkin, T. B., & Venterea, R. T. (2010). Chapter 3: Chamber-based trace flux measurements. In R. F. Follett (Ed.), *Sampling protocols* (pp. 3-39). Washington, DC: USDA-ARS.
- Parkin, T., Venterea, R., & Hargreaves, S. (2012). Calculating the detection limits of chamber-based soil greenhouse gas flux measurements. *Journal of Environmental Quality*, *41*(3), 705-715.
- Paul-Limoges, E., Black, T. A., Christen, A., Nesic, Z., & Jassal, R. S. (2015). Effect of clearcut harvesting on the carbon balance of a Douglas-fir forest. *Agricultural and Forest Meteorology*, *203*, 30-42.
- Pihlatie, M., Pumpanen, J., Rinne, J., Ilvesniemi, H., Simojoki, A., Hari, P., & Vesala, T. (2007). Gas concentration driven fluxes of nitrous oxide and carbon dioxide in boreal forest soil. *Tellus B: Chemical and Physical Meteorology*, *59*(3), 458-469.
- Poblador, S., Lupon, A., Sabaté, S., & Sabater, F. (2017). Soil water content drives spatiotemporal patterns of CO<sub>2</sub> and N<sub>2</sub>O emissions from a Mediterranean riparian forest soil. *Biogeosciences*, *14*(18), 4195-4208.
- R Core Team. (2020). R: A language and environment for statistical computing. R Foundation for Statistical Computing, Vienna, Austria. URL <https://www.R-project.org/>.
- Ramey, T. L., & Richardson, J. S. (2017). Terrestrial invertebrates in the riparian zone: Mechanisms underlying their unique diversity. *Bioscience*, *67*(9), 808-819.

- Raymond, P. A., Hartmann, J., Lauerwald, R., Sobek, S., McDonald, C., Hoover, M., . . .  
Humborg, C. (2013). Global carbon dioxide emissions from inland waters. *Nature*,  
*503*(7476), 355-359.
- Richardson, J. S. (2019). Biological diversity in headwater streams. *Water*, *11*(2), 366.
- Richardson, J. S., & Danehy, R. J. (2007). A synthesis of the ecology of headwater streams and  
their riparian zones in temperate forests. *Forest Science*, *53*(2), 131-147.
- Richardson, J. S., Naiman, R. J., & Bisson, P. A. (2012). How did fixed-width buffers become  
standard practice for protecting freshwaters and their riparian areas from forest harvest  
practices? *Freshwater Science*, *31*(1), 232-238.
- Richardson, J. S., Naiman, R. J., Swanson, F. J., & Hibbs, D. E. (2005). Riparian communities  
associated with Pacific Northwest headwater streams: Assemblages, processes, and  
uniqueness 1. *JAWRA Journal of the American Water Resources Association*, *41*(4), 935-  
947.
- Ruser, R., Flessa, H., Russow, R., Schmidt, G., Buegger, F., & Munch, J. (2006). Emission of  
N<sub>2</sub>O, N<sub>2</sub> and CO<sub>2</sub> from soil fertilized with nitrate: Effect of compaction, soil moisture and  
rewetting. *Soil Biology and Biochemistry*, *38*(2), 263-274.
- Schade, J. D., Bailio, J., & McDowell, W. H. (2016). Greenhouse gas flux from headwater  
streams in New Hampshire, USA: Patterns and drivers. *Limnology and Oceanography*,  
*61*(S1), S165-S174.
- Serrano-Silva, N., Sarria-Guzmán, Y., Dendooven, L., & Luna-Guido, M. (2014).  
Methanogenesis and methanotrophy in soil: A review. *Pedosphere*, *24*(3), 291-307.

- Shrestha, R. K., Strahm, B. D., Sucre, E. B., Holub, S. M., & Meehan, N. (2014). Fertilizer management, parent material, and stand age influence forest soil greenhouse gas fluxes. *Soil Science Society of America Journal*, 78(6), 2041-2053.
- Skinner, C., Gattinger, A., Muller, A., Mäder, P., Fließbach, A., Stolze, M., . . . Niggli, U. (2014). Greenhouse gas fluxes from agricultural soils under organic and non-organic management—A global meta-analysis. *Science of the Total Environment*, 468, 553-563.
- Smerdon, B. D., Redding, T., & Beckers, J. (2009). An overview of the effects of forest management on groundwater hydrology. *Journal of Ecosystems and Management*, 10(1)
- Solomon, S., Manning, M., Marquis, M., & Qin, D. (2007). *Climate change 2007 - the physical science basis: Working group I contribution to the fourth assessment report of the IPCC (vol. 4)*. Cambridge University Press.
- Soosaar, K., Mander, Ü., Maddison, M., Kanal, A., Kull, A., Lõhmus, K., . . . Augustin, J. (2011). Dynamics of gaseous nitrogen and carbon fluxes in riparian alder forests. *Ecological Engineering*, 37(1), 40-53.
- Striegl, R. G., & Wickland, K. P. (1998). Effects of a clear-cut harvest on soil respiration in a jack pine-lichen woodland. *Canadian Journal of Forest Research*, 28(4), 534-539.
- Sun, Q., Shi, K., Damerell, P., Whitham, C., Yu, G., & Zou, C. (2013). Carbon dioxide and methane fluxes: Seasonal dynamics from inland riparian ecosystems, northeast China. *Science of the Total Environment*, 465, 48-55.
- Takakai, F., Desyatkin, A. R., Lopez, C. L., Fedorov, A. N., Desyatkin, R. V., & Hatano, R. (2008). CH<sub>4</sub> and N<sub>2</sub>O emissions from a forest-alas ecosystem in the permafrost taiga forest region, eastern Siberia, Russia. *Journal of Geophysical Research: Biogeosciences*, 113(G2)

- Tan, X., Chang, S. X., & Kabzems, R. (2005). Effects of soil compaction and forest floor removal on soil microbial properties and N transformations in a boreal forest long-term soil productivity study. *Forest Ecology and Management*, 217(2-3), 158-170.
- Tiwari, T., Lundström, J., Kuglerová, L., Laudon, H., Öhman, K., & Ågren, A. (2016). Cost of riparian buffer zones: A comparison of hydrologically adapted site-specific riparian buffers with traditional fixed widths. *Water Resources Research*, 52(2), 1056-1069.
- Tufekcioglu, A., Raich, J. W., Isenhardt, T. M., & Schultz, R. C. (2001). Soil respiration within riparian buffers and adjacent crop fields. *Plant and Soil*, 229(1), 117-124.
- Ullah, S., Frasier, R., King, L., Picotte-Anderson, N., & Moore, T. R. (2008). Potential fluxes of N<sub>2</sub>O and CH<sub>4</sub> from soils of three forest types in eastern Canada. *Soil Biology and Biochemistry*, 40(4), 986-994.
- Ullah, S., Frasier, R., Pelletier, L., & Moore, T. R. (2009). Greenhouse gas fluxes from boreal forest soils during the snow-free period in Quebec, Canada. *Canadian Journal of Forest Research*, 39(3), 666-680.
- University of British Columbia. (2011). Malcolm Knapp Research Forest. Retrieved from <https://www.mkrf.forestry.ubc.ca/>
- Vidon, P., Marchese, S., Welsh, M., & McMillan, S. (2015). Short-term spatial and temporal variability in greenhouse gas fluxes in riparian zones. *Environmental Monitoring and Assessment*, 187(8), 503.
- Vidon, P., Welsh, M., & Hassanzadeh, Y. (2018). Twenty years of riparian zone research (1997–2017): Where to next? *Journal of Environmental Quality*, 28(2), 248-260.
- Walley, F., Van Kessel, C., & Pennock, D. (1996). Landscape-scale variability of N mineralization in forest soils. *Soil Biology and Biochemistry*, 28(3), 383-391.

Watson, K. (2007). *Soils illustrated: field illustrations*. Kamloops, BC: International Remote Sensing Surveys.

Wu, X., Brüggemann, N., Gasche, R., Papen, H., Willibald, G., & Butterbach-Bahl, K. (2011). Long-term effects of clear-cutting and selective cutting on soil methane fluxes in a temperate spruce forest in southern Germany. *Environmental Pollution*, 159(10), 2467-2475.

Zuur, A., Ieno, E., & Smith, G. (2007). *Analysing ecological data*. New York: Springer.

## Appendix

Table A.1 Pairwise difference between Treatment levels (reference, R; buffer B; and no buffer NB) for Chapter 2 using Tukey’s HSD *post hoc* test for the linear mixed effects models explaining the dynamics of carbon dioxide, methane, and nitrous oxide fluxes, respectively. Data includes the influential outliers identified by Cook’s distance. All models included the autocorrelation term “AR1(Week + 0 | Site/Chamber)”. Bolded comparison indicates a significant effect at  $p < 0.05$ .

Model	Comparison	Est.	SE	<i>p</i>
CO <sub>2</sub> ~ Treatment	R - B	-21.47	17.4	0.43
	R - NB	-1.83	17.6	0.99
	B - NB	19.64	17.4	0.50
CH <sub>4</sub> ~ Treatment	R - B			
	R - NB	Model does not converge		
	B - NB			
N <sub>2</sub> O ~ Treatment	R - B	-0.087	0.99	0.99
	<b>R - NB</b>	<b>-2.39</b>	<b>0.98</b>	<b>0.04</b>
	B - NB	-2.30	0.98	0.05

Table A.2 Summarized output of linear mixed effects models explaining the effect of groundwater discharge conditions on environmental variables of soil temperature, soil moisture and depth to groundwater table for Chapter 2. All models included an autocorrelation term. Bolded models indicate a significant effect at  $p < 0.05$ . When comparing groundwater discharge (DIS) and non-groundwater discharge (ND) areas, note that ND is the reference level in the DIS\_ND term.

<b>Model</b>	<b>Est.</b>	<b>SE</b>	<b><i>p</i></b>
Soil temp. ~ DIS_ND	0.003	0.62	0.86
<b>Soil moist. ~ DIS_ND</b>	<b>13.53</b>	<b>2.53</b>	<b>&lt; 0.001</b>
<b>Depth to GW ~ DIS_ND</b>	<b>-9.04</b>	<b>2.5</b>	<b>&lt; 0.001</b>

Table A.3 Pairwise difference between Treatment levels (reference, R; buffer B; and no buffer NB) for soil temperature, soil moisture and depth to the groundwater table using Tukey's HSD *post hoc* test on the results of linear mixed effects models for Chapter 2. Bolded comparison indicates a significant effect at  $p < 0.05$ .

<b>Model</b>	<b>Comparison</b>	<b>Est.</b>	<b>SE</b>	<b><i>p</i></b>
Soil temp. ~ Treatment	R - B	-0.77	1.15	0.78
	R - NB	-1.21	1.15	0.54
	B - NB	-0.43	1.15	0.92
Soil moist. ~ Treatment	R - B	-2.62	4.61	0.84
	R - NB	-7.64	4.62	0.22
	B - NB	-5.01	4.62	0.52
Depth to GW table ~ Treatment	R - B	3.09	3.32	0.62
	<b>R - NB</b>	<b>13.60</b>	<b>3.32</b>	<b>&lt; 0.001</b>
	<b>B - NB</b>	<b>10.50</b>	<b>3.32</b>	<b>&lt; 0.01</b>

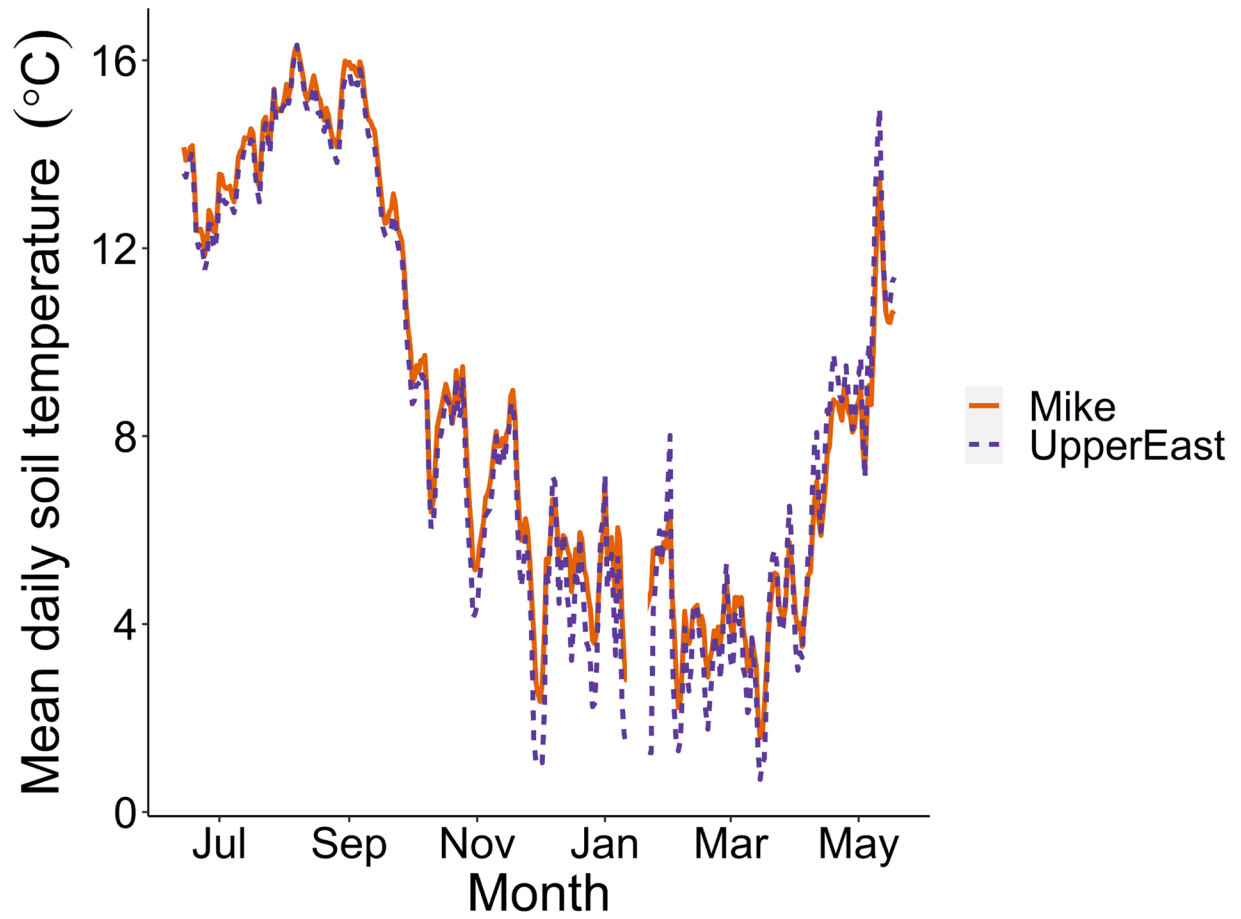


Figure A.1 Mean daily soil temperature measured ~10 cm below the soil surface in the riparian zone of two headwater streams (Mike Ck. and Upper East Ck.) from June 2019 to May 2020.

Table A.4 Weekly high and low seven-day maximum and minimum values, respectively, for soil temperature (°C), soil moisture (volumetric water content, %), and depth to the groundwater table (cm) across groundwater discharge (DIS) and non-groundwater discharge (ND) areas in the riparian zone of Mike Ck. and Upper East Ck. in Malcolm Knapp Research Forest for Chapter 3. The date represents the Monday of the week for which the data are averaged. Data are from May 2019 to May 2020, except soil temperature, which only goes to November 2019.

	Sampling frequency	Mike		Upper East	
		DIS	ND	DIS	ND
Max soil temp. (°C)	Hourly	17.2	16.1	17.6	15.6
Date		2019-08-05	2019-09-02	2019-08-05	2019-09-02
Min soil temp. (°C)	Hourly	3.6	5.1	3.1	5.6
Date		2019-11-24	2019-11-24	2019-10-28	2019-10-28
Max soil moist. (%)	Weekly to monthly	66.1	69.8	56.3	59.5
Date		2019-10-21	2020-02-02	2020-05-18	2020-05-18
Min soil moist. (%)	Weekly to monthly	34.3	24.9	41.9	17.0
Date		2019-05-27	2019-08-12	2019-06-03	2019-07-29
Max depth to GW (cm)	Weekly to monthly	41.7	37.5	38.0	48.4
Date		2019-08-19	2019-08-12	2019-08-26	2019-09-23
Min depth to GW (cm)	Weekly to monthly	-2.0	18.1	24.4	6.6
Date		2019-06-24	2019-11-17	2019-09-23	2019-11-17

Table A.5 Summarized output of linear mixed effects model exploring the spatial dynamics of soil temperature, soil moisture, and depth to groundwater for Chapter 3. All models included the autocorrelation term “AR1(Week + 0 | Site/Chamber)”. Note that ND is the reference level in the DIS\_ND term.

<b>Model</b>	<b>Est.</b>	<b>SE</b>	<b><i>p</i></b>
Soil temperature ~ DIS_ND	0.004	0.01	0.65
Soil moisture ~ DIS_ND	6.84	4.96	0.17
Depth to GW ~ DIS_ND	-0.02	5.61	0.99